

A Study of Loe Bar

A study into the history of the bar and the development of a technique for future monitoring as well as an insight into the geomorphology.



Satellite image of Loe Bar taken from global mapper world imagery.

Submitted by Annabel Pardoe to the University of Exeter as a dissertation towards the degree of Master of Science by advanced study in Surveying with Land and Environmental Management, 7th September, 2015.



Annabel Pardoe

Candidate no. 64007766

Camborne School of Mines

University of Exeter

Abstract

Loe Bar has shown to have a vast and colourful history, witnessing the Cornish mining boom, multiple shipwrecks, wartime efforts and all the time being shaped by means of both human interference and natural processes. While the sea-ward border of the bar appears to have remained in a relatively constant position, the lake-ward side has been moving inland at varying rates. In order to monitor this movement, the development of a method was required to survey the bar effectively and efficiently. A topographic survey was successfully completed using a total station, with further study put towards the testing of a sentripod prism, which was seen to produce resection results of a sufficient quality to be used in future surveys as well as greatly reducing the amount of equipment required.

A resistivity line running the length of the bar gave an insight into the internal structure, as well as possibly determining the depth of the channel that it occupies. Other interesting features included a layer of clay found consistently across the bar at depths of around 10m, and a potential freshwater channel under the location of where the bar was last cut. Recommendations for further study methods include an increased number of resistivity lines as well as undertaking a magnetic survey of the bar.

Table of Contents

A Study of Loe Bar	0
Abstract	1
List of Figures.....	5
List of Tables	8
Acknowledgements	9
Declaration	10
1 Introduction.....	11
1.1 Project Aims.....	12
2 Formation of Loe Bar	13
2.1 The Jan Tregeagle Legend.....	13
2.2 Geomorphological Explanation	13
2.3 Present-Day Characteristics.....	13
3 Environmental Importance of Loe Bar	15
3.1 SSSI.....	15
4 Geology of the Area.....	17
4.1 Superficial Geology	17
5 Characteristics of Shingle Beaches	18
5.1 Characteristics of Loe Bar	18
5.2 Comparisons to Loe Bar.....	21
5.2.1 Slapton Sands	21
5.2.2 Chesil Beach.....	21
6 Management of the Bar	23
6.1 Historical Management	23
6.1.1 Cutting of the bar.....	23
6.1.2 Creation of an Adit.....	25
6.2 Present-Day Management of Loe Bar	25
7 Changing Morphology of the Bar	27
7.1 Chronological profiles of the Loe Bar	28
8 Port Proposals for Loe Bar in 1837	30
9 Shipwrecks at Loe Bar	32
9.1 Loe Bar at War	33
10 Mining History of the local area	34
11 Existing Survey Data of Loe Bar	37
11.1 TELLUS LiDAR	37
11.1.1 Advantages and Disadvantages of LiDAR	40
11.2 Laser scanning	40

11.3 The South West Coastal Group.....	42
12 Possible Survey Methodology for measuring Loe Bar.....	43
12.1 Laser Scanning	43
12.2 Aerial Photography	43
12.3 GPS Surveys	43
12.4 Total Station Surveys	44
13 Topographic Survey of Loe Bar.....	45
13.1 Installing the Baseline at Loe Bar.....	45
13.2 Survey Method	48
13.3 Findings of the Survey	50
13.4 Difficulties encountered	50
13.5 Possible Improvements	51
14 The Sentripod	52
14.1 Creating a suitable Baseline.....	53
14.2 Resection accuracies using Sentripods at Loe Bar.....	55
14.3 Testing the Sentripod in the Field.....	58
14.3.1 Method	58
14.3.2 Problems Encountered when Using the Sentripod	60
14.3.3 Transferring Coordinates to a Bolt	61
14.4 GPS Error Ellipse	63
15 Recommendations for Future Surveys	64
15.1 Recommended Method.....	64
16 Geophysical Investigation of Loe Bar	65
16.1 The ZZ array	68
16.1.1 Induced Polarisation	68
16.2 Survey Method	68
16.3 Results and Interpretation.....	70
16.3.1 Line 1 Resistivity	70
16.3.2 Line 1 Induced Polarisation	76
16.3.3 Line 2 Resistivity	78
16.3.4 Line 2 Induced Polarisation	79
16.4 Correlation with Rendel's Bores.....	80
16.5 Further Study	81
16.5.1 Flooding in Helston – a solution?	81
17 Recommendation for Further Study at Loe Bar	82
18 Conclusion	83
References	84

Appendix A: Loe Bar Since 1984	88
June 1985.....	88
April 1986	88
June 1987.....	89
May 1988.....	89
June 1989.....	90
December 1989	90
June 1990.....	91
January 1991.....	91
March 1993.....	92
March 1994.....	92
January 1997.....	93
September 1998	93
October 2001.....	94
June 2003.....	94
Appendix B: Loe Bar historical maps	95
1878-1880.....	95
1888	95
1907-1908.....	96
1908-1909.....	96
1962-1963.....	97
1974	97
1978-1981.....	98
Appendix C: Sentripod Accuracies.....	99
C.1 Resection results	99
C.2 Resection Errors.....	101
C.3 Errors encountered at Each Resection	103
C.4 Average Errors of Each Prism	105
Appendix D: Bolt Coordinates	106
Appendix E: Project Timeline.....	107

List of Figures

Figure 1: Location map of Loe Bar. Area in red box is displayed in figure 2.	11
Figure 2: Location of Loe Bar, at the foot of Loe Pool.	12
Figure 3: Map showing the location of Loe Bar within an Area of Outstanding Natural Beauty (Green). (Information source: Cornwall Council; Map source: Digimap).....	15
Figure 4: Map showing the location of Loe Bar within an Area of Scientific Value (Orange). (Information source: Cornwall Council; Map source: Digimap)	16
Figure 5: Map showing the extent of the Site of Special Scientific Interest at Loe Bar and Pool (blue). (Information source: Cornwall Council; Map source: Digimap).....	16
Figure 6: Map showing Conservation Areas near Loe Bar (purple). (Information source: Cornwall Council; Map source: Digimap).....	16
Figure 7: Bedrock and superficial geology of the area (Information source: BGS interactive mapping, Base map: Edina Digimap).....	17
Figure 8: Typical differences in morphology characteristics between sandy and cobble beaches (Source: Davidson-Arnott, 2010).	18
Figure 9: Effects of sea level in relation to bar height. The diagrams left to right show an increase in sea level and the associated effects on bar morphology. (Source: Coastal Processes Research Group, University of Plymouth, 2015).	19
Figure 10: Over-wash during storms pushes sediment onshore and over the top of the barrier (left) where it will stay and not return to the beach (right) (Masselink, 2015).	19
Figure 11: Diagram displaying results found from a pre- and post-storm survey at Loe Bar completed in February 2014 (note: vertical exaggeration) (Masselink, 2015). This can be compared to the diagrams in the left side of figure 9 above and the process demonstrated in figure 10.	19
Figure 12: The amount of landward movement of the boundary between Loe Bar and Loe Pool going by OS maps produced in December 2013 and May 2014 (Base map: Edina Digimap).....	20
Figure 13: Satellite imagery of the Bar with the landward movement between December 2013 and May 2014 overlain. Note the visible break in vegetation (satellite image source: Global Mapper).....	20
Figure 14: A comparison of geomorphological form between Slapton Sands, enclosing a large lagoon, and Loe Bar, blocking a narrow estuary (Source: May and Hansom, 2003).	21
Figure 15: Chesil beach, showing the location in relation to the cliffs at the Western end and lagoon at Eastern end of the pebble bar. 'First attack' represents the location of shoreline first attacked at the dates shown (Source: May and Hansom, 2003).	22
Figure 16: Photograph of the 'cut' being made to release water from Loe Pool to the sea in November 1984, looking southeast (Davies, 2012).	23
Figure 17: Satellite Image of Loe Bar. The lack of vegetation is visible in a linear NE-SW direction, caused by the cutting of the bar to let water out to the sea in November 1984 (Source: World Imagery, Global Mapper).	24
Figure 18: Changes in morphology of Loe Bar at various intervals between 1878 and present day (Source: Edina Digimap Historical & Mastermap data).	27
Figure 19: Changes in morphology of Loe Bar. Lines 1 to 5 represent chronological profiles shown in figure 20 a to e.	28
Figure 20 (a to e): Profiles showing the change in thickness at 5 sections on the bar from 1887 to present day. Lines are represented in figure 19 (source : Digimap Historical Mapping).	29
Figure 21: Plan of proposed design for a harbour to be built at the mouth of Loe Pool, Loe Bar (Rendel, 1837).	30
Figure 22: Catchment area of the River Cober (Base map: Edina Digimap, information source: loepool.org)	34
Figure 23: Mine features in the area surrounding the Loe, mainly dating from the 18 th and 19 th Centuries (Source: historical maps, Digimap).	34
Figure 24: Closer look at the locations of mine features in the area surrounding the Loe (source: historical maps, Digimap).....	35

Figure 25: Generalised North-South section of the top few metres of sediments in Loe Pool (O’Sullivan et al, 1982).	35
Figure 26: Loe Bar topography represented in contour lines generated in Global Mapper from LiDAR data taken by Ferraccioli et al in 2014.	37
Figure 27: Slope direction of the bar enabling the distinction of the approximate location of the crest of the bar as marked (Source: Ferraccioli et al, 2014).	38
Figure 28: View of Loe Bar in Global Mapper’s ‘slope shader view’, showing slope characteristics and morphological features (Source: Ferraccioli et al, 2014).	39
Figure 29: 3Dview of Loe Bar and surrounding area using LiDAR data from TELLUS, looking approximately east (vertical exaggeration: 1.2500, Source: Ferraccioli et al, 2014).	39
Figure 30: 3D view of the TELLUS LiDAR data showing the lake-ward edge of the bar, looking west (vertical exaggeration: 1.2500, source: Ferraccioli et al, 2014).	40
Figure 31: Top and right: Photos showing the deployment of the laser scanner at Loe Bar, Lower left: beach profile with locations of the equipment used during the survey (Almeida et al (2014).	41
Figure 32: Part of the equipment used in the 2012 beach morphology observations made at Loe Bar by Poate et al (2013).	41
Figure 33: Locations of the GPS base stations established for use in surveying the bar.	45
Figure 34: GPS Base station set up over an ‘X’ marked in the rock at Base SE.	46
Figure 35: A GPS base station set up over an existing survey point at base NW.	46
Figure 36: The existing survey point placed by the Environment Agency and used as a point for ‘Base NW’.	47
Figure 37: The rock used for the location of Base SE, firmly embedded into the ground to avoid error.	47
Figure 38: The ‘X’ marked on the rock in figure 37 above, created with a hacksaw and marker pen.	47
Figure 39: Leica prism set up on a tripod over base SE, used in resection.	49
Figure 40: The Trimble M3 total station used in the topographical survey carried out.	49
Figure 41: Photograph of a Sentries. Height of target is marked (not to scale).	52
Figure 42: Access Routes to the bar from public car parks and another possible location for parking if permission is granted by the National Trust (base map: Edina Digimap).	53
Figure 43: Photograph of the mark made in the pipe which will be the new base station point.	53
Figure 44: Photograph of the GPS station set up over a point marked on the pipe to create another base station for future resection use.	54
Figure 45: Location of ‘Base Pipe’ in relation to OS stations at Camborne (CAMO) 16.787km away and The Lizard (LIZD) 13.796km away (base map: Digimap).	54
Figure 46: Locations of the three base stations established on Loe Bar which can be used for future surveys (base map: Edina Digimap).	55
Figure 47: Map showing the distance between Base NW and the new Base Pipe to be 105.38m (base map: Edina Digimap).	55
Figure 48: Accuracies stated by manufacturers of the sentripod applied to Loe Bar. A description of this is in table 8.	56
Figure 49: Possible range of resection angles displayed with areas of optimum accuracy for using sentripods as resection tools.	57
Figure 50: Examples of possible locations for resection which use an angle of 90°.	57
Figure 51: Sentripods in place at Base Pipe (left) and Base NW (right).	58
Figure 52: Locations of instrument set-ups, from where 5 resections were made using both sentripods and circular prisms.	59
Figure 53: Circular prism placed on the bolt for determining coordinates. Note the collar to the right of the prism which obstructs the view to the sentripod from certain places on the bar.	61
Figure 54: Locations where resection was used to establish a location and measurements taken to the circular prism on the bolt (base map: Edina Digimap).	62

Figure 55: Sentries placed on bolt a held level and in place using tac. This can be used in resection if view of Base NW is obstructed. Note the sentripod fits over the 5mm tall bolt, providing the need to adjust the target height to 0.027 rather than 0.032.....	62
Figure 56: Sequence of measurements used to build up a pseudo-section when and arrangements of electrodes needed. 'a' represents spacing between electrodes, with deeper readings taken using electrodes further apart (Source: Loke, 1999).	66
Figure 57: The roll-along method involving linear movement of the line to increase the data coverage at depth (source: Loke, 1999).	67
Figure 58: Pseudo-sections created from differing arrays, covering a rectangular block target (source: Loke, 1999).	67
Figure 59: Location of resistivity lines 1 and 2 displayed on satellite imagery, with electrode numbers labelled (satellite imsgs source: Global Mapper).	69
Figure 60: Photographs of the placement of the resistivity line 1 rolled across the bar looking NW (left) and SE (right).	69
Figure 61: Typical ranges in resistivity values of Earth materials (Palacky, 1988).	70
Figure 62: Resistivity pseudo-section of line 1 using a Wenner array (processed by Mr N.A. Wood). Smoothing coefficients: Horizontal = 9, Vertical = 3.....	71
Figure 63: Resistivity pseudo-section of line 1 using a ZZ array (processed by Mr N.A. Wood). Smoothing coefficients: Horizontal = 9, Vertical = 3.....	72
Figure 64: Resistivity pseudo-section of line 1 using a ZZ array. Contours are applied to clarify values in the image (processed by Mr N.A. Wood). Smoothing coefficients: Horizontal = 9, Vertical = 3.	73
Figure 65: Resistivity pseudo-section of line 1 using a ZZ array. Scale is altered to show a maximum value of 1200 Ωm (processed by N.A. Wood). Smoothing coefficients: Horizontal = 9, Vertical = 3. Scale units Ωm	74
Figure 66: Position of cross section generated for comparing the morphology of the channel feature with that of the surrounding valley in figure 67.....	74
Figure 67: Cross section through LiDAR data (location marked in figure 66) with resistivity data superimposed (top scale of 1200 Ωm), showing a realistic match between the shape of the valley and the increase in resistivity potentially showing the bottom of the ria.	75
Figure 68: Vertical Cross-section showing typical interactions of fresh and saline water in an unconfined coastal aquifer (Todd, 2005).	76
Figure 69: Induced polarisation pseudo-section of line 1 using a Wenner array (processed by N.A. Wood). Smoothing coefficients: Horizontal = 13, Vertical = 3.	77
Figure 70: Induced polarisation pseudo-section of line 1 using a ZZ array (processed by N.A. Wood). Smoothing coefficients: Horizontal = 9, Vertical = 3. Scale units Ωm	78
Figure 71: Spatial relationship between resistivity lines 1 and 2 and the changes in shoreline over time.	78
Figure 72: Resistivity pseudo-section of line 2 using a ZZ array (processed by N.A. Wood). Smoothing coefficients: Horizontal = 9, Vertical = 3. Scale units Ωm	79
Figure 73: Induced Polarisation pseudo-section of line 2 using a ZZ array (processed by N.A. Wood). Smoothing coefficients: Horizontal = 9, Vertical = 3.....	80
Figure 74: Cross section with pseudo-section superimposed (as in figure 67) with the addition of probable locations of Rendel's bores (subject to assumptions). Points on the bore locations represent features of interest found.	80

List of Tables

Table 1: Borehole findings observed by James Rendel, published in his report of 1837.....	31
Table 2: Wreckages at Loe Bar recorded by Larn and Carter (1969).....	33
Table 3: Rates of erosion in the catchment area of the River Cober as determined from lake sedimentation rates (O’Sullivan et al, 1982).....	36
Table 4: Times during which the GPS base stations were running in order to obtain coordinates.....	45
Table 5: Coordinate values pre- and post-RINEX and the differences encountered.....	48
Table 6: Prism Constants, Centring accuracies and ranges of a number of prisms which can be used in topographic surveys with a total station (information source: http://surveyequipment.com/)	50
Table 7: Coordinates pre- and post-RINEX calculations and the differences. Information obtained by Dr Andy Wetherelt, Camborne School of Mines.	55
Table 8: Key for information visualised in figure 48, based on the stated accuracies of the sentripod by the company responsible for their invention and manufacture (www.sentripod.com).	56
Table 9: Distances from each station to the bases and angles of resection.	58
Table 10: Coordinates of the bolt on the sluice derived from multiple resections and weighted averages. The height was derived by levelling from base NW.	62
Table 11: Coordinates which should be used when resecting, as established by work done in this project (* elevations derived by levelling from Base NW).....	64
Table 12: RMSD values of each array on both lines before and after the stated number of processing rounds, as well as the number of points taken by each survey and those filtered out.....	70

Acknowledgements

A great deal of thanks must go to my supervisor, Mr Neill Wood for supplying the project idea and materials, including running the resistivity lines and processing the data. Thank you for all your support and putting up with my abundant queries.

Thanks also to Dr Andy Wetherelt for help in establishing the three base station coordinates with RINEX and also providing a great deal of support and knowledge on surveying techniques.

Interpretation of resistivity was greatly aided by input and suggestions from Dr Robin Shail and from Dr Dave Watkins.

None of the field work would have been possible without my very dedicated field assistant Kris Larby, who has spent many days guarding tripods and holding the staff. Thank you for all your help.

Declaration

I certify that all material in this dissertation which is not my own work has been identified and that no material is included for which a degree has previously been conferred on me.

Signed

1 Introduction

Loe Bar is located around 4km to the South West of Helston on the Cornish Coast (figures 1 and 2) and comprises a stretch of sand and shingle approximately 400m long, dividing Loe Pool and the Atlantic Sea. It is part of a beach system extending over 4km in length which extends in a NW-SE direction from Porthleven to Gunwalloe forming a single sediment cell that can be divided into three parts: the cliffs and beach known as 'Porthleven Sands', the bar itself and the cliffs and beach known as 'Gunwalloe Fishing Cove Beach'.

The bar intercepts the river Cober creating Loe Pool behind it, the largest freshwater lagoon in Cornwall. The linear features of the pool come from the flooding of a sunken channel or 'ria'. Loe Bar and Pool are managed by the National Trust as part of the Penrose Estate and are accessible to the public on foot, with the South West Coastal Path running the length of the bar. Material on the bar is mainly flint shingles and coarse sand, which give the bar a distinctive steeper gradient on its sea-ward side, different to that of a beach containing finer sand.

The lake-ward side of the bar is understood to be moving inland, causing the bar to gradually widen. Storm events can increase this effect on the bar and accelerate its movement. Determining an effective monitoring method by which to record movement would be beneficial for the future study and management of the bar.



Figure 1: Location map of Loe Bar. Area in red box is displayed in figure 2.



Figure 2: Location of Loe Bar, at the foot of Loe Pool.

1.1 Project Aims

The aims of this project are:

1. Establish a successful method for future monitoring of the lake-ward side of the Loe Bar.
2. Test the success of the sentripod prism as a tool for future surveys, noting advantages and disadvantages.
3. Distinguish information on the internal structure of the bar and the ria in which it sits.

2 Formation of Loe Bar

2.1 The Jan Tregeagle Legend

The remorseful spirit of Jan Tregeagle, the most evil man believed ever to have lived in Cornwall is said to be forever chased by demons. To hide from the demons, Tregeagle was put to work by priests to carry out indefinite tasks. After St Petroc had bound him in chains and led him to Helston, he was given the task of carrying all the sand from the beach below Berepper to Porthleven, across the estuary of the River Cober. One day however, the ever-watching demons contrived to trip him up as he was wading across the river, making him drop the sack of sand that he was carrying, causing the Cober to dam, and thus forming Loe Pool and bar (Cornwall Guide, 2015).

2.2 Geomorphological Explanation

The geomorphological formation of Loe Bar has always been a subject of debate, with many feasible theories proposed. The initial reason for its existence is thought by some to be a result of eustatic sea level rise after the last glacial period. Throughout the ice age huge levels of erosion were caused by glaciers flowing over the land and taking with them vast quantities of sediment. When the ice began to thaw, this material was dropped by the melting glaciers and huge levels of deposition occurred. As the sea level rose very gradually, this sediment was slowly pushed up, causing the beaches to move landwards, until they reached their present position around 6,000 years ago (Davies and Matthews, 2002). Loe Bar is not alone in its formation and characteristics. Other examples in the South West believed to have been formed as a result of this process are Swan Pool, Long Rock and Eastern Green in Cornwall as well as Slapton Ley in South Devon and Chesil Beach, Dorset. All of these beaches notably contain a large proportion of non-local material, mainly comprising of flint, yet are isolated from any present-day sources. Over 90% of the sediment that forms the 4.3 km stretch of beach in which Loe Bar is included, is flint of a non-local provenance (May and Hansom, 2003), and falls into two size categories: medium to very coarse sand (between +0.5 and -1.0 phi) and small pebbles (above -4.0 phi). This has prompted theories such as that from Bird and Swartz (1985) to describe the material as having been washed up from the sea floor. May and Hansom (2003), describe these beaches as being in the form of barrier beaches which were gradually moved onshore during the rise in sea level in the Holocene. The flint is believed to have come from the drowned pathways of the river formerly flowing down what is now the English Channel, and seen to exist across the entire Mounts Bay coast, from Marazion to Mullion (Coard, 1987).

King (1972) described the bar as being an example of a case where very low discharge occurs at an estuary or a very permeable barrier, whereas Toy (1934) made the suggestion that two spits had formed across the narrow estuary from either side, with the bar being gradually formed when the process led to their joining, creating the bar, as was witnessed at Pagham Harbour in West Sussex. This theory was also suggested in a report by James Rendel in 1837. Loe Bar is then believed to have been developed by longshore drift, being kept from washing out to sea.

2.3 Present-Day Characteristics

The Bar is said to be growing by the cause of longshore drift and its position as a sediment sink. Every incoming tide brings a strong South Easterly current, linking the sand in the beaches from Porthleven to Gunwalloe and in doing so, deposits a continuous supply of sediment on the bar. The ebb tide however is not as strong and so does not take the same amount of sediment back. As a result the bar is accreting material and gaining stability. The amount of sediment in the bar is considered to be incredibly high, with Rogers (1859) reporting that a boring made in 1834 reached a depth of 22m without reaching bedrock (May and Hansom, 2003). Huge waves from the Atlantic Ocean can deposit hundreds of tonnes of material onto the bar and occasionally overtop it, creating washover fans on the lake-ward side of its structure, although this only occurs on occasions of extreme swash (Loe Pool Form, 2015; May and Hansom, 2003). Such waves were seen in June and October 1859 and in April 1868, the latter described as a 'succession of hundreds of great waves for more than an hour' (Davies and Matthews, 2002). In 1924, a vast tidal wave destroyed part of Porthleven, claiming huge amounts of material

from the cliffs, which was deposited onto and over the bar, significantly altering its shape. Similar effects were seen by the storms in 1979 (Coard, 1987). Climate change is believed to cause an increase in such events in the future, with the rising frequency of strong storms coupled with rising sea level. Today the lake-ward edge of the bar is believed to be slowly moving inland at a rate of around 1m per year and in the next 50 years is expected to move inward by between 25m and 74m (SMP2, 2011).

3 Environmental Importance of Loe Bar

Loe Bar and the surrounding landscape has been categorised as one of the Cornwall Areas of Outstanding Natural Beauty (AONB) and Area of Scientific Value, as well as being classed as a Site of Special Scientific Interest (SSSI) on account of both its ecological and geomorphological significance (figures 3-6).

3.1 SSSI

The pool and bar provide a rare habitat for flora and fauna which is not found anywhere else in Cornwall. Rare species of higher plants, bryophytes and algae, along with many rare and local species of insect are found in the area, which also hosts up to 80 species of wintering birds, accounting for 1,200 wildfowl (Designated Sites, 2015).

The pool is known to support several rare aquatic plant species with the bar also supporting several local plant species, namely Sea Holly (*Eryngium maritimum*), Sea Fern-grass (*Catapodium marinum*), Yellow Horned-poppy (*Glaucium flavum*), Sea Sandwort (*Honkenva peploides*), Sea Mayweed (*Tripleurospermum maritimum*) and the very rare Strapwort (*Corrigiola litoralis*) (Designated sites, 2015).

Loe Pool is currently Britain's only known site where the Cornish subspecies of the Sandhill Rustic Moth and a rare species of woodlouse can be found. High levels of nutrients present in the pool itself have also encouraged an abundance of benthic invertebrates. The surrounding areas of the lake area also considered to be of importance, being home to a number of reed species. A relatively undisturbed ancient oak wood lies to the west of the lake and an extensive mat of maritime grassland exists on the cliffs either side of the bar (Designated sites, 2015).

The site is also of great importance with regards to coastal geomorphology, with the bar being described as a classic coastal landform and a rare example of a bay-bar, as well as contributing to a suite of beaches which are predominantly formed and maintained by south-west wave regimes (May and Hansom, 2003).



Figure 3: Map showing the location of Loe Bar within an Area of Outstanding Natural Beauty (Green). (Information source: Cornwall Council; Map source: Digimap)



Figure 4: Map showing the location of Loe Bar within an Area of Scientific Value (Orange). (Information source: Cornwall Council; Map source: Digimap)



Figure 5: Map showing the extent of the Site of Special Scientific Interest at Loe Bar and Pool (blue). (Information source: Cornwall Council; Map source: Digimap).

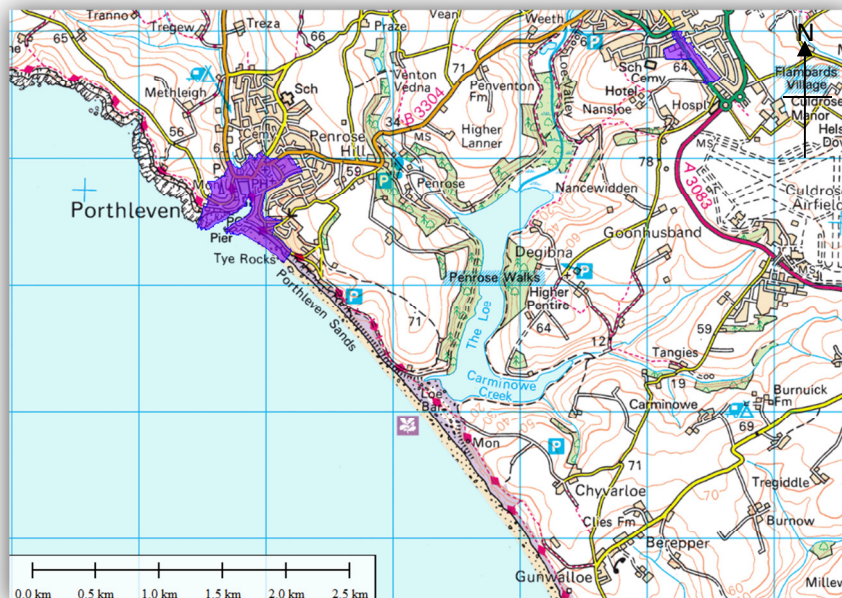


Figure 6: Map showing Conservation Areas near Loe Bar (purple). (Information source: Cornwall Council; Map source: Digimap)

4 Geology of the Area

The underlying geology of The Loe is predominantly divided into the Portscatho and Mylor Slate formations (figure 7). The Portscatho consists of interbedded sandstone and argillaceous rocks formed in a deep oceanic environment and dates from approximately 375 to 392 million years ago. The Mylor Slate Formation is made up of slates and siltstones formed approximately 359 to 385 million years ago in an open sea environment. Despite being older than the Mylor Slate, the Portscatho lies above it, due to the emplacement of the Carrick Thrust (Le Gall et al., 1985). The projected offshore continuation of the Carrick Thrust is seen to coincide with a notable seismic reflector dipping to the south east at around 30-35° in both Plymouth Bay and Mounts Bay (Day and Edwards, 1983). Despite this, the South easterly dipping fault separating the Mylor Slate and Portscatho formations near Bar Lodge shows characteristics of a normal (extensional) fault implying the occurrence of reactivation (Selwood et al, 1998). This extensionally reactivated fault could be expected to cross Loe Bar and continue along the Helford River (Selwood et al, 1998).

To the Northwest of Loe Bar a metamorphic aureole exists, representing a thermal alteration of the Mylor Slate to that containing Hornfelsed slates and siltstones (BGS, 2015). The Mylor Formation forming the cliffs to the north of the bar is recorded as being slower to erode than the cliffs to the south and so provide the bar with less material (May and Hansom, 2003). Other rocks in the surrounding areas are mainly silica-poor igneous intrusions of a north east orientation which range in date, with the youngest formed 299 million years ago. A number of mineral veins are also seen in the area, supporting the strong mining history of the area (BGS, 2015).

4.1 Superficial Geology

The Bar is mapped by the British Geological Survey as being marine beach deposits containing sand and gravel, forming up to 3 million years ago in the Quaternary period. The river pathways and in particular Loe Pool, show an alluvium deposit of sediment composed of a mixture of clay, silt, sand and gravel, deposited less than 2 million years ago in the Quaternary Period. This sediment has been transported here by river systems and has settled in the pool. Some areas along the headlands either side of the bar show 'head' sediments also consisting of clay, silt, sand and gravel, deposited by sub-aerial processes acting on the cliffs, and are less than 3 million years old (BGS, 2015). Soils which have developed over the surrounding area of the lake and bar predominantly consist of acidic brown earths (May and Hansom 2003).

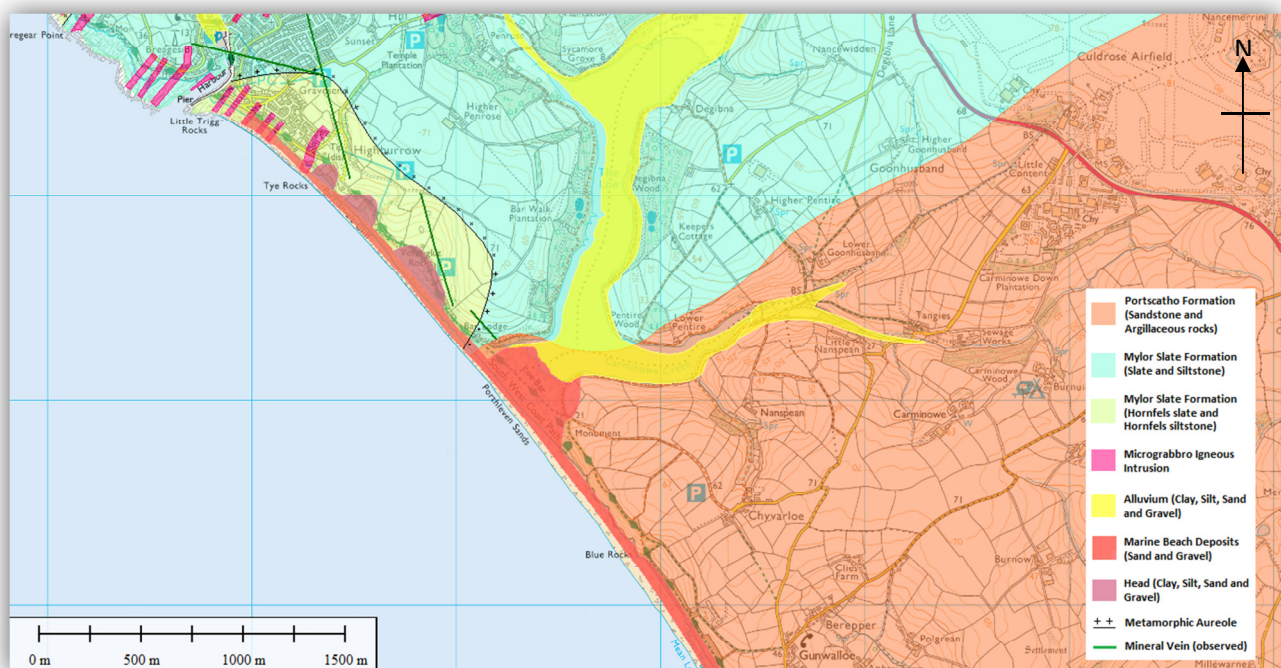


Figure 7: Bedrock and superficial geology of the area (Information source: BGS interactive mapping, Base map: Edina Digimap)

5 Characteristics of Shingle Beaches

Gravel or shingle beaches tend to occur on paraglacial coasts such as Canada or the UK or on coastlines backed by mountains, as seen in New Zealand (Almeida et al, 2014). They differ physically from sandy beaches in that they tend to show much steeper gradients and higher sediment permeability (Buscombe and Masselink, 2006). This morphology promotes early and more violent breaking of waves than is seen at sandy beaches, with most of the sediment transport taking place nearer to the shore in the swash zone rather than in the surf zone. This creates very different features from those of sandy beaches (figure 8). The higher level of permeability seen at gravel beaches leads to more significant effects of infiltration and exfiltration, specifically showing greater swash infiltration losses, which can create asymmetry in the swash transport potential (Austin and Masselink, 2006).

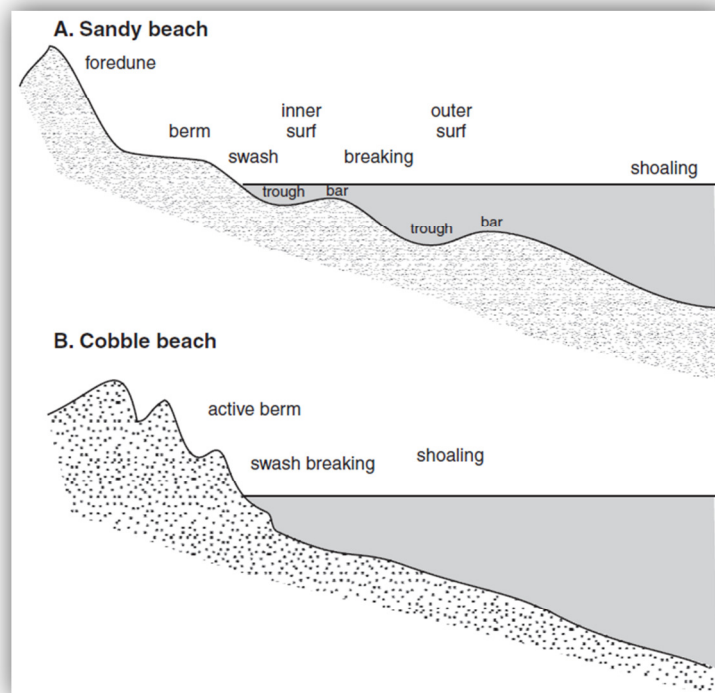


Figure 8: Typical differences in morphology characteristics between sandy and cobble beaches (Source: Davidson-Arnott, 2010).

5.1 Characteristics of Loe Bar

Loe Bar is very seldom overtopped by the sea and the high tide level is clearly marked in OS maps as not covering the bar. The situation here therefore shows a positive freeboard, where the crest height of the bar is higher than the run-up height of the waves, representing the morphology seen on the left side of figure 9. The amount of freeboard available is directly related to occurrences of overtopping (Orford et al, 2003), meaning that only the seaward side of the bar is affected by wave action, apart from on the rare occasions on which overtopping occurs.

A rise in sea level which is believed to occur in the future as a result of climate change will alter this relationship between the sea and the bar, reducing the available freeboard and changing the situation to resemble the scenarios further to the right side of figure 9. It will also however result in increased erosion of the adjacent cliffs which in turn will supply more material to the bar with the known trends in longshore drift, which may counter some of the effects of sea level rise.

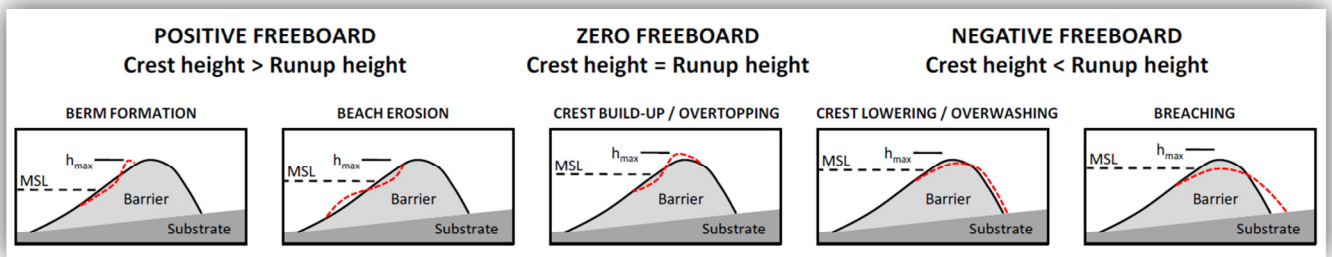


Figure 9: Effects of sea level in relation to bar height. The diagrams left to right show an increase in sea level and the associated effects on bar morphology. (Source: Coastal Processes Research Group, University of Plymouth, 2015).

At the rare occurrence of overtopping, material can be taken from the beach and carried over the crest of the bar, changing the morphology of both the bar and the beach, as demonstrated in figure 10. Surveys have been carried out by researchers at Plymouth University to monitor the effects that the storm has on the bar morphology. In 2014 the occurrence of a significant storm event showed a change in both the position and height of the crest of the bar (figure 11), as well as a notable movement of the lake-ward edge of the bar.

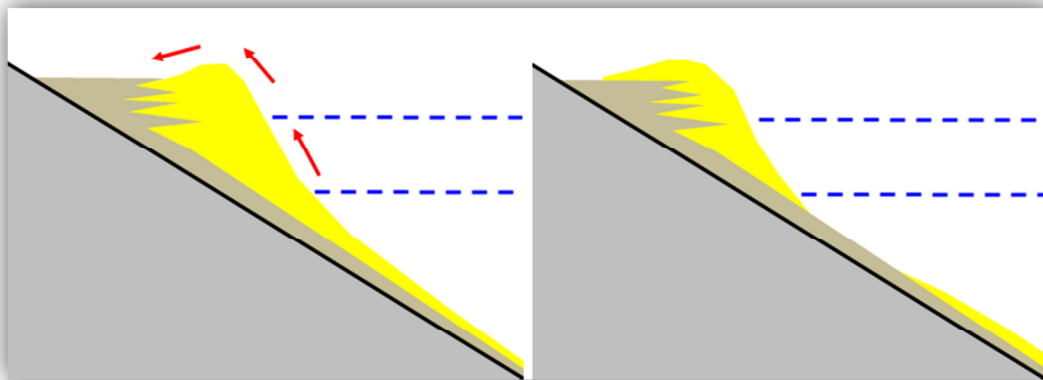


Figure 10: Over-wash during storms pushes sediment onshore and over the top of the barrier (left) where it will stay and not return to the beach (right) (Masselink, 2015).

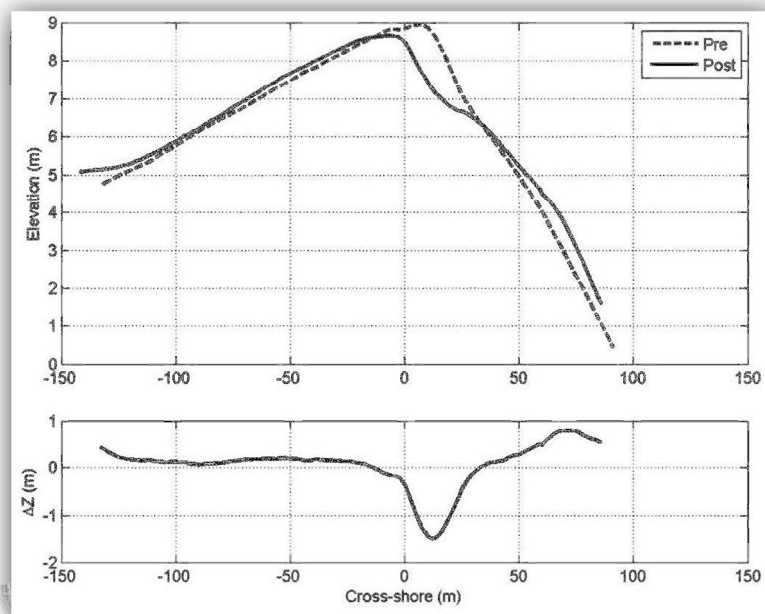


Figure 11: Diagram displaying results found from a pre- and post-storm survey at Loe Bar completed in February 2014 (note: vertical exaggeration) (Masselink, 2015). This can be compared to the diagrams in the left side of figure 9 above and the process demonstrated in figure 10.

Using topographic OS maps from recent years it is possible to see the effects of the storm which caused the landward movement of the lake border. The location of the landward side of the bar remained constant in maps published from June 2007 to December 2013. It is between December 2013 and May 2014 that the shift can be seen, with the landward side of the bar moving up to almost 25m in some areas, gaining around 4,052m² in area on the landward side (figures 12 and 13).



Figure 12: The amount of landward movement of the boundary between Loe Bar and Loe Pool going by OS maps produced in December 2013 and May 2014 (Base map: Edina Digimap).

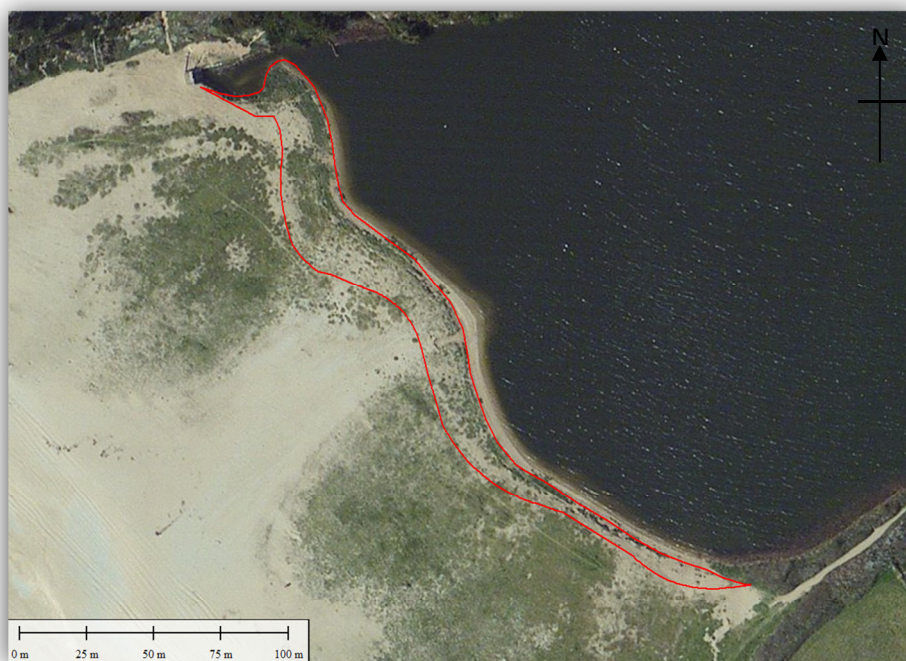


Figure 13: Satellite imagery of the Bar with the landward movement between December 2013 and May 2014 overlain. Note the visible break in vegetation (satellite image source: Global Mapper).

5.2 Comparisons to Loe Bar

5.2.1 Slapton Sands

The shingle bar at Slapton Sands encloses a freshwater lagoon, Slapton Ley. The location of this bay-bar differs greatly from that of Loe Bar with it being more sheltered from the dominant Atlantic wave systems, demonstrating very effectively the possibility for similar landforms to have developed in differing wave conditions. Another similarity between the two shingle bars is that the level lake or lagoon behind both of them is higher than that of the sea, making them appear perched (May and Hansom, 2003).

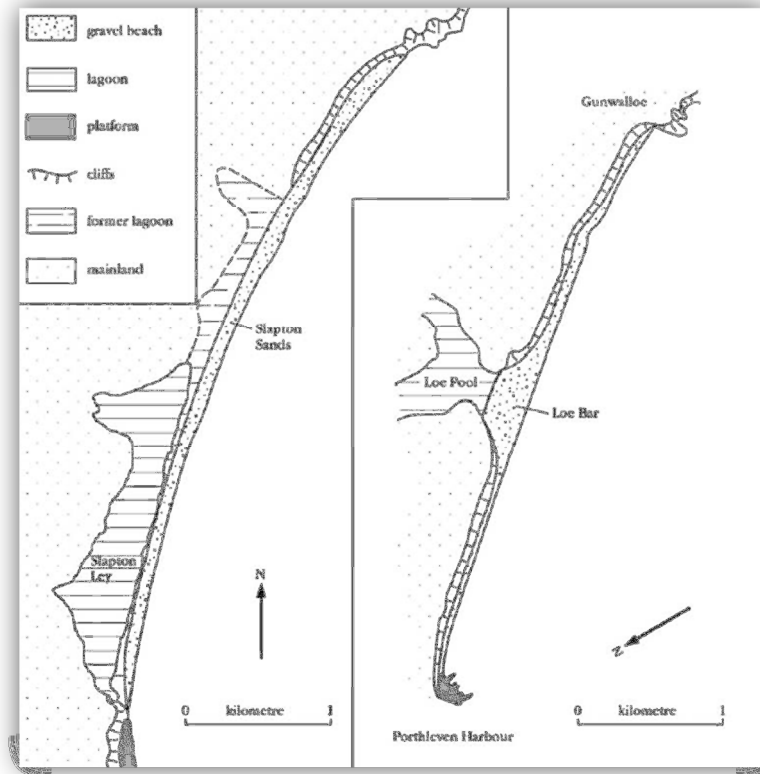


Figure 14: A comparison of geomorphological form between Slapton Sands, enclosing a large lagoon, and Loe Bar, blocking a narrow estuary (Source: May and Hansom, 2003).

5.2.2 Chesil Beach

Chesil Beach is significant in size, stretching more than 18km in length and 14m high. Its linear form consists of pebbles and cobble, backed by cliffs at its western end and a lagoon, 'The Fleet', to the east. The formation of Chesil Beach is a subject of debate, but is believed by Bray (1990) to be a result of the erosion of river gravels and other offshore sediments during a time in the Devensian when sea level was approximately 100m below its present position, and has since been maintained by longshore sediment transport. Other views suggest the early deposition of an original sand bar upon which a cobble ridge was later established as part of a two-phase development (May and Hansom, 2003).

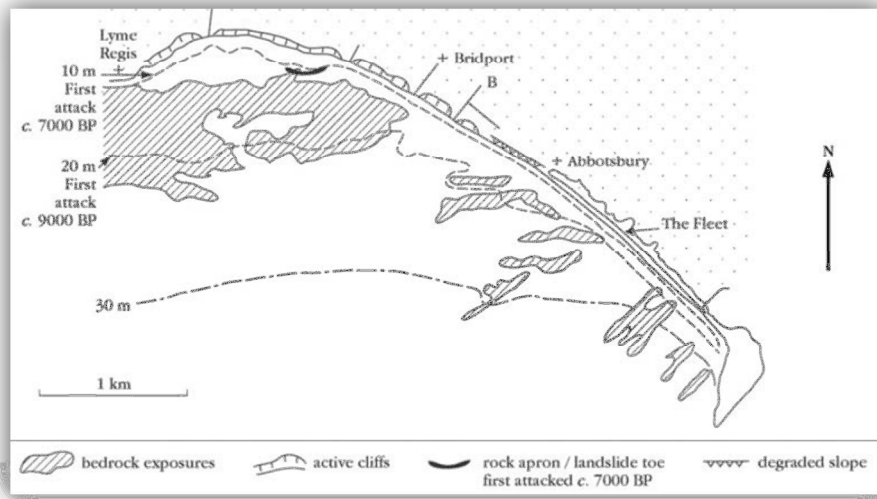


Figure 15: Chesil beach, showing the location in relation to the cliffs at the Western end and lagoon at Eastern end of the pebble bar. 'First attack' represents the location of shoreline first attacked at the dates shown (Source: May and Hansom, 2003).

6 Management of the Bar

6.1 Historical Management

Human intervention of the Bar has been prevalent in its history, with both sediment extraction and forced breaching taking place. The natural passage of water through the bar from the lake to the sea has been compromised by the mining which took place in the area during the eighteenth and nineteenth centuries, depositing large amounts of fine material into the Cober, consequently blocking pore spaces in the bar (Davies and Matthews, 2002).

6.1.1 Cutting of the bar

The level of Loe Pool has been linked to flood risks in Helston, with an increased risk posed when levels are high. This has historically resulted in management of the pool in the form of breaching the bar to release its water. The last time this was done was in November 1984 when, like on previous occasions, a trench was dug from the lake to the sea (figure 16). The location of this trench can still be seen today by the 'scarred' area in the central part of the bar, displaying a lack of vegetation in satellite images (visible in figure 17). The rapid sedimentation rate at the bar has always allowed the cut to close naturally. A series of photos taken in the years since the cut show the gradual recovery of the bar and are available in appendix A.



Figure 16: Photograph of the 'cut' being made to release water from Loe Pool to the sea in November 1984, looking southeast (Davies, 2012).

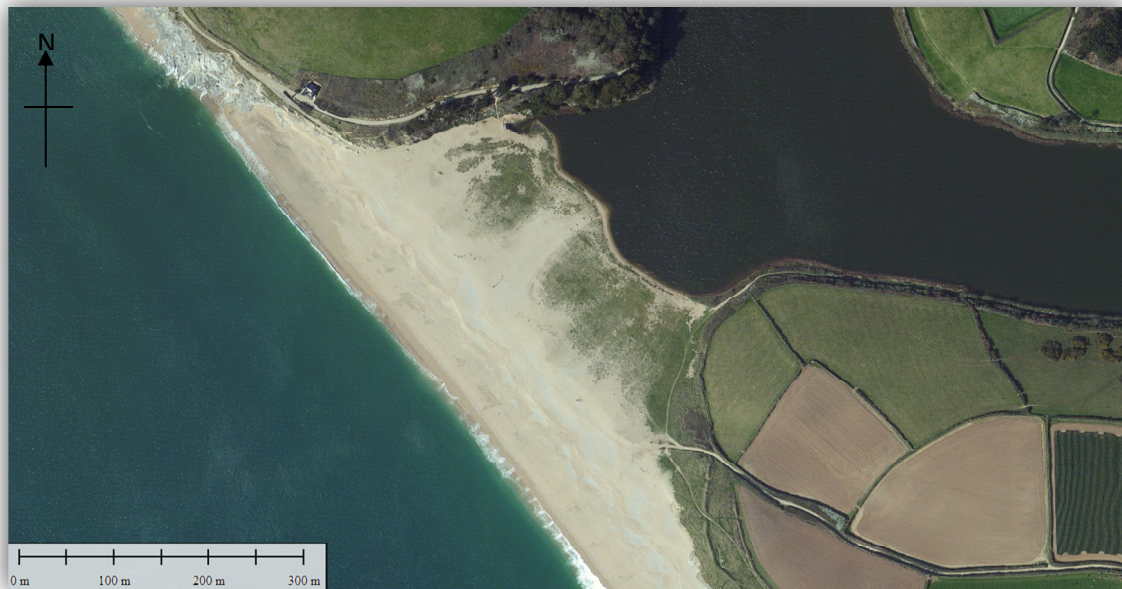


Figure 17: Satellite Image of Loe Bar. The lack of vegetation is visible in a linear NE-SW direction, caused by the cutting of the bar to let water out to the sea in November 1984 (Source: World Imagery, Global Mapper).

The bar is mentioned in accounts as early as that made by Leland's itinerary of 1535-1543, which describes a bar of sand impounding a freshwater lake, which can occasionally reach levels that will cause it to overflow (Coard, 1987). Artificial cutting of the bar is something which has reportedly been done many times throughout history. Traditionally, the Lord Mayor of Helston would apply for permission to cut the bar from the Lord of Penrose Manor, who would receive a dated leather purse containing three half-pennies, some of which are still in existence at Penrose House. Once permission was obtained, a channel was dug into the bar by the townsmen of Helston using shovels (Loe Pool Forum, 2015). The bar has never been helped in the process of resealing itself, rather always re-establishing itself through natural rates of sedimentation. Leland's Itinerary also mentions the presence of floods in Helston and the stopping of the mills, leading to the need to cut the bar and release the water. During the sixteenth century, the bar was cut several times due to these economic pressures and the process is thought to have been well established by the mid-18th century. Between 1848 and 1874, the bar was cut approximately every two to three years. During the cut, marine fauna were able to enter the lake before its resealing (Coard, 1987). Leland's itinerary also reports that with each cut, water in the lake became momentarily brackish and marine fish and shrimps have been known to enter. The lake has always returned to fresh water after each break, the speed of which being dependent on the amount of rainfall after the resealing of the bar (Loe Pool Forum, 2015).

The shape of the bar is believed to have been dictated by the frequency of the cuts taking place. When regular, it is likely that the growth of the bar was not prominent due to the removal of thousands of tonnes of shingle and sand taking place every time (Coard, 1987), leading to the indented profile seen in maps of the bar before 1900 (appendix B).

When the bar is cut a narrow channel is made with shovels or, in more recent times, a small digger. The volume and speed at which water leaves the lake causes the cut to be greatly widened. In 1865 an account of the breach described it as having become 'wider than a stone could be thrown across with a strong arm' (Davies and Matthews, 2002). The breach carried out in 1984 by South West Water is recorded to have evolved from being a small one metre wide opening in the evening to that which was sixty metres wide and 10 metres deep by the early hours of the next morning (Davies and Matthews, 2002). Rendel (1837) notes that the bathymetry of the sea at the location of the bar became greatly altered when compared to the rest of the coast due to the amount of

sand which is washed out to sea during each cut. The resealing of the bar is documented by Johns (1874) as sometimes taking many days, but is greatly accelerated in the event of a storm (Coard, 1987), giving an idea of how rapidly the bar closes after cutting.

Since the cutting of the bar was stopped in the late 1800s, a natural widening of the bar has taken place. The increasing width over time has led to a reduction in seepage from the lake to the sea as well as less breaching by waves. The deposition of fine mine waste material onto the landward side of the bar has also greatly contributed to the decrease in water seepage. In 1967 the Cornwall River Authority stated that no significant movement of water exists through the bar in either direction, a significant contrast to estimations by Rendel in 1837 claiming the volume of water seeping through to be approximately 198,000m³ per day (Coard, 1987). Rendel noted that the level of water in the pool greatly impacted the rate of water movement through the bar. At times when the lake was at a level of approximately six to eight feet above high water sea level, a drop of around four inches a day could be seen in the lake for several successive days. After accounting for the influx of the river, this reduction in the lake's volume was calculated to amount to seven million cubic feet of water exiting the lake through the bar in a 24 hour period (Rendel, 1837).

6.1.2 Creation of an Adit

In 1790, the miners at the nearby Castle Wary silver mine cut an adit taking water from the lake to the sea in order to prevent their mine workings from flooding. High sedimentation rates caused the adit to occasionally become blocked, until it was enlarged by Captain Rogers in 1887. This increased the flow of water passing through, helping to keep it free from blockage (Loe Pool Forum, 2015). Despite this, the adit was still prone to occasional blocking, one example of which was the tidal wave event of 1924, when the adit became completely covered with sand. Blockages such as this have led to the more recent occurrences of artificial cutting of the bar by South West Water both in 1979, when a minor channel was made after storms blocked the adit; and 1984, when the substantial size of the bar had again engulfed the adit, requiring a full-scale cut (Coard, 1987). In 1986 the adit was modified by the Water Authority, fitting a smooth concrete lining to improve the flow. The tunnel was also lengthened by 100m and the sluice gate upgraded to decrease its vulnerability from future storms. This now controls the level of the pool and has greatly reduced the fluctuation in lake level as well as the amount of flooding experienced by Helston.

The pool is mainly fed by the river Cober, which is responsible for 93% of the water supply, the rest of which is accounted for by two large streams, Penrose and Carminow (Coard, 1987). With the level of the lake being higher than that of the sea, the lake should remain freshwater given that overtopping of the bar even in large storms is exceptionally rare (Coard, 1987).

6.2 Present-Day Management of Loe Bar

In the late 1990s a Shoreline Management Plan (SMP) was put in place stating a 'hold the line' approach allocated to the coastline running from Porthleven to Gunwalloe, including Loe Bar (SMP2, 2011). This was reviewed in 2011, with a new SMP stating that a change in strategy would be implemented, using less engineering techniques and giving more of an emphasis to natural processes. The policy adopted for the seaward shore of Loe Bar was changed to 'managed retreat' and the adjacent headlands changed to 'no active intervention'. This latest approach to the management of the coastline here may lead to an increase in the erosion of the headlands, providing more material to the bar. As previously discussed, combining this with rising sea level and increasing occurrences of storms may lead to further landward migration of the bar (SMP2, 2011).

In 2013 a report was issued by the Environment Agency, detailing a list of options for measures which could be put in place to reduce flood risk to Helston from the River Cober. A total of sixteen options were considered, including do nothing, upstream storage, and the dredging of Loe Pool in order to increase its capacity. Five of the proposed options involved making changes at Loe Bar, and are listed below (Northey et al, 2013) although it is uncertain whether any of these will be acted upon:

- I. Emergency breach of Loe Bar when required at the section already scarred by previous cuts (five day flood warning required).
- II. Creation of a concrete, stepped spillway structure in the scarred area to take water over the bar when the tunnel was at full capacity.
- III. Creating a new tunnel adjacent to the existing tunnel to provide additional discharge when required as an alternative to pumping.
- IV. Improving the hydraulic performance and discharge capacity of the existing tunnel, by means such as using a spray lining and modifying the recent extension.
- V. Abandoning the existing tunnel and constructing a new one with larger discharge capacity, either adjacent to the current tunnel or at the southern end of the bar, eliminating the need for pumping.

7 Changing Morphology of the Bar

When the bar was cut in 1979, its internal structure was noted as being comprised of banded coarse shingle. These layers are thought to be representative of how the bar has built up and become increasingly stabilised over time, with episodes of construction predominantly taking place during storms (King, 1972).

The cut made in 1984 involved a much deeper channel than was dug in 1979, involving the use of mechanical excavators. During the creation of this cut large amounts of red clay were witnessed within the landward side of the bar's structure, potentially providing evidence for deposition of fine mine waste material responsible for the significant reduction in seepage of water through the bar (Coard, 1987).

Historical OS maps dating from 1878 to present day show clear widening of the bar over time since 1878 (figure 18). The seaward side has remained relatively constant, yet the landward side has notably moved inland by a considerable amount. Despite the bar being cut in 1984, a clear recovery has been made, with the present day lake line being further inland than it was seen to be in historical maps published in 1978-1981, before the cut was made. This implies that the cut did not greatly affect the growth of the bar and that in order to have an effect on its width, a significant frequency of cuts would be required. With no more, or at least very seldom, cutting taking place, the bar has been able to return to its natural rate of growth through onshore deposition (Loe Pool Forum, 2015). Whilst OS maps are subject to a degree of error, a confident representation of how the bar used to be in the past is determinable from the information available.

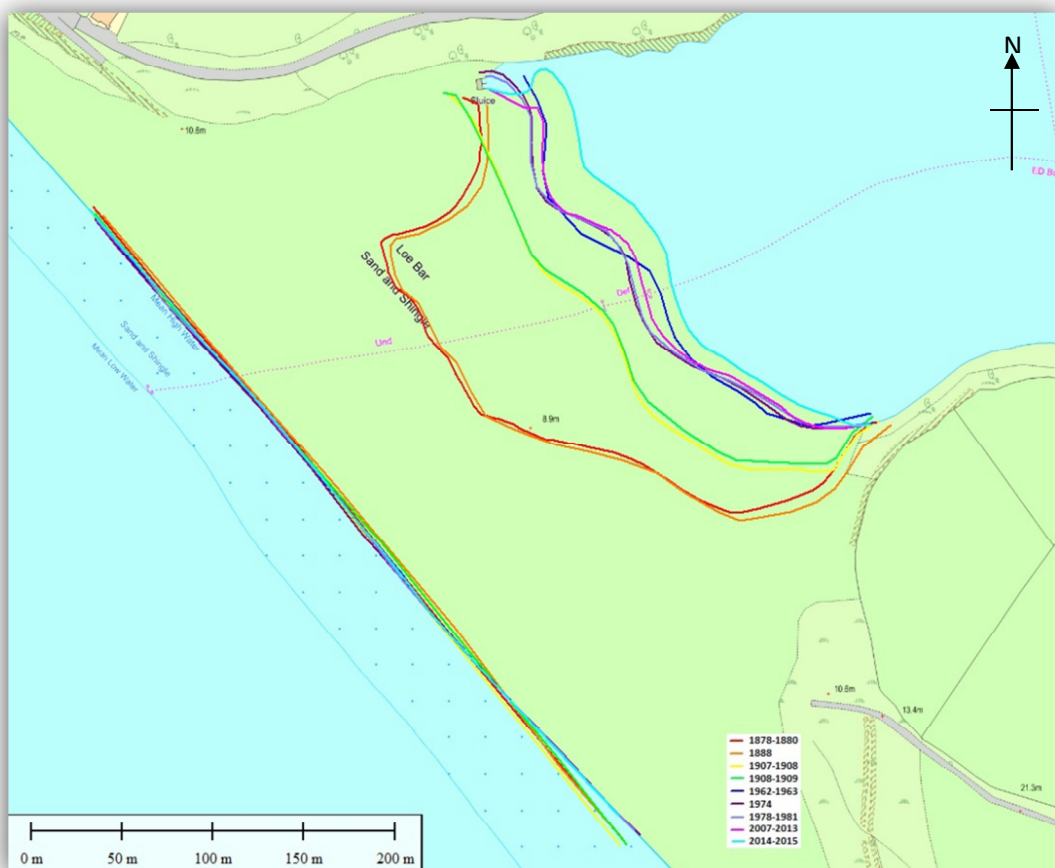


Figure 18: Changes in morphology of Loe Bar at various intervals between 1878 and present day (Source: Edina Digimap Historical & Mastermap data).

7.1 Chronological profiles of the Loe Bar

Chronological profiles of the growth of the bar towards the lake allow an idea of the speed of growth at times since 1878. No readily available data exists prior to 1878, making the morphology of the bar before such prolific human interaction and management unknown. Figure 19 shows the migrating edge of where the lake meets the bar and the locations of five profiles created, to show chronological changes in width. The profiles are represented in figures 20 (a to e). Zero thickness on each scale has been started at the western-most point of time where the sea meets the bar for that profile.

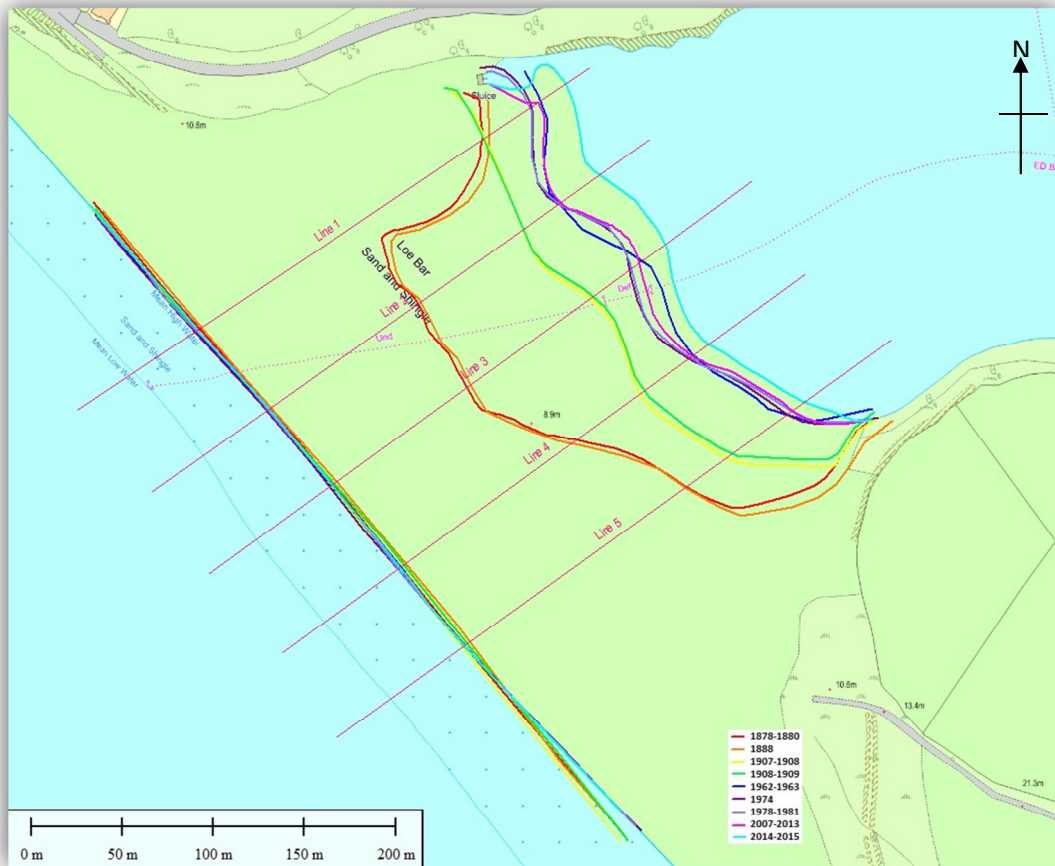


Figure 19: Changes in morphology of Loe Bar. Lines 1 to 5 represent chronological profiles shown in figure 20 a to e.

Line 1 shows the least amount of movement during the time represented, whereas lines 2 and 3 show a rapid widening of the bar between 1878 and 1907, with the sand travelling around 75m in the direction of the lake. Profiles 4 and 5 show approximately a 50m expansion towards the lake between 1888 and 1907, after a small seaward movement which took place in the 10 years prior to this.

A period of steady growth is seen in all profiles from 1908 to 1963, before a brief seaward movement between 1963 and 1974. From 1974 to 2013 the centre of the bar has remained relatively constant in profiles 1 to 4, only moving lake-wards by a maximum of approximately 5m, while line 5 shows a growth of 25m in the same period of time.

The effects of the February 2014 storm are evident in every profile, with the greatest lake-ward movement of 25.8m taking place at the location of line 2. Storm events such as the one which occurred in 2014 provide evidence that growth of the bar tends to occur in sudden events rather than gradual slow growth. These chronological profiles are therefore somewhat misrepresentative of the probable true growth of the bar, which is likely to be more sudden and sporadic moments of growth, rather than the steady rate implied.

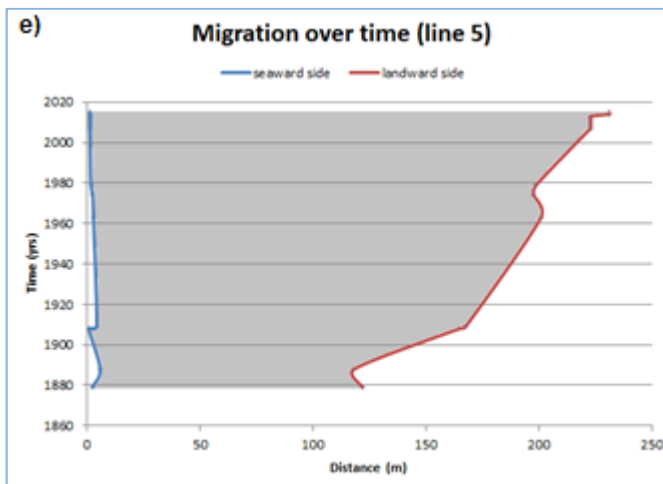
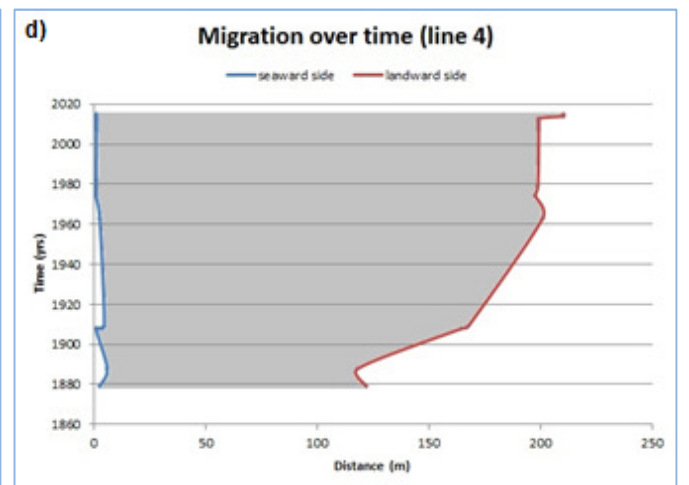
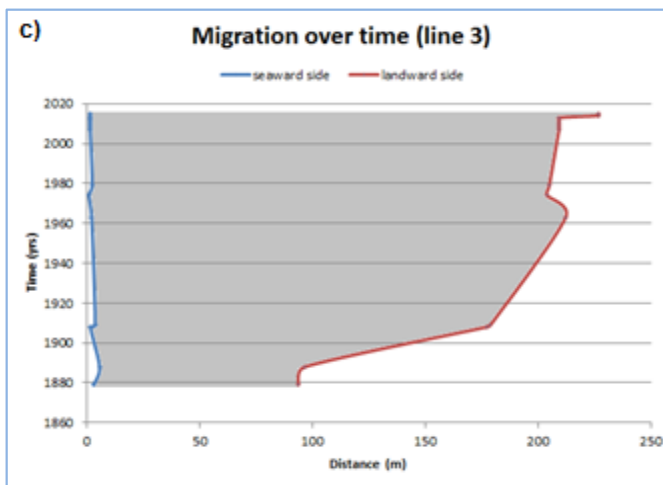
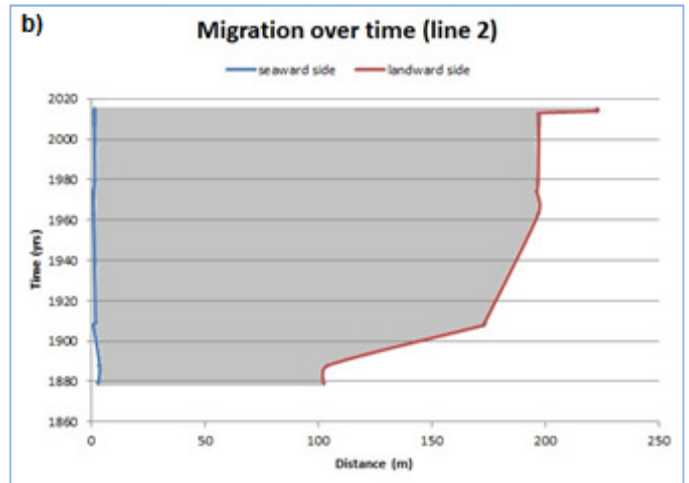
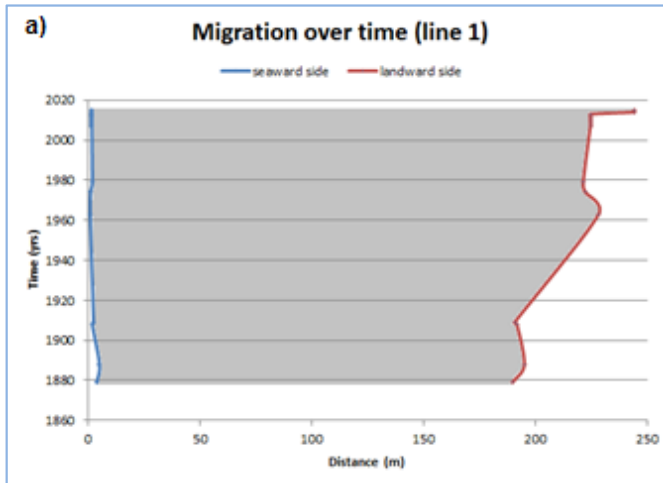


Figure 20 (a to e): Profiles showing the change in thickness at 5 sections on the bar from 1887 to present day. Lines are represented in figure 19 (source : Digimap Historical Mapping).

8 Port Proposals for Loe Bar in 1837

In 1837 plans were drawn by engineer J.M. Rendel to assess the viability of developing Loe Pool into a harbour. Plans included the construction of piers through the bar and two dams across Loe Pool and Carminow Creek (figure 21) (Rendel, 1837). Locations were proposed for the construction of the piers, the eastern one to be built using the Clijer rocks at Carminow Point to build from and the western one designed to shelter the harbour from the prevailing southwest winds as well as the sea. The opening between these two piers was planned to be 1,150 feet (approx. 300m), which would enable vessels to enter under limited wind conditions as well as eliminating the possibility of closure by means of sediment build-up. Once removed, it was believed the prevailing onshore winds would keep the gravel from returning to the opening. The harbour itself would be kept clear from sedimentation by the undertow of returning waves, believed to be more sufficient in stronger winds and resulting in equilibrium (Rendel, 1837).

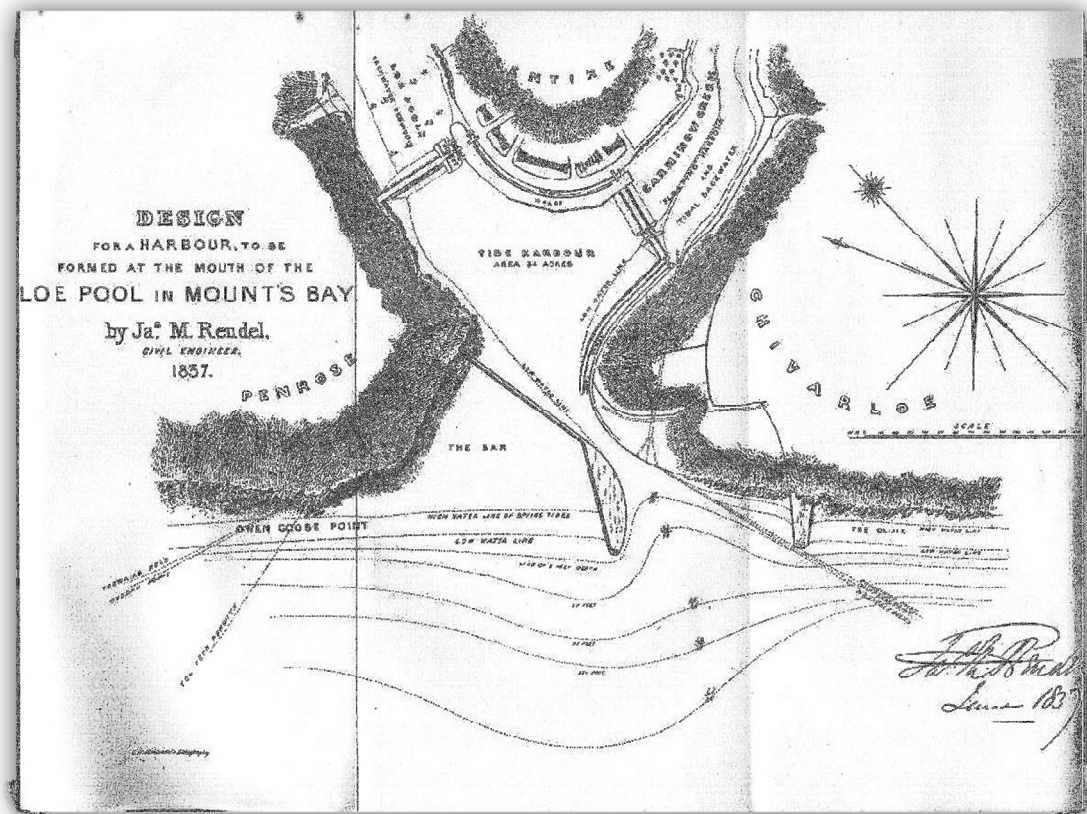


Figure 21: Plan of proposed design for a harbour to be built at the mouth of Loe Pool, Loe Bar (Rendel, 1837).

With the bar being composed of sand to a considerable depth, construction of the piers using stone was seen to be impracticable, leading instead to the proposal that they should be built using a double row of very strong piling with a concrete fill to a depth of two feet below the low water level. This design was believed to provide better stability, and all concrete used on site was to be made using the gravel and sand on the bar. The piling was expected to last around 50 years, by which time the concrete was thought to be ready to stand on its own without support. Previous success of this technique had been seen on gravel beaches at Brighton and Woolwich in the years before the proposal of this harbour (Rendel, 1837).

The dams which were to be formed, both across Loe Pool and Carminow Creek, would be able to open for letting in the tide and the passing through of vessels. Loe Pool would be kept at a level of around ten feet above the high water mark and a canal 12 feet deep would be dug to allow vessels of three hundred tons burthen to pass through to Helston, regardless of tide, along with a basin made at the head of the Canal, for which a number of eligible sites were identified. It was believed that the ability for large vessels to travel to Helston would provide a

huge advantage to the town and in particular to its businesses as well as playing a large part in trade coming to the English Channel. In turn, this anticipation was expected to provide capital and investment in the harbour. The locks would also provide a place for vessels to rest, with larger vessels being able to enter Loe Pool and smaller ones in the more tidal Carminow Creek (Rendel, 1837). The construction of buildings around the harbour was expected and suitable land suggested, with North Pentire Point being identified as a possibility and shipwright's yards suggested to be cut into the shores of Carminow Creek. The elevated level of Loe Pool was thought to have a potentially positive effect on the fish found and the beauty of the lake, however the construction of the harbour and its associated likely building in the area would have had an impact on the Privacy of the Penrose Estate despite endeavours by Rendel in his decision to keep particularly the more busy sections of the harbour away from the grounds of Penrose (Rendel, 1837).

During the initial investigation to gain information about the geomorphology of the bar and devise a sufficient design for the harbour, a number of bores were completed in the area. Several of these were carried out on the bar and results recorded by James Rendel, who's findings are summarised in table 1.

Boring	Location	Depth	Findings
A	450 ft (137m) from the foot of the western shore	68 ft (21m)	Coarser material nearer the surface, becoming finer with depth. Several fine and coarse beds were cut through. At 50 ft (15m) depth a layer of fine silt was seen.
B	400 ft (122m) from the opposite shore	51 ft (15.5m)	Layer of fine silt at 20 ft (6m), resting on a layer of fine sand.
C	100 ft (30.4m) from Carminow Point	Unknown	Fine sand resting on killas at a depth of 37 ft (11m)
D	200 ft (61m) nearer the sea than the last	Unknown	Rock is 4 ft (1.2m) below the level of low water and is covered with a floor of hard quartz, impenetrable to the boring tools.
E	The same distance from Carminow Point, near the water line of the Pool	22 ft (6.7m)	Rock at the bottom is 2 ft (60cm) under low water.
F, G and H	A direct line across the bar in the Weeth Green	Unknown	First 15 ft (4.5m) saw alternate layers of mud and sand and several rotten trees. A layer of granite sand about 18 inches (45cm) covered the surface of the killas which was 28 ft (8.5m) below the surface.

Table 1: Borehole findings observed by James Rendel, published in his report of 1837.

9 Shipwrecks at Loe Bar

The Cornish coast has been host to many ship wrecks in its history, with the coast From Gunwalloe to Porthleven seeing a large share. To the South of the Bar along the cliff stands a white cross, erected as a memorial to all who lost their lives on this stretch of coast. The main hazard associated with Mount's Bay is the sudden change in wind encountered by sailors as they exit the sheltered channels and find themselves pushed into the bay by the strong South Westerly winds. The main wrecks are recorded by Larn and Carter (1969) and are listed in table 2 below. Over 120 ships are said to be wrecked on Loe Bar alone (Spalding, 2015) and many more across Mount's Bay. Many other shipwrecks are also well documented by Treglown (2011).

From the late 1870s, a decrease occurred in the number of wrecks in the Mount's Bay area. This was due to a combinations of efforts, such as the new Wolf Rock lighthouse and improvements to those at the Lizard along with developments also made to Longships, and the decline of certain types of sailing ship.

Date		Wreckage
1782	Winter	A winter's gale saw the brig <i>Maria Elizabeth</i> , laden with wine and fruit lost below Predannack Head and the ship <i>Torrington</i> , carrying wines, run aground at Loe Bar.
1802	18 th May	A large French mackerel boat drove ashore during a heavy south-westerly gale, losing eight members of her crew. The remaining six were put up in lodgings at the Fishmonger's Arms by Mr John Rogers of Penrose.
1807	29 th December	<i>HMS Anson</i> , a 44-gun fifth-rater, was towed out of Falmouth Roads on Christmas Eve of 1807, yet forty-eight hours later a storm was spotted, forcing Captain Lydiard to take bracing measures. The ship rode safely until dawn of the following morning when her cables parted and Captain Lydiard ordered a helmsman to run her ashore. As she breached, the mainmast fell to the sand, acting as a bridge by which many were able to escape, yet still 120 lives were lost, including the captain, who died trying to save a young boy. He was later interred with military honours at Falmouth. The ship was very well salvaged with many dives taking place in the late 19 th century. In 1905 a large cannon was raised and many others in the years that followed. A large bell also found is reputed to have been from the <i>Anson</i> . In 1964, Naval divers found and recovered the brass pintle and rubber supports and two iron cannons, the larger of which can now be found sitting outside Helton museum. Nine or ten cannons are still believed to be located under the sand.
1808	6 th April	The wreckage of the Hamburg ship <i>Herman and August</i> carrying wine at Loe Bar during a southwest gale.
1809	6 th January	The 110-ton brig <i>Royal Recovery</i> destroyed on Loe Bar and little over a month later the big sloop <i>Mars</i> came ashore close by.
1809	16 th November	The Scots sloop <i>Clio</i> carrying barilla and a Spanish brig laden with wine were also lost on Loe Bar.
1815	24 th October	A French sloop carrying wine lost on Loe Bar. Her crew all had a lucky escape.
1817	24 th January	Captain Guillème and eleven sailors perished when <i>L'Hameçon</i> carrying wine struck the bar during a westerly gale.
1819	11 th December	The brig <i>Montreal Packet</i> , carrying nuts, was embayed and driven onto Loe Bar. The crew were swept out to sea.
1826	5 th February	The ketch <i>Ida</i> , carrying oranges was wrecked on the western end of Loe Bar. A daring

		rescue by Frederick Rogers of Penrose saved the captain and mate, but the rest of the crew, including the mates two sons were swept overboard. Rescues such as this by local men became increasingly frequent in subsequent shipwrecks, with medals awarded by the RNLI for daring rescues carried out.
1833	7 th February	The crew of the 47-ton Scilly Isles schooner <i>John and Mary</i> were dragged ashore when the ship struck Loe Bar.
1859	7 th November	The largest sailing vessel to be wrecked on Loe Bar, the 1,894-ton wooden full-rigger <i>Chincas</i> laden with 3,000 tons of cannel coal and bound for Rio de Janeiro encountered the Royal Charter storm and was driven into Mount's Bay, where she was anchored off Loe Bar until cables parted and the ship was in the surf. A group of rescuers were on the beach, intercepting the sailors who ran to them at each wave, yet despite their efforts, 8 or 9 men were swept away and drowned. The ship's cargo of coal was eagerly collected by villagers, whose fires were well stocked that winter. Pieces of the coal are still believed to be found on the bar.
1874	22 nd September	A French schooner the <i>Seudre que Tremblade</i> laden with pitwood was wrecked at Loe Bar during a SSW gale.
1877	22 nd April	The Dutch galliot <i>Margaretha Hellegina</i> carrying beans was beached on Loe Bar, breaking apart.
1912	26 th December	The 2,297-ton steamer, <i>Tripolitania</i> of Genoa was caught in bad WSW winds, scraping past Land's end. Knowing the ship was doomed, Captain Reppito beached her on Loe Bar. The crew threw ropes down and of the twenty eight men who climbed down, only one was swept away. The Tripolitania was swept further up the sands in the days that followed, yet suffered little damage and work began to re-float her. After months of digging, a south-west gale on 4 th November along with a high spring tide undid all the work that had been done towards saving the ship. Furthermore, the ship had been pushed another 300 yards inland by the storm and was settled even deeper into the sand. Over the next two years she was broken up where she lay.

Table 2: Wreckages at Loe Bar recorded by Larn and Carter (1969).

9.1 Loe Bar at War

During the Second World War, a number of sites around the UK were designated as possible amphibious landing sites for enemy ships. Loe Bar was named as one of these sites and a series of defences were put in place. The only visible evidence of this today is the type 24 pillbox on the cliffs to the North of the Bar heading towards Porthleven, however during the time of the war, the bar is said to have been covered in obstacles from convoluted scaffolding and barbed wire to mines and gun emplacements (English Heritage, 2015). Many of these defences are said to be still there and occasionally visible when the shingle is disturbed by storms (Spalding, 2015).

10 Mining History of the local area

Although the area has a history of being mined for many centuries, it is within the 18th and 19th centuries that the mines were of a significant scale, mainly dealing in tin. In the last 150 years, over 30 mines are known to have been in operation within the catchment boundary of the River Cober (figures 22 to 24), with the river being used as a means of both transportation and disposal of mining waste. The sediment from the mine was transported downstream, to settle in Loe Pool, resulting in the presence of haematite (Fe_2O_3) and tin (Sn) laminations in the lake bed sediments (Roberts, 1998).

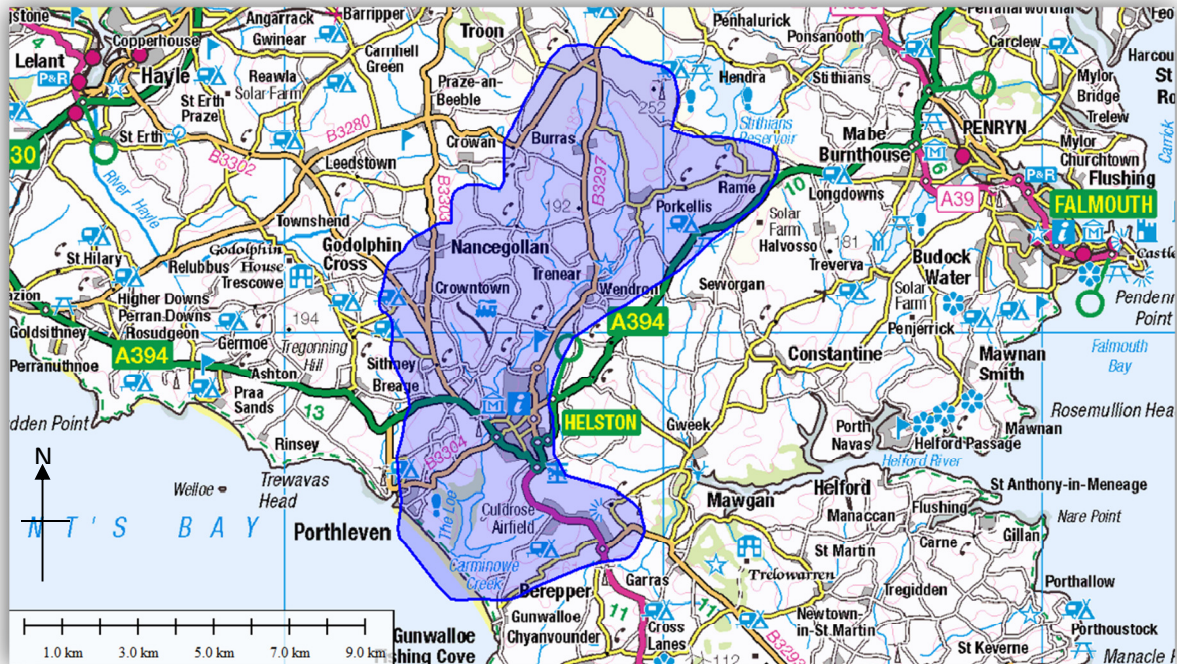


Figure 22: Catchment area of the River Cober (Base map: Edina Digimap, information source: loepool.org)

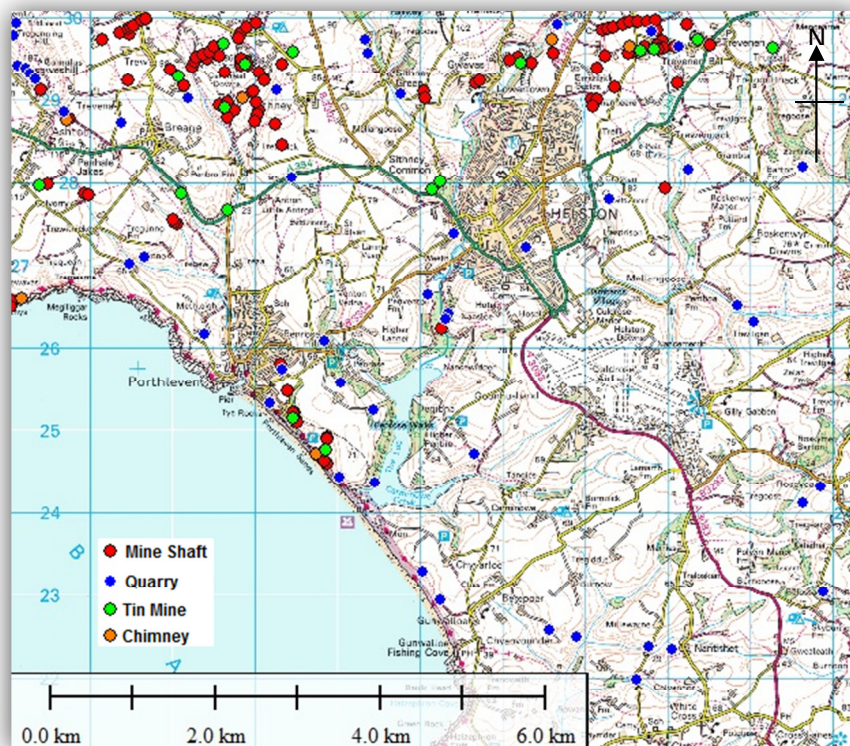


Figure 23: Mine features in the area surrounding the Loe, mainly dating from the 18th and 19th Centuries (Source: historical maps, Digimap).



Figure 24: Closer look at the locations of mine features in the area surrounding the Loe (source: historical maps, Digimap).

This abundant sediment was of some concern, given the difference it made in reducing the capacity of the lake and likelihood of increased flooding in Helston. A study into the sediment at the bottom of the lake (figure 25) suggested that the top 3m was most likely deposited after 1820, implying a rapid sedimentation rate in the time during which mining was prominent in the area (O'Sullivan et al, 1982).

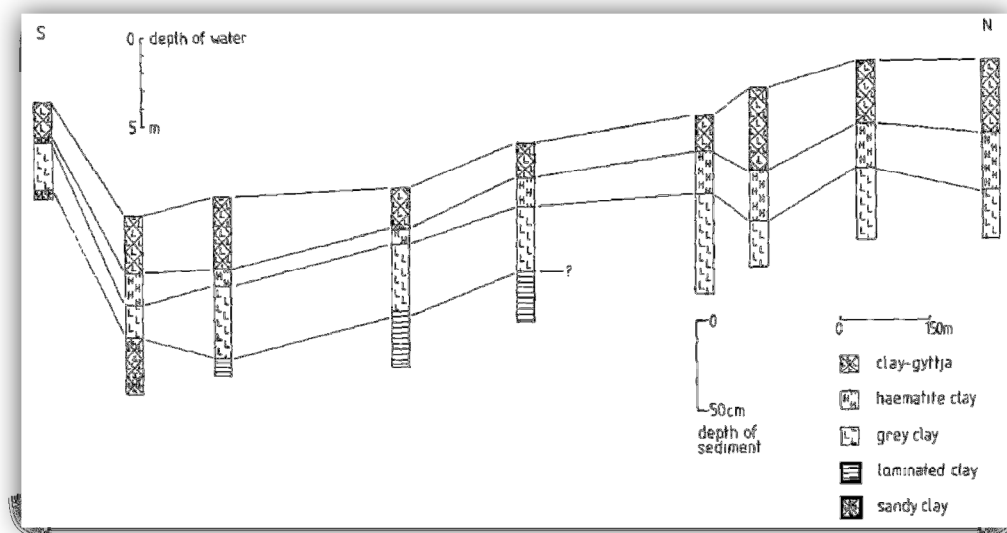


Figure 25: Generalised North-South section of the top few metres of sediments in Loe Pool (O'Sullivan et al, 1982).

At times when the bar has been broken to reduce the level of the lake, it is believed that quantities of the mine waste material can be seen flowing out to sea. Some records describe the Cober as having had a reddish tint and also tell of large plumes of discoloured water entering the sea at times when the bar was cut. Sediment in the river was found to contain workable quantities of tin, which was exploited by the Helston Valley Tin Company Ltd between 1914 and 1918, putting the sediment through processing works on the eastern side of the valley (Coard, 1987).

Porkellis, the last mine to cease operation in the Cober catchment, finished producing tin in 1938. Since then, the sedimentation rates in Loe Pool have greatly decreased (table 3), despite two major events which could have increased the rate of sedimentation being carried to the pool by the Cober – those being the canalisation of the river's lower reaches in 1946 and the construction of a road approximately 2km upstream from the pool in 1968, from which a large amount of sediment is believed to have been deposited into the river (C.R.A., 1946; Coard, 1987).

Date	Activity	Rates of erosion ($\text{t km}^{-2}\text{y}^{-1}$)
1860-1920	Mining and Agriculture	174
1930-1936	Intensive Mining and Agriculture	421
1937-1938	Intensive Mining and Agriculture	361
1938-1981	Agriculture	12

Table 3: Rates of erosion in the catchment area of the River Cober as determined from lake sedimentation rates (O'Sullivan et al, 1982).

11 Existing Survey Data of Loe Bar

11.1 TELLUS LiDAR

A LiDAR system consists of three main components: a laser range finder, GNSS receiver and an internal navigation system, all of which are built into a fixed wing aircraft or helicopter (Uren and Price, 2010). A LiDAR (Light Detection and Ranging) survey was carried out in the South West of England by the British Antarctic Survey (BAS) as part of the TELLUS project funded by the National Environment Research Council (NERC) (Ferraccioli et al, 2014). The area covered by the LiDAR measured around 9,424 km² which includes all the land to the west of Exmouth. The LiDAR data produces a Digital Terrain Model (DTM), representing a topographic model of the earth as it is seen from the sky. Data was collected on 17th March 2014 in 1 km blocks and published on 29th April of the same year. The data is available to the public, with the capability to be loaded into GIS software.

The results can be displayed in a number of ways with features such as contour lines generated from them to give a clear indication of elevation (figure 26). In the case of Loe Bar, contours show its characteristics as being a gentler slope on the landward side than that of the seaward side and a distinct feature where the last cut was made in 1984. Here a depression is seen to occur in the elevated parts of the bar towards the crest, which evolves into a risen channel towards the lower areas of the bar near the lake. The lack of vegetation in this area and consequent instability of sediment may be causing material in this section to be blown towards the lake by the prevailing winds approaching the bar from the south west.

It must be taken into account that where vegetation occurs, the LiDAR is unable to penetrate to the ground beneath, leading to a potential inaccuracy in height data in these areas.

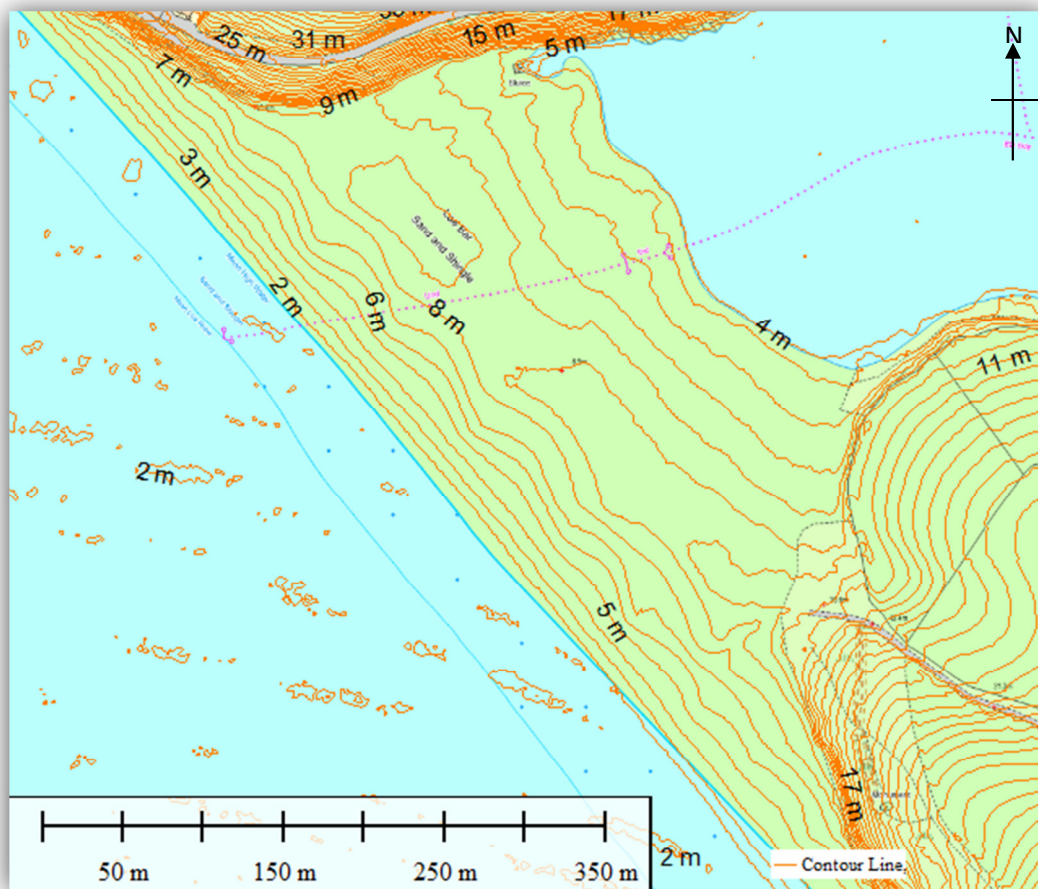


Figure 26: Loe Bar topography represented in contour lines generated in Global Mapper from LiDAR data taken by Ferraccioli et al in 2014.

GIS can also be used to look at the direction of the slope detected by the LiDAR data. In this case, figure 27 shows a distinct change in slope direction running NW-SE. This can be used to approximate the position of the crest along the bar, as is displayed.

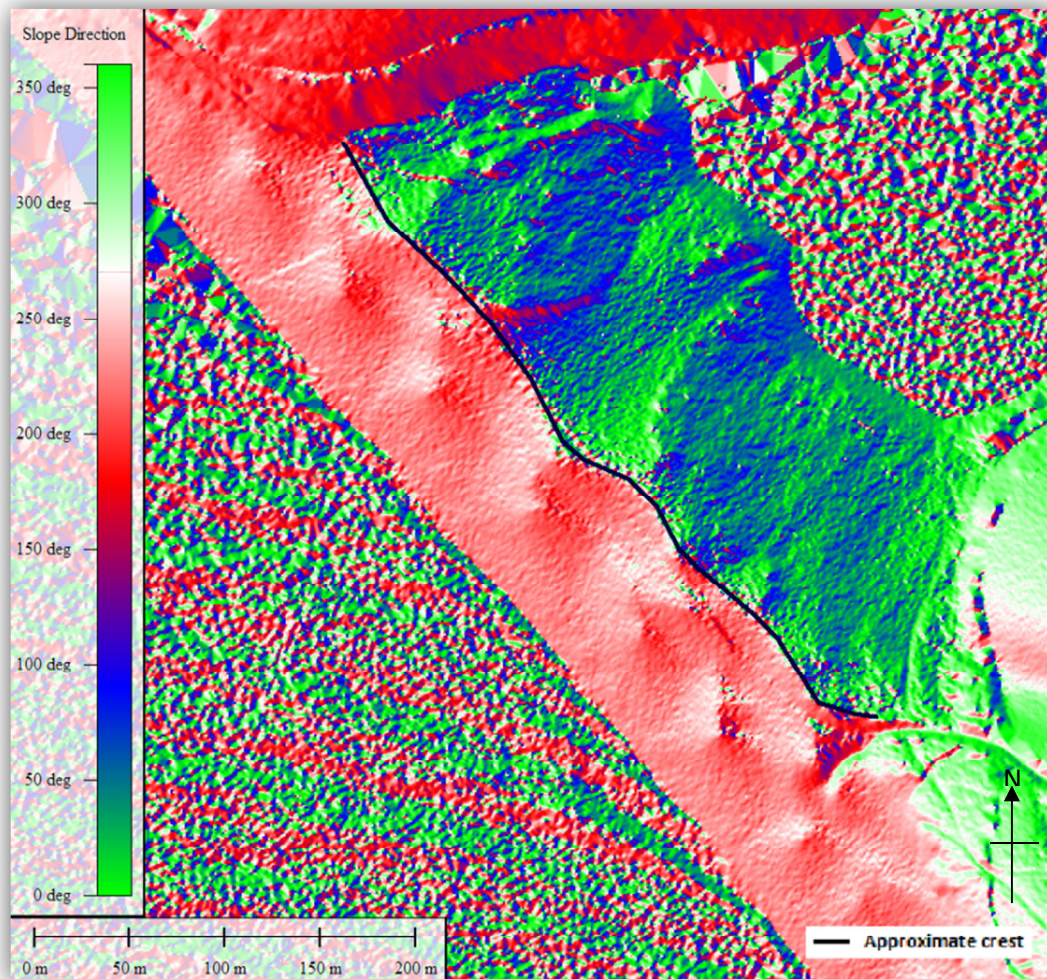


Figure 27: Slope direction of the bar enabling the distinction of the approximate location of the crest of the bar as marked (Source: Ferraccioli et al, 2014).

Another possibility with the use of GIS, is to display the LiDAR data using the gradient of slope. Figure 28 shows areas of steep gradients as dark and vice versa. Displaying the data like this can show a vast amount of detail regarding the morphology of the bar. The area of the cut carried out in 1984 is easy to see, and with the aid of 3D visualisation the bar can be seen in its context with the surrounding cliffs as well as showing clear differences between the landward and seaward sides of the bar (figures 29 and 30).

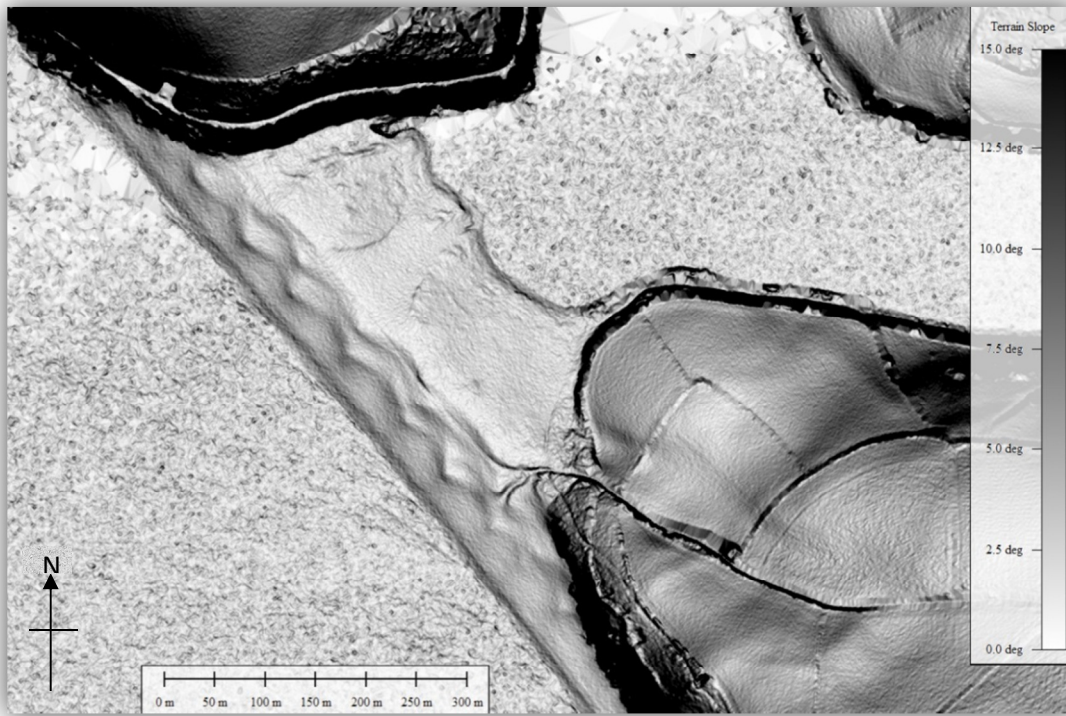


Figure 28: View of Loe Bar in Global Mapper's 'slope shader view', showing slope characteristics and morphological features (Source: Ferraccioli et al, 2014).

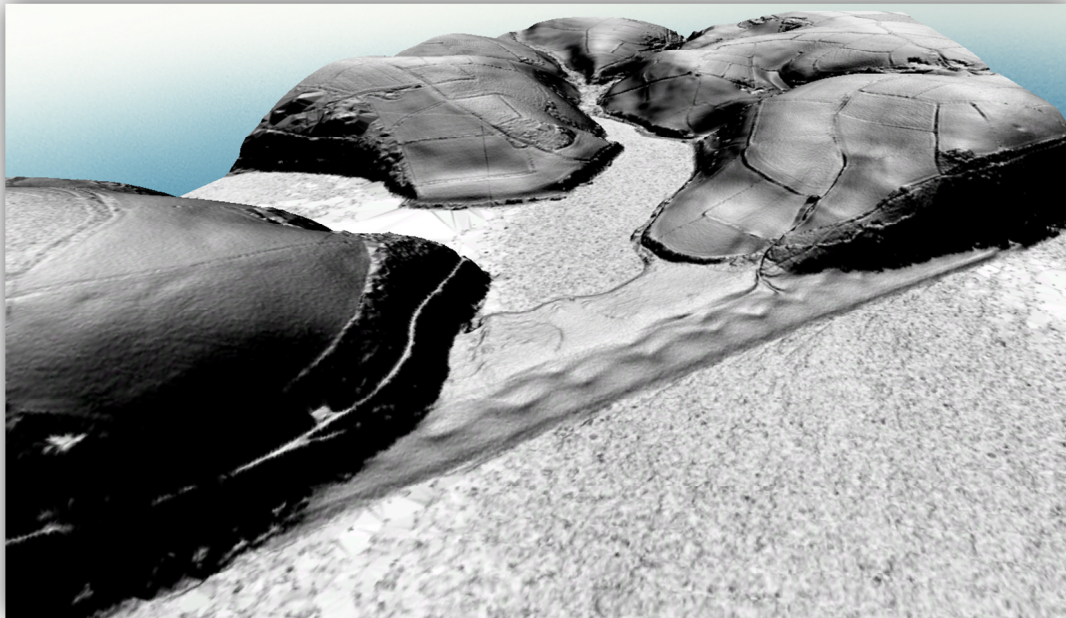


Figure 29: 3Dview of Loe Bar and surrounding area using LiDAR data from TELLUS, looking approximately east (vertical exaggeration: 1.2500, Source: Ferraccioli et al, 2014).

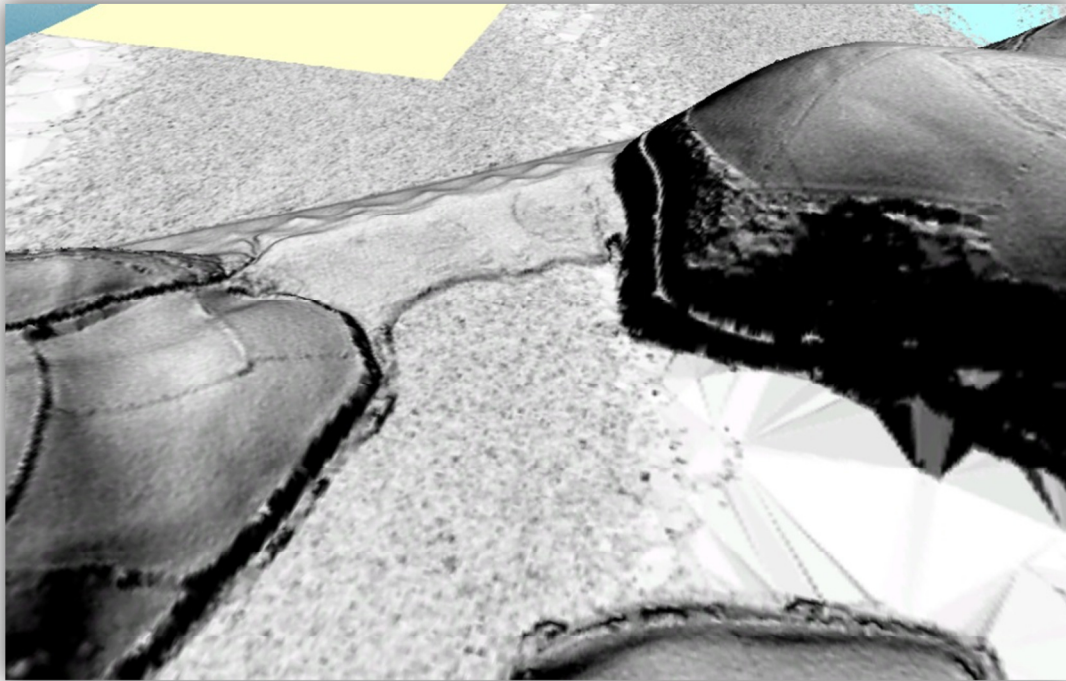


Figure 30: 3D view of the TELLUS LiDAR data showing the lake-ward edge of the bar, looking west (vertical exaggeration: 1.2500, source: Ferraccioli et al, 2014).

11.1.1 Advantages and Disadvantages of LiDAR

Accuracy of the survey was calculated by using the Root Mean Square Error (RSME) to compare the coordinates of 74 ground survey stations to the points collected by the LiDAR. The RMSE value was found to be 0.095 which equates to approximately 9.5cm accuracy (Gerard, 2014). While this is well within the 25cm zone of acceptance set for the survey and seems impressive for the rapid data collection, a higher level of accuracy can be achieved using simpler methods which focus on a smaller area, such as a total station. As a general overview of the morphology of a feature like Loe Bar and its surroundings, extracting pieces of information from the LiDAR survey can be beneficial, however conducting the survey is expensive and seldom carried out.

11.2 Laser scanning

Loe Bar has been the locality for a number of studies observing how morphology of gravel bars changes during a storm. Almeida et al (2014, 2013) mounted a 2D laser scanner atop an aluminium tower, 5.2 m in height, which was fixed to a scaffold frame inserted into the beach at around the high tide run-up level, stabilised with guy ropes (figure 31). The laser scanner covered approximately 90 m of the beach in cross section, showing an average horizontal resolution of around 6 cm, with values of 20cm to 1m at the far reaches of the data collection zone, due to the undesirable angles of incidence. A compromise had to be made between the area reached by the laser scanner and the resolution of the data by deciding on an appropriate height for the tower. Lowering the instrument would increase the clarity, yet would greatly reduce the data coverage (Almeida et al (2014).

This method is effective for measuring a 2D profile over a short period of time and has provided a clear and valuable insight into the movement of material on the seaward side of Loe Bar in response to wave motion. For the purpose of monitoring gradual changes of the shape of the bar however this would be an unsuitable technique, given the amount of data points which would be collected by the laser scanner and the number of set ups that would be required in order to achieve sufficient accuracy, given the unsuitable ground morphology for the angle of incidence.

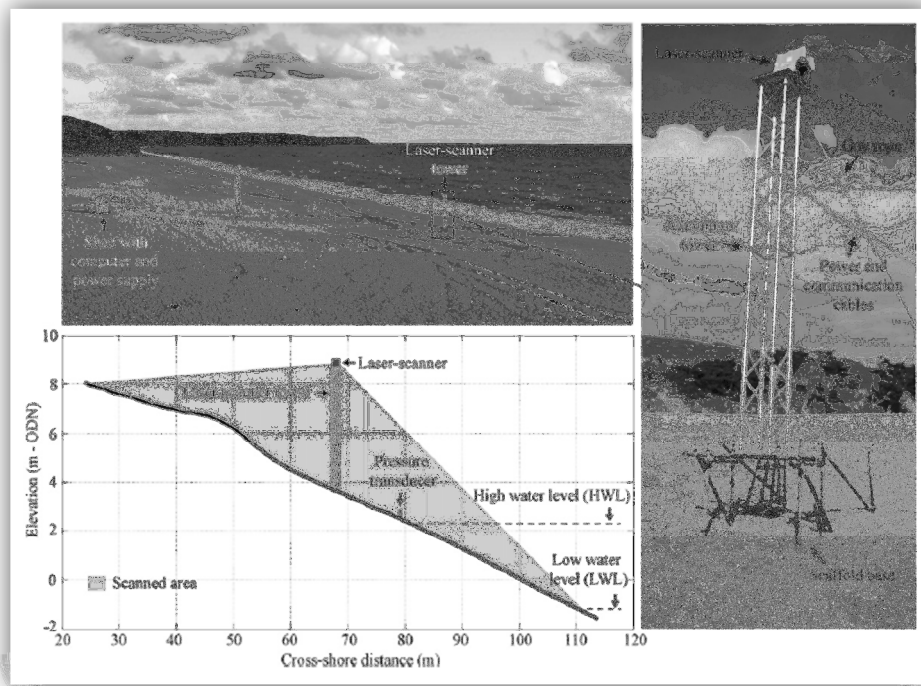


Figure 31: Top and right: Photos showing the deployment of the laser scanner at Loe Bar, Lower left: beach profile with locations of the equipment used during the survey (Almeida et al (2014)).

A comparable study to this was carried out by Poate et al (2013) where a similar mount was constructed on the seaward side of the bar and hosting a single beam LiDAR with the addition of an acoustic bed level sensor (BLS) measuring 70m, extending from the Mean High Water Springs (MHWS) to the crest of the bar (figure 32). This structure, supported by 3m vertical scaffold poles driven 2m into the bar, held 45 acoustic bed level sensors positioned between 1.5m and 2m apart and 1-1.5m above the bed. An all-terrain vehicle (ATV) was also used to measure 3D topography across the bar recording points every 1m using RTK GPS. In addition, a limited number of points were also collected on foot. Accuracies gained by the ATV were $\pm 0.080\text{m}$, compared to $\pm 0.030\text{m}$ when done on foot at 3m intervals. This was due to the sinking of ATV tread into the beach, compared to a flat-bottomed staff used by the surveys which were completed on foot (Poate et al, 2013).



Figure 32: Part of the equipment used in the 2012 beach morphology observations made at Loe Bar by Poate et al (2013).

11.3 The South West Coastal Group

Established in 2009, the South West Coastal Group was formed by the merging of the South Devon and Dorset Coastal Group and the Cornwall and Isles of Scilly Coastal Group. The objectives of the Group are to provide advice regarding coastal issues as well as to influence strategic and sustainable policies and plans to effectively manage the risk from sea flooding and coastal erosion (SWCG, 2015). As part of the need for effective shoreline management, monitoring must be carried out to model any changes and note which areas are under threat. Under the current South West Regional Monitoring Program, all beaches undergo a full baseline beach survey every 5 years, using either a GPS system or total station (SWCG, 2015).

12 Possible Survey Methodology for measuring Loe Bar

In order to develop an appropriate monitoring technique for the landward side of the bar, a number of things must be taken into account. For example, the SMP2 in 2011 reported that the landward movement of the bar was calculated to be approximately 1m per year, and is likely only to move by 25 to 74m in the next 50 years, although the proven movement of sediment in 2014, increasing the bar's thickness by up to 25m in places does highlight the unpredictable nature of sediment transport at the bar.

Keeping the method as simple as possible would be desirable, so that the possibility exists to survey the bar with little man power, sufficient accuracy and on potentially short notice. Whilst a high accuracy is desirable, a beach survey covering an area the size of Loe Bar would find an acceptable accuracy to be within $\pm 3\text{-}5\text{cm}$.

12.1 Laser Scanning

Recent advancements have seen laser scanners mounted onto vehicles and driven along a survey area. Such adaptations have led to effective and accurate surveys being completed, however they require a GPS base station and despite reducing the time taken to collect data, a great deal of post-processing is needed for the vast quantity of points. This number of points is advantageous to commercial surveys, where accurate calculations of volumetric information may be required, however for the means of the survey which would be required at Loe Bar and the size of the survey area, using one of these machines may provide far more information than needed, as well as being expensive. The issue witnessed by Poate et al (2013) of sinking tyres causing inaccuracies would also play a part here.

12.2 Aerial Photography

Measuring the changes in beach characteristics in some cases can be done using aerial photography. Photographs can be taken either at a vertical angle and used in GIS software or on an oblique angle and used in photogrammetry techniques. Training and experience in photogrammetry is required for this and although a clear idea of the morphology can be obtained, the data would require georeferencing and scaling in order to be used. For use at Loe Bar, aerial photography could be used to see a general change in the outline of the bar, yet with the potentially low level of accuracy combined with the high cost and required expertise of flying a plane over the area, this would not be recommended for collecting the data needed.

Satellite imagery is also increasingly being used in some instances, however resolution for monitoring the bar would not be of a sufficient level to carry out the survey required in monitoring the changes in position of the bar's edge. Difficulties also arise when trying to obtain the time and date of when the satellite data was captured and sourcing its provenance (RICS, 2014).

12.3 GPS Surveys

Using a GPS Rover to carry out a survey such as that required at Loe Bar could be very effective. The accuracies required for such an area are likely be achievable and effective coverage of the beach achieved by walking multiple lines.

Real-time Kinematics (RTK) can improve a GPS survey by eliminating the need for post-processing of the data points, and compensates for potential errors such as atmospheric delay and orbital errors. In early 2015, Loe Bar was surveyed using the GPS technique as part of the South West Coastal Group 5-year survey plan for aiding in coastal management. This technique requires a base station and rover system, which is quite possible to achieve and is a realistic method to survey the bar.

Advancements in GPS have led to the development of a UK-wide control network, where survey stations can be accessed using a mobile phone signal. This can be effective in areas where a strong signal is achievable, however areas, such as the Northern end of the bar are void of mobile phone signal, so this development would not be a suitable means by which to carry out the survey.

12.4 Total Station Surveys

Once two base stations have been installed, the TPS can be taken to the site as many times as necessary, using methods of either resection or known back sight to orientate. From then topography and other characteristics can be mapped using the prism and staff and features such as the ridge and lake edge can be determined and recorded in the machine. Accuracies achievable with the use of a total station and prism are well within those required for the sand bar survey which would be required to monitor the bar. Total stations are applicable to a vast number of surveys due to their versatility, consistently accurate results and low cost usage. Accuracies most commonly range from 1 to 5 seconds and can be specified prior to use. The simplicity and repeatability of this method has led to this being the chosen method to carry out the survey at Loe Bar for this project.

13 Topographic Survey of Loe Bar

13.1 Installing the Baseline at Loe Bar

In order to set an accurate baseline to work from throughout the survey, two GPS points were derived at opposite ends of the bar (figure 33). To establish these points, Leica 1200 GPS base stations were set up over two marked points (figures 34 and 35) and left to run for three hours each in order to fully capture the satellite information available (table 4).

Station	Time started (approx.)	Time ended (approx.)
Base SE	10:30	13:30
Base NW	11:00	14:00

Table 4: Times during which the GPS base stations were running in order to obtain coordinates.

In determining where each station should be positioned, a location had to be identified which would not move or be altered in any way between establishing the coordinates of the bases and the survey completed from them. The lack of these features in the middle areas of the bar led to both of the stations being established towards the edges. This would have potential advantages as any errors which may occur along a long baseline like this will lead to errors being minimised as much as possible.

Base NW was set up over an existing survey station previously placed by the Environment Agency which involved centring and levelling over the existing point (figure 36). Base SE was determined by finding a patch of ground which could be returned to and would not be manipulated by human traffic or the elements. This was chosen as a patch of rock bedded very firmly into the grass (figures 37 and 38). An 'X' was marked into the rock with both a hacksaw and a marker pen and the instrument set up over it.



Figure 33: Locations of the GPS base stations established for use in surveying the bar.



Figure 34: GPS Base station set up over an 'X' marked in the rock at Base SE.



Figure 35: A GPS base station set up over an existing survey point at base NW.



Figure 36: The existing survey point placed by the Environment Agency and used as a point for 'Base NW'.

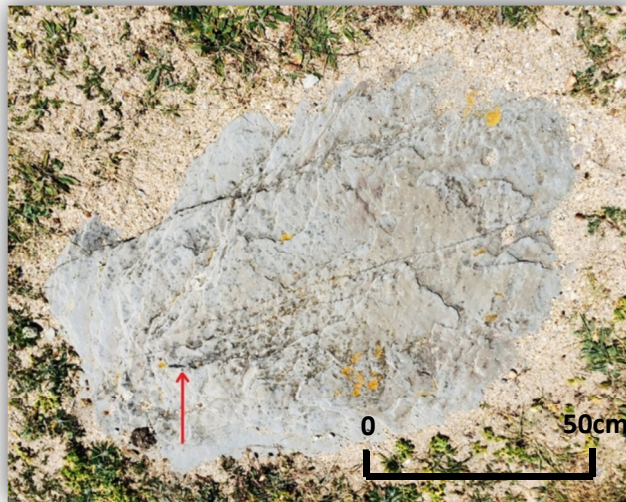


Figure 37: The rock used for the location of Base SE, firmly embedded into the ground to avoid error.



Figure 38: The 'X' marked on the rock in figure 37 above, created with a hacksaw and marker pen.

13.1.1 RINEX

Receiver Independent Exchange Format (RINEX) is a method applied to GPS coordinates to increase their accuracy. The UK has a network of Global Navigation Satellite System (GNSS) base stations which record the positions of the satellites in orbit. If any satellites have drifted from their designated path this is recorded by the station in data obtainable from the OS website. If the local base line for the survey was established during the time when one of the satellites was out of position, the coordinates produced can contain inaccuracies. In order to stop this happening, the data must be uploaded to the Ordnance Survey (OS) website where the coordinates can be altered for the time during which the base stations were running. In this case, the RINEX process was completed by Dr Andy Wetherelt of the Camborne School of Mines.

In this case, the corrected coordinates were seen to have differences of about 0.5m to those collected in the field. This amount can have a serious effect on the accuracy of the survey which will be carried out from them, making it of particular importance that they were corrected. If this is not carried out, the modelling of the bar will be incorrect and may not be sufficient for comparing future models.

		Pre-RINEX	Post-RINEX	Difference
Base NW	Easting	164317.976mE	164317.4075mE	-0.5685m
	Northing	24276.821mN	24276.3314mN	-0.4896m
	Height	5.062m	6.151m	1.089m
Base SE	Easting	164484.183mE	164483.5679mE	-0.6151m
	Northing	23915.507mN	23915.1322mN	-0.3748m
	Height	10.455m	11.1627m	0.7077m

Table 5: Coordinate values pre- and post-RINEX and the differences encountered.

13.2 Survey Method

To carry out the topographic survey a circular Leica prism was placed over both base stations using a tripod and tribrach to ensure sufficient centring and levelling (figure 39). These could then be used in distance resection to set up the Trimble M3 total station (figure 40) wherever required on the bar. During resection care was taken to ensure that the standard error was sufficiently low for Eastings, Northings and Height. Measurements were taken on face left and right when sighting to the base stations. Using an instrument with automatic target recognition (ATR) may reduce the errors encountered, however for surveying a sand bar, the accuracies acquired were deemed acceptable. The benefit of using this resection method is that the possibility arises to set up anywhere that these stations are visible, allowing flexibility and accessibility to a vast amount of features which may not be accessible if the known back sight method was to be used.

The Trimble M3 has an accuracy of 2" and 2mm+2ppm. For the majority of the survey a mini prism was used, at a constant staff height of 1.300m and a prism constant of 18mm. These constants were programmed into the machine before commencing the survey. When collecting points at the water's edge, the mini prism and staff (table 6) were occasionally found to be of an insufficient height to extend over the ridge line. When this problem arose, a longer staff was used with the ability to extend up to a height of 2.150m, hosting a circular Leica prism. The prism constant and staff height were changed whenever necessary, and kept at lengths as short as possible, in order to reduce error from staff wobble. Both staffs which were used had a pointed end, and were expected to cause accuracy problems from sinking into the sand. To combat this, a flat-bottomed plastic bottle was put over the end of the staffs to stop the sinking from occurring and eliminate potential errors.

The survey covered the area from the lake edge to just over the crest of the bar. This was deemed acceptable as the main feature of interest is the lake-ward side of the bar. The location of the seaward edge has predominantly remained constant, as demonstrated previously in the historical OS mapping data. The survey produced can be seen at the back of this report.



Figure 39: Leica prism set up on a tripod over base SE, used in resection.



Figure 40: The Trimble M3 total station used in the topographical survey carried out.



Prism Type	Prism Constant	Centring Accuracy	Range	Photograph
Leica GMP111-0 Basic Mini Prism	18mm	2.0mm	2000m	
Leica GRZ4 360° Prism	23.1mm	2.0mm	600m (ATR)	
Leica GPR121 Professional Prism	0.00mm	1.0mm	3500m	
Leica GPR113 Circular Prism	0.00mm	2.0mm	2500m	

Table 6: Prism Constants, Centring accuracies and ranges of a number of prisms which can be used in topographic surveys with a total station (information source: <http://surveyequipment.com/>)

13.3 Findings of the Survey

The survey findings show a contour pattern similar to that which was recorded by the LiDAR data of the TELLUS program, with the highest elevations of the bar running in a NW-SE direction. The topography slopes gently towards the lake. At the lake edge, a distinct increase in gradient can be seen, marked on the plan as a 'top ridge' signifying the start of a steep slope towards the water's edge. Another top ridge runs parallel to the crest of the bar, representing the start of the steeper slope gradient heading towards the sea.

A shallow depression in elevation exists in the crest, at the location of the scar towards the centre of the bar. The feature then evolves to a raised section at lower elevations, extruding slightly into the lake. This coincides with a lack of vegetation in this section, which leads to the sand being less stable and more prone to movement by the strong winds approaching from the southwest. Towards the lake, more shelter is provided from the wind, creating a depositional environment, in contrast to the area at the crest.

Near the sluice, a distinct conduit shape exists. With natural widening of the bar taking place, this narrow pathway to the sluice may be threatened by the high rates of sedimentation, particularly in storm events, as has been witnessed in the past.

13.4 Difficulties encountered

While there were not many difficulties encountered during the survey, the bar is a place of public access, hosting the South West Coastal Path and is a popular location for the public to visit for recreational purposes. Inevitably, inquisitive members of the public often touch and alter the equipment. This was not found to be a problem with the total station as it was never unattended, however leaving the prisms on tripods at either end of the bar produces difficulties when attempting to resect. For base NW, its location inside the wire fencing created some protection, however base SE, nearer to the path (figure 39), was often played with by both people and animals. This was hugely inconvenient as it then required checking before resection could be resumed to ensure that it would not lead to any errors. A shorter baseline may be beneficial in future to reduce the distance between the surveyor and the prisms. To minimise public interaction with the equipment and for security reasons, the tripods

at the base stations were dismantled after each resection and erected again if another resection was required. This lengthened the time taken for the survey to be completed, although fortunately the gentle topography of the bar required minimal setups.

13.5 Possible Improvements

Using a total station which has ATR would increase the accuracy of the survey by a small amount, and would be particularly beneficial for resection, as previously mentioned. Another benefit of ATR is that the machine could track a 360° prism on a staff and be operated from a remote. This would eliminate the need for a field assistant, although may still present a potential issue of security for the total station which would be unattended while the operator is up to 250m away. Regular calibration of the equipment such as tribrachs would also lead to a reduction in errors.

14 The Sentripod

The sentripod (figure 41) is a piece of surveying equipment which can be used as a prism, as it makes use of retro reflective technology, set on a cylindrical target. Observations are made by sighting to the centre point of the cylinder using a prism constant of 4.4mm.



Figure 41: Photograph of a Sentripod. Height of target is marked (not to scale).

The sentripod's small size makes it easy to transport and is also visible from almost any angle, making it more versatile than a circular prism. The 5/8th imperial thread on the top and bottom make it mountable onto a tripod or pole or fixed to a surface of any angle. If mounted on an oblique surface, a magnetic strip can be applied to the back and the prism can be adjusted within its plastic casing to maintain a vertical position. Accuracies stated by the manufacturer of the sentripod are 1mm to a distance of 60m and 3mm for distances up to 150m, making them competitive to regular prisms at short distances.

A disadvantage of using the sentripod is their relatively short range, particularly when considering the length of the bar. Applications such as building surveys, where for example they are often mounted on a building across the road and used for resection may therefore be more suitable. They also cannot be used with ATR, and so rely on manual accuracies, which can lead to increased error.

The simplicity of the sentripod set up is desirable, particularly when considering the difficulties encountered with the stations used in resection when surveying the bar. The sentripod can replace two tripods, tribrachs and prisms which can greatly ease the process of transporting equipment to the survey site. Access to Loe Bar via public car parks is 944m from the North, much of which is on a single track, or 784m from the south (figure 42), although permission can be granted by the National Trust to park at Bar Lodge, reducing the distance to 98m.

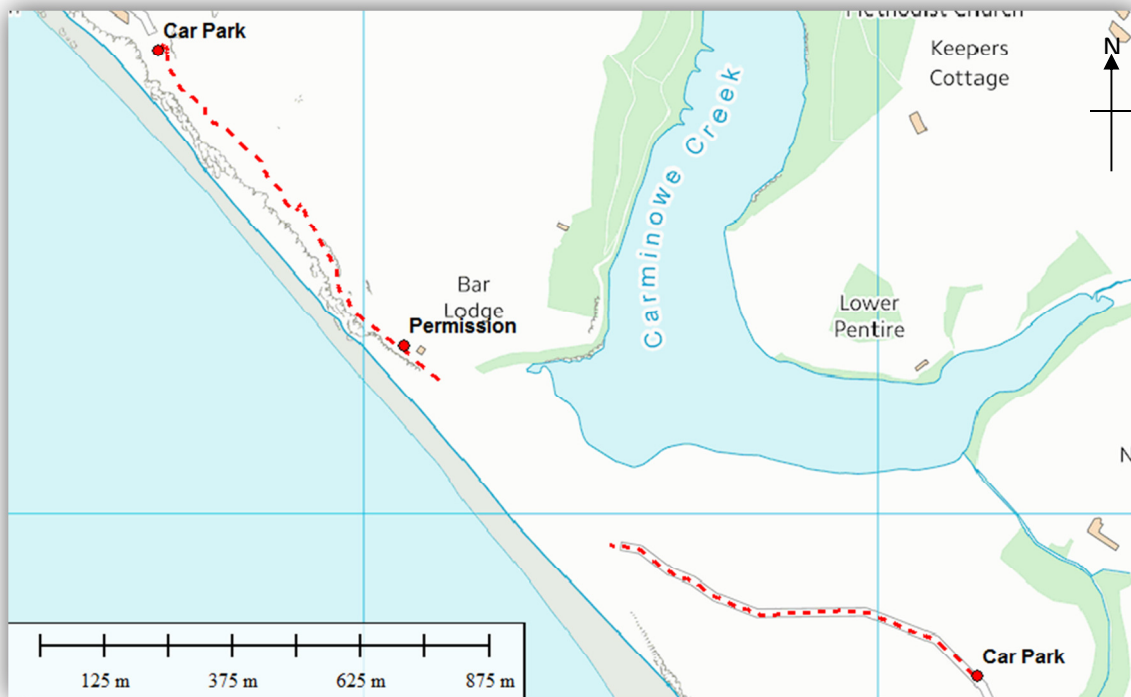


Figure 42: Access Routes to the bar from public car parks and another possible location for parking if permission is granted by the National Trust (base map: Edina Digimap).

14.1 Creating a suitable Baseline

Although the number of fixed locations for placing base stations is limited, another potential location for a base station was identified at the northern end of the bar. This was on a metal pipe sticking out of the sand. A mark was made in the edge of the pipe with a hacksaw and marker pen (figure 43) and a GPS station was set up and run for three hours (figure 44), similar to the technique used for Base SE and Base NW.



Figure 43: Photograph of the mark made in the pipe which will be the new base station point.



Figure 44: Photograph of the GPS station set up over a point marked on the pipe to create another base station for future resection use.

When obtaining RINEX information for the coordinates of this station, it was found that the GNSS base station located at The Lizard (LIZD) had been out of action for several days. This meant that the RINEX corrections for this point were obtained from the next closest station at Camborne (CAMO). This should not significantly affect the results as the station is less than 3km further from the bar than that of the Lizard (figure 45). The location of the new base point can be seen in figure 46 and the coordinates before and after RINEX corrections in table 7.



Figure 45: Location of 'Base Pipe' in relation to OS stations at Camborne (CAMO) 16.787km away and The Lizard (LIZD) 13.796km away (base map: Digimap).

		Pre-RINEX	Post-RINEX	Difference
Base Pipe	Easting	164215.7	164214.6	-1.1356
	Northing	24253.04	24253.01	-0.0256
	Height	9.786	8.9238	-0.8622

Table 7: Coordinates pre- and post-RINEX calculations and the differences. Information obtained by Dr Andy Wetherelt, Camborne School of Mines.

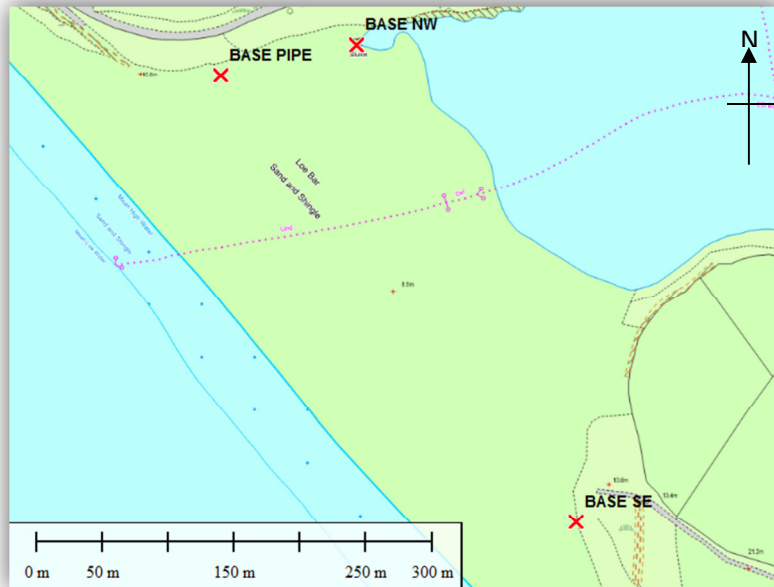


Figure 46: Locations of the three base stations established on Loe Bar which can be used for future surveys (base map: Edina Digimap).

14.2 Resection accuracies using Sentripods at Loe Bar

The distance between Base NW and Base Pipe is approximately 105.38m (figure 47). Locating the total station in the centre of these points will create a distance of less than 60m from each one to the instrument, meaning it will be inside the zone of highest accuracy stated by the manufacturer, however this would involve using an angle of around 180°, whereas the method of resection ideally uses a geometry showing an angle closer to 90°. Figure 48 shows how the accuracies of the sentripod prism stated on the website (www.sentripod.com) will apply to the proposed resection scenario on the bar.

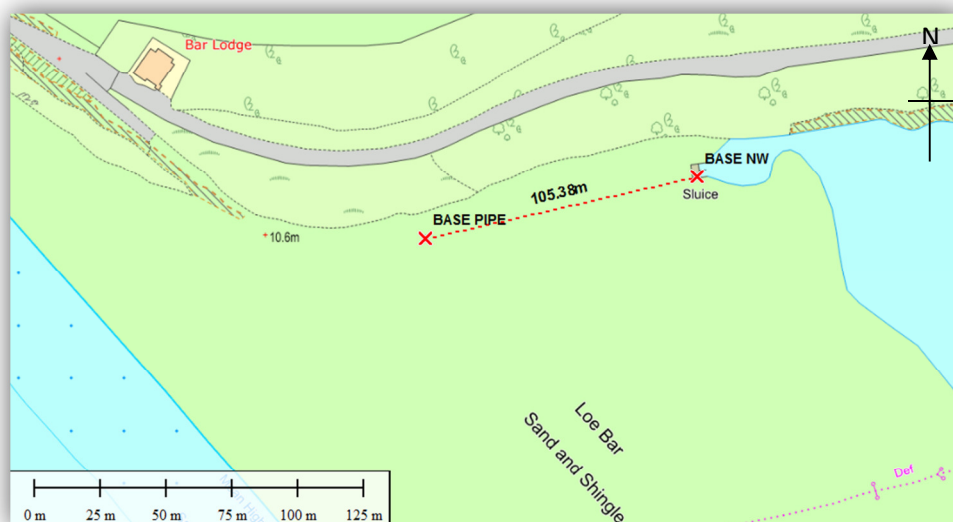


Figure 47: Map showing the distance between Base NW and the new Base Pipe to be 105.38m (base map: Edina Digimap).

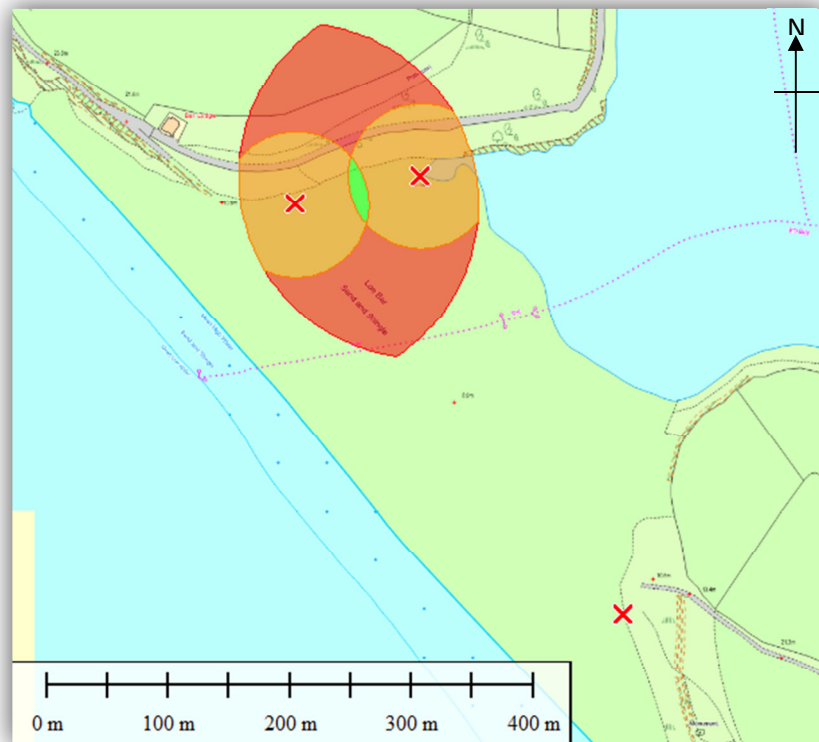


Figure 48: Accuracies stated by manufacturers of the sentripod applied to Loe Bar. A description of this is in table 8.

Area	Description
Green	Less than 60m from both stations
Orange	Less than 60m from one station and between 60m and 150m from the other
Red	Between 60m and 150m from both stations

Table 8: Key for information visualised in figure 48, based on the stated accuracies of the sentripod by the company responsible for their invention and manufacture (www.sentripod.com).

The ideal angle of resection is as close to 90° as possible, yet sufficient accuracies can still be produced with a range of around 30° to 150°. Figure 49 shows the compromise which must be made between the angle of resection used and the distance from the base stations, with the stated accuracy boundaries of the sentripod also represented in colour blocks. The location can also be moved East or West, for example, to gain a 90° angle and bring the resection location into a section of a higher accuracy for the sentripod and therefore also for the resection (figure 50). In the field however, determining an exact position such as those mapped here is difficult.

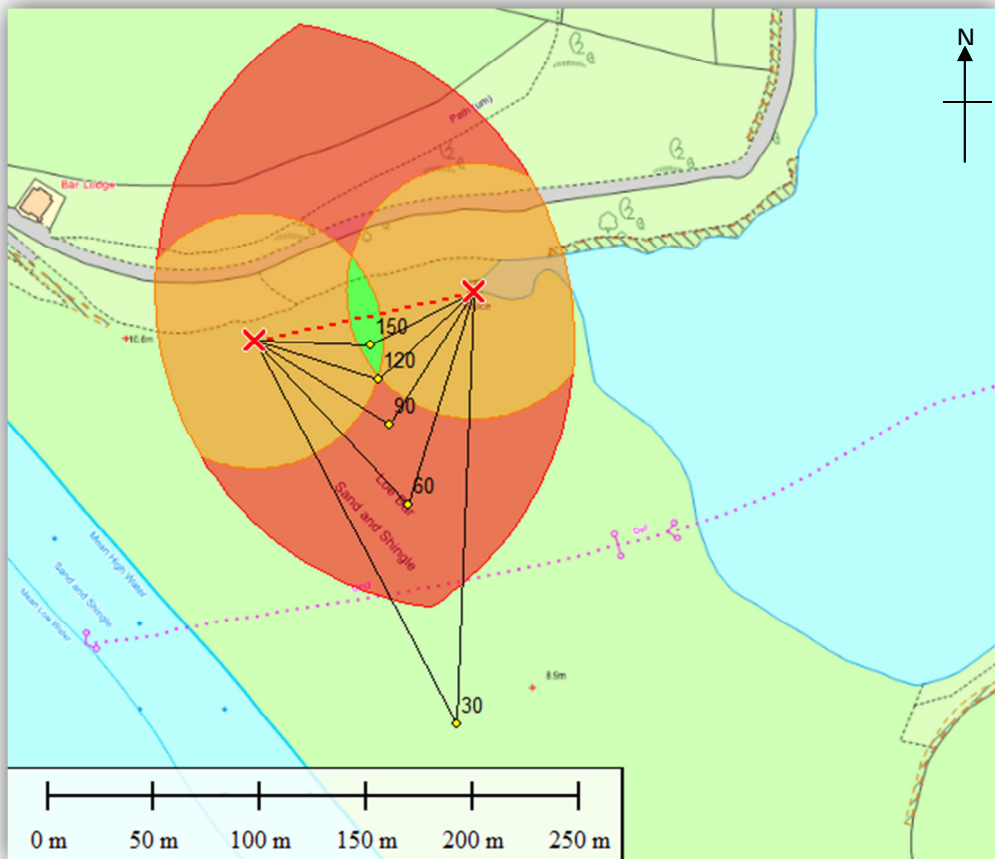


Figure 49: Possible range of resection angles displayed with areas of optimum accuracy for using sentripods as resection tools.

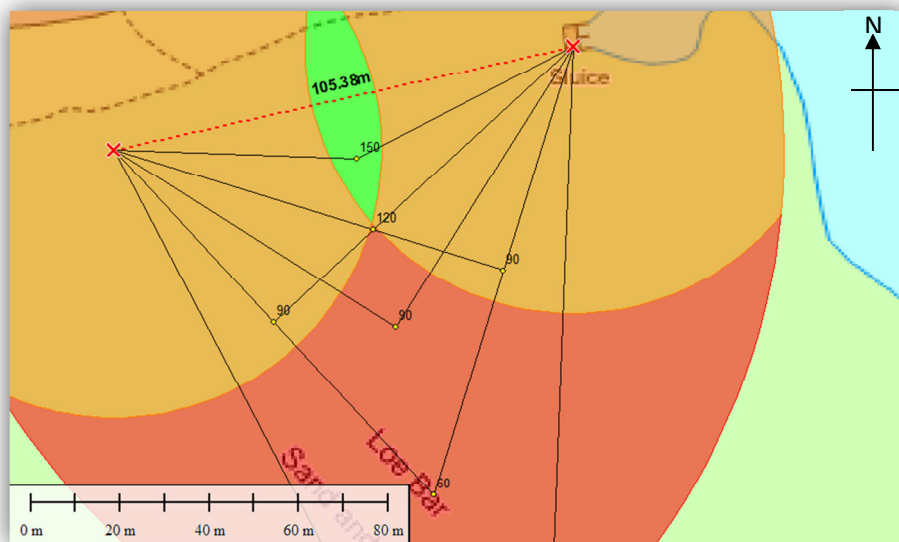


Figure 50: Examples of possible locations for resection which use an angle of 90°.

In setting up the total station towards the northern end of the bar, the southern end will be surveyed topographically from further away. It would be beneficial to use a total station with automatic target recognition (ATR) for measuring topography because as the prism becomes further from the instrument, it appears smaller, providing the possibility for increased human error. If ATR was used, the instrument would more easily lock on to the target and the human error involved in aiming the site of the instrument at the target would be eliminated.

14.3 Testing the Sentripod in the Field

14.3.1 Method

At points Base NW and Base Pipe, a sentripod was fixed to the points using a small amount of tac in order to keep them level and unaffected by wind (figure 51). Tripods were also set up over the points with Leica circular prisms mounted on them. The Trimble M3 was set up at a total of five stations, involving a variation in both angles of resection and distances to the bases (table 9). Five resection measurements were completed for both the prisms and the sentripods at each of the stations. Locations of the 5 points (A to E) are shown in figure 52. Care was taken to ensure that the sentripods were correctly positioned over the points, so as to reduce any potential error.

The target heights used for the sentripods were 32mm for Base Pipe, yet only 30mm for Base NW, due to the thread in the bottom fitting over the small point from which the height was calculated when obtaining GPS coordinates.



Figure 51: Sentripods in place at Base Pipe (left) and Base NW (right).

Distances from bases (m)			
Station	Base NW	Base Pipe	Angle of resection
A	46.6	65.6	139°
B	77.4	63.5	96°
C	133.81	94.263	51°
D	42.7	91.5	83°
E	104.5	18.4	87°

Table 9: Distances from each station to the bases and angles of resection.

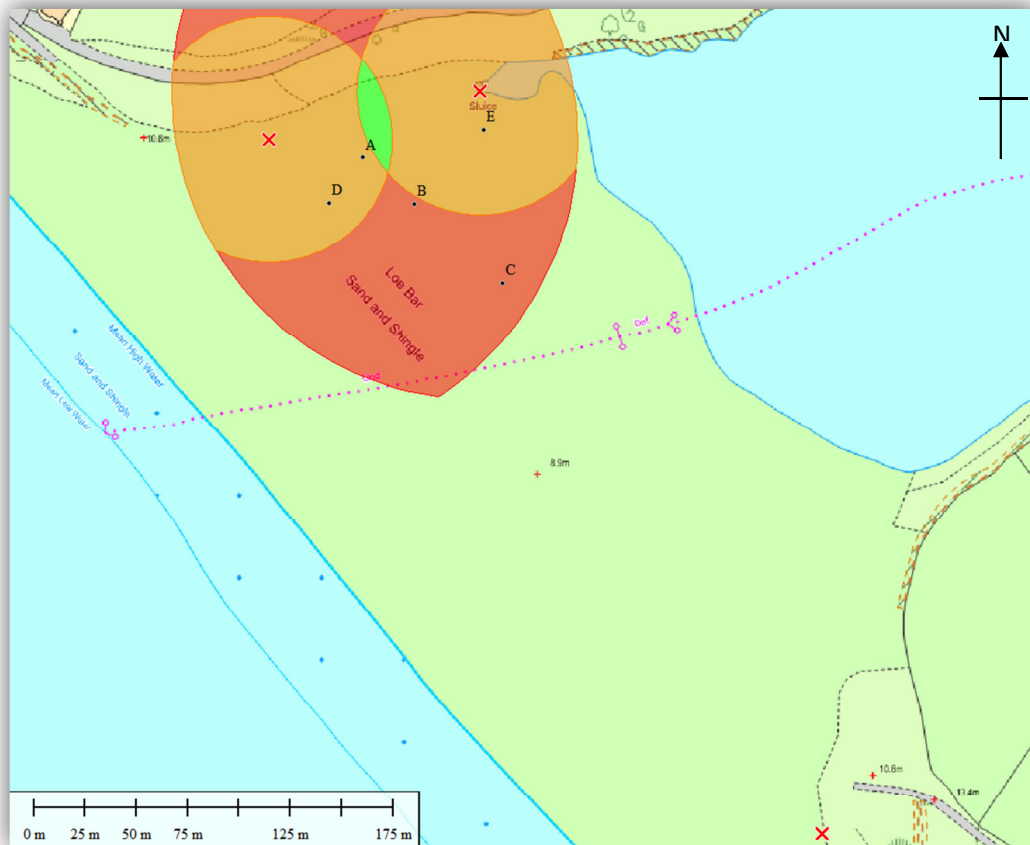


Figure 52: Locations of instrument set-ups, from where 5 resections were made using both sentripods and circular prisms.

At each site, the resulting coordinates from the multiple resections were recorded as well as the resection errors that were stated by the instrument. Graphs of these results are presented in Appendix C. A clear trend appears to exist in that the coordinates calculated by resection from the sentripod always appeared to be further North than those calculated using the circular prisms (appendix C1). For sites A, B, C and D the sentripod resections also produced results slightly further to the west, yet for site E, shows the sentripod results to be slightly to the east of the circular prism results. These graphs also show how consistent each method was, with a tight cluster of points showing a greater consistency of results. For example, coordinates of location C obtained using the sentripod appear more spread out than those with the prisms, implying that the consistency and repeatability for the sentripod at this distance is not as good as the prism. The length of time taken to record each point at C was noted as being as much as 20 seconds, suggesting that the Trimble may have encountered problems when trying to find the sentripod, yet never had an occasions where the sentripod was unable to be found. Location C was the furthest away, showing how the results can change when distance from the sentripods is increased.

Graphs in appendix C2 show that the errors obtained in the measurements between the sentripods and the circular prisms were fairly consistent for all set-ups. In all locations, each resection showed consistent errors, regardless of the prism type that they were being calculated from. This shows that no matter which prism is used or where the instrument is set up, a small error will nearly always occur. The Standard errors produced by the sentripod resections were consistently larger in both Eastings and Northings (appendix C3). The bar charts in appendix C4 show the differences in average standard errors between the sentripods and prisms. These show that for every value of easting and northing measured, the sentripod is out-performed by the prism, yet for elevation there appears to be mixed results.

Despite tight clustering of coordinates witnessed at location D, large differences exist in the results produced from each prism type. This implies that the readings are consistently inaccurate for both types of prism, yet the

errors seen in the Eastings for the sentripod are larger than those seen for the circular prism. This implies that the true coordinates are closer to those produced by the prism than by the sentripod.

Location E shows a similarly high consistency and tight grouping, particularly for the sentripod, however the coordinates produced are as much as 24mm further north than those produced by the circular prism. The high errors seen in the northings of this location therefore imply that the true location is further towards the coordinates produced from resection using the circular prism than that of the sentripod. With the standard errors showing higher inaccuracies for the sentripod than the circular prism, this will be the case for every station.

Locations A and B do not show particularly tight cluster of coordinates but do show the smallest differences between the two sets of coordinates calculated. The errors in the Eastings are relatively high, considering their close proximity to the base stations at both of these locations.

In terms of accuracy required for the survey, the errors experienced in this small test have shown that the maximum errors in Eastings are 28mm, which were collected using the sentripod at station C. The maximum errors in Northings are 23mm, also with the sentripod at station C, which was the only station to generate any errors larger than 16mm. While the sentripod has shown to produce coordinates with a higher error than that of a circular prism, the results are of an acceptable standard for a beach survey of this type. It could therefore be possible to use the sentripod to carry out a resection ahead of surveying the bar, with the knowledge that the larger the distance from the bases, the higher the errors are likely to be.

Other possible causes for error in the test may have been from aspects such as the tripods being set up on sand and moving very slightly; the sentripods not placed quite on the target; or even the issue of parallax, which was occasionally noticed when readings were being taken.

The clear advantage of using a sentripod is the obvious reduction in the amount of potentially heavy kit needed to carry out the survey. Rather than setting up two tripods with tribrachs and prisms, a sentripod can be placed at two known locations and used for resection. The topographic survey can then be continued using a staff with either a circular or 360° prism.

The issue of tripods being 'played with' or stolen by members of the public no longer remains due to the easy set up and removal of the sentripod. If another station set up is needed via resection then the sentripods can simply be placed back in their positions and used for resection in a matter of just a few minutes before being removed again if necessary.

14.3.2 Problems Encountered when Using the Sentripod

A number of difficulties were encountered when using the sentripods as a resection tool. The main issue encountered was the limited number of locations from which a resection could be conducted, caused by a combination of slight undulations in topography and their near-ground positions. Another issue was that the sentripod at Base NW had to be positioned behind a wire fence. The fence itself did not appear to cause a problem, however when positioned nearer to the lake, the sentripod was mostly hidden by a metal collar running around the bottom of the wire. Care also had to be taken to avoid the railings around the sluice blocking the line of sight. This greatly restricted the locations from which a resection could be made. To combat this, either one or both sentripods could be mounted on a small foot which would only need to be a few centimetres tall. The problem was seen to exist more prominently with increasing distance from the points, particularly in the case of the station on the pipe, given its low position. This however is not hugely significant, given the accuracy levels seen in the trial resections, where it was deduced that increasing the distance from the base stations creates larger errors. Staying closer to the bases therefore has advantages for both the resection quality and the visibility of targets.

14.3.3 Transferring Coordinates to a Bolt

The issue of the fence by Base NW inhibiting the possibility for resection at locations closer to the lake can be aided by transferring coordinates onto a more accessible part of the sluice structure. An obvious location for this point was a bolt on the edge of the concrete platform, upon which a sentripod can easily be placed and secured with tac. Gaining a coordinate for this point using GPS would be problematic due to the difficulty which would arise in placing a tripod there, therefore a method was adopted using the total station.

Method

To obtain coordinates for this point, a tripod was set up at the bases NW and Pipe, with a Leica prism on each. Another Leica prism was placed on the bolt and secured using tac to ensure its position was level (figure 53). Leica prisms were used rather than sentripods due to the higher accuracy which can be achieved, as previously seen. The Trimble M3 total station was set up at five different locations (figure 54) using resection and from each, a total of 10 readings were made to the prism on the bolt, turning the instrument away, both horizontally and vertically, between each reading. A statistical analysis was then carried out to reject any outliers in the results from each setup. These averages were then weighted according to their resection error and an overall coordinate was produced which could be attributed to the bolt (table 10). The height of the bolt was determined by using a level, recording the differences in height between Base NW and the bolt. Appendix D contains the tables of how the coordinates were derived.

While these coordinates will not be as accurate as those of Base NW which were obtained using GPS data, they are likely to be of a sufficient accuracy for that required of the survey. If an incident arises where the view to the sentripod at Base NW is obscured it is likely that using these coordinates will be sufficient. A brief test using five resections from one station set-up was completed. When tested using sentripods at a later date, errors in coordinates produced using the bolt showing to be exactly the same as those recorded from Base NW. This makes the bolt an acceptable alternative to use when base NW cannot be seen.



Figure 53: Circular prism placed on the bolt for determining coordinates. Note the collar to the right of the prism which obstructs the view to the sentripod from certain places on the bar.

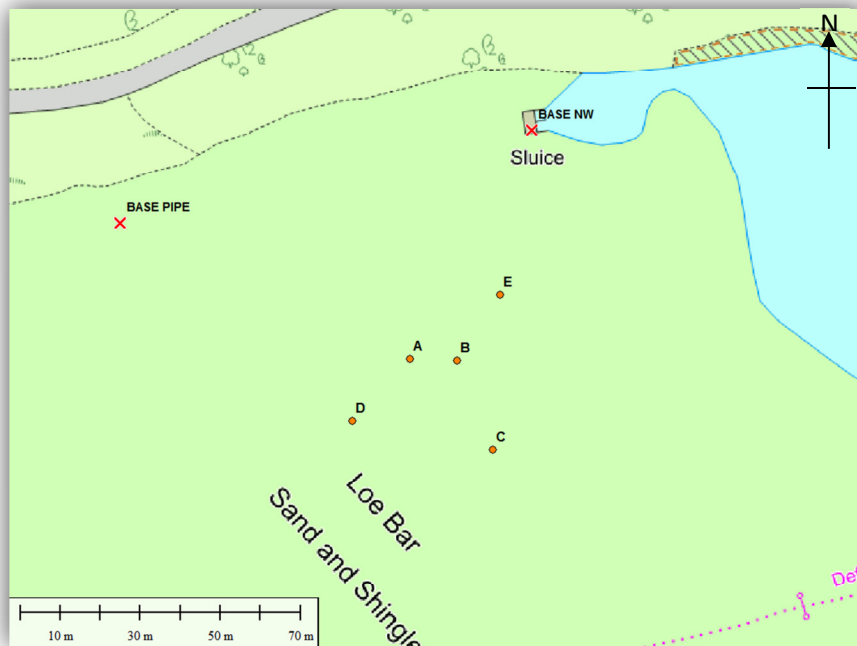


Figure 54: Locations where resection was used to establish a location and measurements taken to the circular prism on the bolt (base map: Edina Digimap).

Coordinate	
Easting	164317.2006m
Northing	24275.77618m
Height	6.154m

Table 10: Coordinates of the bolt on the sluice derived from multiple resections and weighted averages. The height was derived by levelling from base NW.



Figure 55: Sentrypod placed on bolt a held level and in place using tac. This can be used in resection if view of Base NW is obstructed. Note the sentripod fits over the 5mm tall bolt, providing the need to adjust the target height to 0.027 rather than 0.032.

14.4 GPS Error Ellipse

A technique often used in surveying is to derive a single point of elevation from which all other elevations on the site will be measured. This is due to the errors witnessed in using GPS techniques, which show a lesser accuracy when looking at the 'Z' dimension in comparison to those of the 'X' and 'Y'. If the baseline is very long or on uneven or densely vegetated ground, difficulties in levelling between them may encounter inaccuracies and the elevations produced by GPS stations are often accepted. Baselines such as that set up on Loe Bar from Base SE to Base NW would have encountered errors if attempting to level between the points due to the amount of soft sand and the length of the line, however between Base NW and Base Pipe, levelling is possible.

The difference in heights between Base NW and Base Pipe according to their GPS results is 2.7728m, however levelling between the two points showed a different result of 2.8274m, giving a difference of 0.0546m. The point at the pipe therefore shows a relative elevation of 8.978m above sea level, rather than 8.9238m previously obtained by the GPS. This could be attributed to a number of possible reasons. GPS coordinates of the points were collected on different days and the RINEX for the base at the pipe was done from a different GNSS station. Both points are also positioned within close proximity to the cliff which may have blocked signal from certain satellites and reduced the optimum viewing angles or created a multipath effect from signal reflection. If the satellites used by the GPS were closer to the horizon, the signal would have been exposed to higher levels of ionospheric and tropospheric delay, yet this should have been accounted for by the RINEX process, which acts similarly to the differential GPS technique. This should also correct other errors such as clock errors.

When determining an elevation using GPS, the measurement is made from an arbitrary point on an ellipsoid to the point at which the device is located. The ellipsoid is most commonly located beneath the surface of the earth, although some areas, for example in areas of the United States the ellipsoid is located above the earth (Kaplan and Hegarty, 2006). The ellipsoid used in GPS is the GRS80 (Geodetic Reference System 1980) and is considered to be a best fit of the earth, however other local ellipsoids exist, for example the Airy 1830 ellipsoid which fits best to Britain, but is not relevant for other countries (OS, 2015). Determining a 'zero height' to which all measurements will be in relation, involves the creation of a Geoid, which is a more irregularly shaped ellipsoid and corresponds to the average surface of the oceans over the whole earth. Every point on the Geoid has exactly the same height anywhere throughout the world. Similarly to the ellipsoids, local geoids also exist, which are occasionally offset from the global Geoid. The UK records its elevation relative to the tide gauge in Newlyn, Cornwall measured between 1915 and 1921, which is around 80cm below the global Geoid (OS, 2015). Errors can arise when using the ODN local geoid model due to the fact that it is only tied to the mean sea level at one point, making it tilt when compared to the true Geoid and susceptible to slope error. This error is small however and only amounts to approximately 20cm across the 1000km model (OS, 2015). In Cornwall it is unlikely to have a noticeable effect so will not be altering the results at Loe Bar.

When establishing points using GPS, horizontal and vertical accuracies differ. Horizontal measurements can be achievable to within 2mm at the highest precision, yet to get accuracies as fine as this, the GPS receiver must be permanently installed in a network. Collecting measurements in the field can see higher errors which can reach to a few centimetres, with vertical position quality generally seen as 2.5 times worse than that of horizontal (OS, 2015).

A small test was done to investigate how levelling between the points compares to using the elevations derived from the coordinates produced by the GPS. A sentripod was placed on both Base Pipe and Base NW and five resections were carried out from one setup location. The errors in height saw a reduction from 15mm to 4mm when using the new height for Base Pipe. In future surveys the elevation of 8.978m created by the levelling should be used for Base Pipe.

15 Recommendations for Future Surveys

It is clear that the bar is currently changing shape today as it has been since the earliest records have been made. Monitoring of the lake edge and crest height will be useful in the future in order to see how the bar is changing and the distribution of material over time.

15.1 Recommended Method

In future monitoring of the bar, sufficient accuracies of resection can be achieved by placing the sentripod prisms over the points at Base NW and Base Pipe. These can be levelled and stabilised effectively using a tac. When establishing a suitable location to set up the total station, consideration must be given to the pattern seen here, showing resection errors increase with distance from the sentripods. If the sentripod at Base NW is unable to be seen through the cage, the bolt can be used to combat this issue, particularly if positioned nearer to the water's edge. Potential adaptation or the addition of a foot would raise the sentripods to allow for their occasional obstruction due to the undulating ground. When resecting, the coordinates which should be used are those in table 11. The correct target heights should also be included, as well as the prism constant, stated by sentripod.com as 4.4mm.

Base	Easting (mE)	Northing (mN)	Elevation (m)	Target Height (m)
Base Pipe	164214.600	24253.010	8.978*	0.032
Base NW	164317.408	24276.331	6.151	0.030
Bolt	164317.201	24275.776	6.156*	0.027

Table 11: Coordinates which should be used when resecting, as established by work done in this project (* elevations derived by levelling from Base NW).

Once the position of the total station has been established showing an acceptable error of resection (approximately ± 30 mm for easting, northing and height), the topographic survey can begin. Either a circular prism or a 360° prism can be mounted to a staff, which should be able to extend to approximately 2m in order to be seen at the lake edge. The bottom of the staff should be adapted to have a flat surface to minimise sinking into the sand. The accuracy of the equipment used should be adequate to require only one set up, with the southern section of the bar being surveyed from further away. If a total station with ATR capability is used, accuracy for this may be increased. Robotic tracking of the prism will eliminate the need for a second person but may imply security issues given the distance between the total station and the operator at times.

The topographic survey should include features such as the edge of the lake, the ridge above it and a number of points in the space between. Paths, other ridges and the sluice should also be recorded in detail. The rest of the bar should then be surveyed on a grid of around 20 paces, from the lake as far as the crest and just over. This will show the changing height of the crest as well as any advance in sand towards the lake.

With resection taking place at the Northern end of the bar, the possibility exists for any errors to be increased with distance towards the southern end. During the survey, a measurement should be taken with the staff placed on Base SE. This can then be used as a quality observation to compare the coordinates obtained by the GPS stations with those produced from the survey.

16 Geophysical Investigation of Loe Bar

Resistivity surveys are an effective, unobtrusive method to gain an insight into the structure and characteristics of the ground below the surface. In running a resistivity line along the ground with electrodes inserted into the top soil, a two-dimensional cross section of the line can be created and visible features attributed to various parameters can enable assumptions to be made as to the interpretation of the subsurface. This is done by inserting a current into a number of linearly placed electrodes and recording the amps observed compared to the volts applied. These values are defined by the resistance in ohms between opposite faces of a unit cube of the material through which the current is being passed. If a material of resistance R , has a cross sectional area A and a length L , the resistivity can be expressed by using the equation below (Todd, 2005). This generates units of ohm meters (Ωm).

$$\rho = \frac{R A}{L}$$

Resistivity surveys are used in a number of investigations, namely determining the location of archaeological and engineering features such as ancient buildings or tombs and disused mine shafts, and can also be used in exploration of mineral ore bodies as a quick and inexpensive preliminary method to map the extent of a resource. Their advantages include the rapid, economical and linearly extensive data collection, which can be far more insightful than boreholes (McDonald et al, 1998).

Resistivity surveys originated in the 1920s from work carried out by the Schlumberger brothers. Throughout the next 60 years, sounding surveys were the method most commonly used to produce a quantitative interpretation of the subsurface (Loke, 1999). In this method an array of electrodes are placed extending from a fixed central point and spaces between them gradually increased to gain values at greater depths. This method gives values for varying depths but not for lateral variance. By contrast, the profiling method can create lateral rather than depth variation by keeping the electrodes at the same distances from one another and moving the entire array in a straight line. Both of these survey methods give only a one-dimensional view of the data, showing only changes in resistivity at certain depths, as opposed to two-dimensional surveys which show both lateral and depth features along the line (Loke, 1999).

Resistivity values vary greatly depending on the medium that the current is passed through. Water has a low resistivity, meaning a sedimentary rock which is more porous and prone to water saturation will show a lower resistivity value than in its equivalent dry state. Mineral and salt content of water can also show a significant decrease in resistivity values, giving groundwater a variable resistivity of 0-100 Ωm , dependent on the salinity content, with sea water for example showing value of around 0.2 Ωm (Loke, 1999).

A number of surveys involving 2D resistivity in coastal areas have been carried out, including an airborne electromagnetic survey completed by Beamish (2012) in order to establish the extent of saltwater incursion on a beach in Anglesey. Saline parts of the beach were then able to be modelled in 3D by extrapolating data between the lines and with the aid of several boreholes, with rough volumes able to be calculated. Mc Donald et al (1998) also carried out a resistivity survey to investigate saline intrusion and geological structures beneath areas of tidal coastal wetland at Langstone Harbour in Hampshire.

A two-dimensional survey can be restricted by the lack of data perpendicular to the line, leading to lateral assumptions. A three-dimensional survey will show this information, yet is expensive and often unnecessary, particularly when looking at geological strata which can be reasonably assumed to have minimal lateral variation. One application for three-dimensional resistivity recently carried out was by Allah et al (2013) to measure the interaction between salt water and ground water at a beach in Japan. This was done using a Grounded Electrical-Source Airborne Transient Electromagnetic (GREATEM) system, hung below a helicopter, giving results for material as deep as ~350m and reached a distance of more than 500m from the shoreline.

Two-dimensional imaging or tomography surveys have been developed to involve large numbers of electrodes connected with a multi-core cable. A laptop and electronic switching unit automatically select the type of array, sequence of measurements and the current to use and will select the electrodes for each measurement. In order to obtain an effective two-dimensional cross-section, a series of points must be taken at sufficient locations along the line regarding both depth and linear position (Loke, 1999). Measurements should be made in a systematic manner in order to maintain good data quality (Dahlin and Lock, 1998).

A procedure known as a 'pole-pole' array, if using 20 electrodes, would take 19 measurements with a spacing of $1a$ between the electrodes, followed by 17 measurements of $2a$ spacing and so on, with the readings becoming deeper with the increasing distance between the electrodes (figure 56). For dipole-dipole, Wenner-Schlumberger and pole-dipole arrays the spacing between the inside and outside electrodes is changed (Loke, 1999). All of these methods create an array which is seen to taper off with depth. Should a survey be required which contains more lateral information at depth, the cable can be moved along the line and a smaller array run to pick up only data which hasn't already been recorded, known as the 'roll-along' method (figure 57). The pole-pole array provides the widest horizontal coverage with increasing depth, whereas the Wenner array is the quickest to taper, evident in figure 58.

The output of these resistivity surveys is generally to create a pseudo-section using contouring which provides a crude pictorial representation of resistivity values in the subsurface. The shape of the contours depend on the type of array used to gather the data (figure 58), with each having their own advantages.

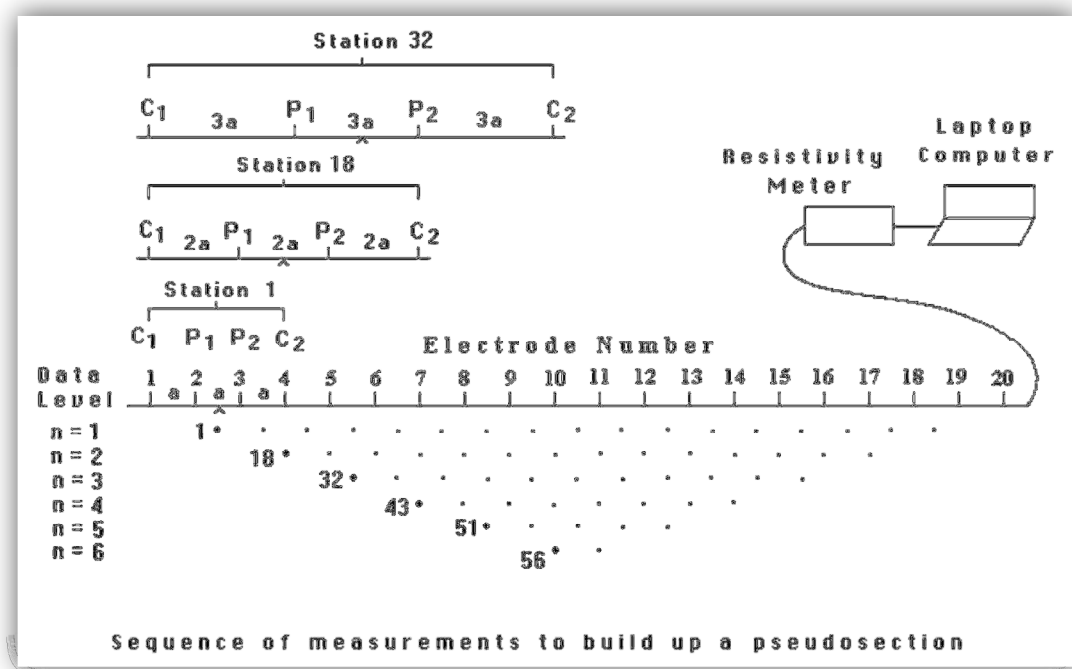


Figure 56: Sequence of measurements used to build up a pseudo-section when and arrangements of electrodes needed. 'a' represents spacing between electrodes, with deeper readings taken using electrodes further apart (Source: Loke, 1999).

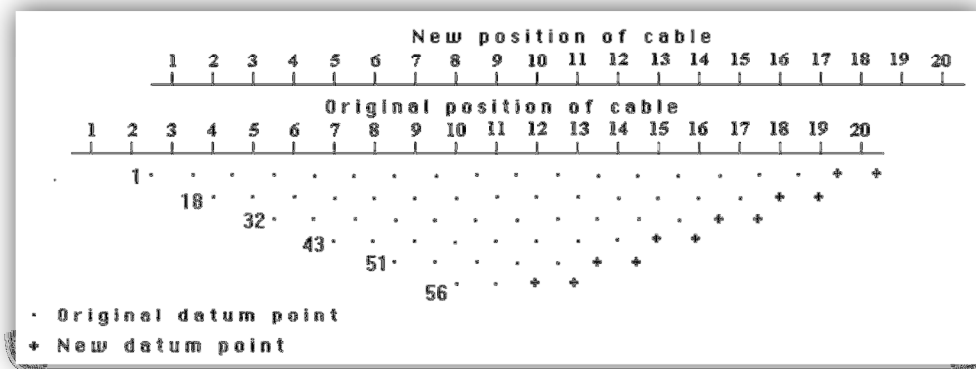


Figure 57: The roll-along method involving linear movement of the line to increase the data coverage at depth (source: Loke, 1999).

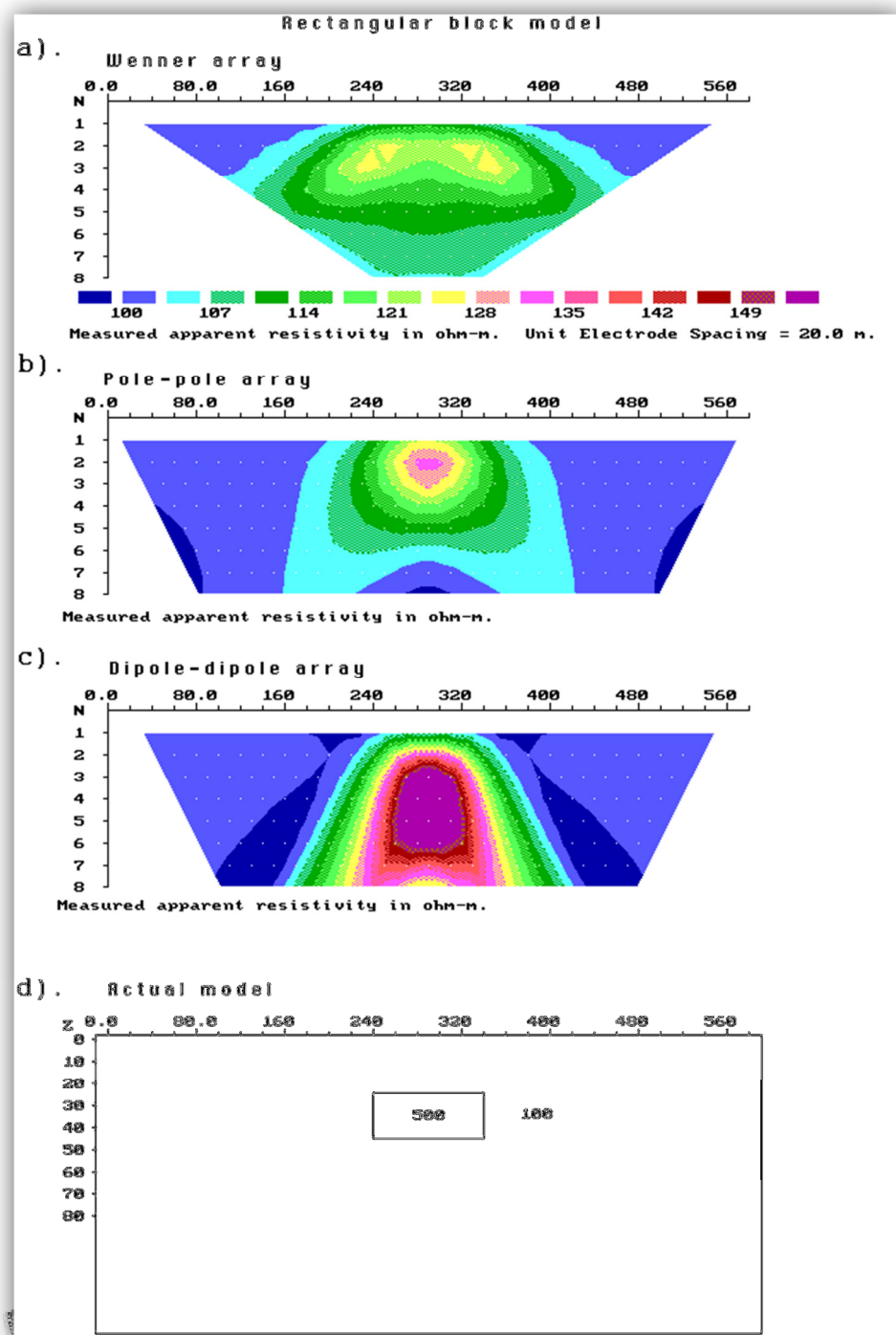


Figure 58: Pseudo-sections created from differing arrays, covering a rectangular block target (source: Loke, 1999).

16.1 The ZZ array

One of the more recently developed arrays is the ZZ array. While older types such as the Wenner array can produce data points in the hundreds, a ZZ array uses a more complex algorithm for its data collection, which can provide data points in the tens of thousands. The FlashRes resistivity meter uses any two electrodes to insert a current, with a maximum of 256 possible pairs. This can be run using each electrode in turn to act as the common reference electrode, so can be done a total of 61 times in an array consisting of 64 electrodes (ZZGeo, 2014). This increased number of points reduces the root-mean-square deviation (RMSD) of the ZZ array to be typically much lower than that of the Wenner array.

The resolution produced by each array is dependent on the length of the line used. At full extension, electrode spacings of 5m would create a line around 315m long and reach to an approximate depth of around 62-79m (ZZGeo, 2014). The manufacturer of the resistivity instrument, ZZgeo, states that exploration resolution decreases with depth, with tests showing the resolution to be about 10% of depth. For example, the exploration resolution at 50m below the surface is around 5m. The general rule of the equipment is that the best resolution gained for each array is half of the electrode spacing, meaning that if the electrodes are placed with 5m intervals between them the best resolution obtainable is 2.5m.

16.1.1 Induced Polarisation

Induced Polarisation (IP) is measured by the time that it takes for voltage in the ground to decay after the DC input has been switched off. When collecting resistivity data, voltage is usually applied to the ground in a pattern of 0.6s on and 0.1s off, however when also recording IP values, the voltage requires longer intervals in order to measure the decay curve, using 0.6s on and 0.6s off, lengthening the time taken for the data collection process. IP values recorded are demonstrated as a function of time. The main classes of materials that retain their charge are clays and some ores – notably sulphides, making IP a useful tool for also detecting mine wastes. The fine grained mine wastes which are recorded to have been transported to Loe Pool by the River Cober may show high levels of IP, particularly expected in the lake-ward side of the bar, following the account by Coard (1987), stating visible quantities of mine waste last time the bar was cut. The mining techniques used during the time when the mines in the River Cober catchment area were most active are less efficient than those used by mining companies today, with higher percentages of ore being discarded as waste than is seen in present day mining. This provides the possibility for there to be relatively strong readings of IP if waste material exists.

16.2 Survey Method

The instrument used in collection of resistivity data at Loe Bar was the FlashRes 64 Universal manufactured by ZZgeo. It has 61 channels, and the ability to carry out multiple data arrays in a single run, along with the capacity to collect over 62,000 data points in an hour. Two resistivity lines were installed at Loe Bar in directions perpendicular to one another (figure 59). Before the survey was commenced, around 50ml of water was poured onto the ground at the location of each electrode in order to generate a sufficient electrical contact between the electrode and the ground. A voltage of 350V (DC) was passed through the rods with a pulse of 0.6s on and 0.6s off with resistivity and induced polarisation being recorded for each line using a ZZ and Wenner array for line 1 and only a ZZ array for line 2. In the time during which the data collection was taking place, a relative topography of the lines was recorded using a total station. This allowed for later topographic correction of the pseudo-section. The position of the end of each line was recorded using a hand-held GPS device, accurate to approximately 2m.

Line 1 was 315m in length, running sub-parallel to the coastline of the Bar with 5m spacings between electrodes (figure 60). Line 2 ran in a perpendicular orientation to that of the bar with electrodes spaced at 1m, giving the line a total length of 63m.



Figure 59: Location of resistivity lines 1 and 2 displayed on satellite imagery, with electrode numbers labelled (satellite image source: Global Mapper).



Figure 60: Photographs of the placement of the resistivity line 1 rolled across the bar looking NW (left) and SE (right).

16.3 Results and Interpretation

The quality of the data appeared very good, demonstrating consistent readings and low 'Q' values. RMSD values created in the processing of the data were reduced by continual rounds of processing by the program to find a sufficient model. Table 12 shows the reduction in RMSD and the number of processing rounds performed, as well as the number of points which were obtained by the survey and those which were filtered out on the basis of quality. The difference in points collected by the ZZ array compared to that of the Wenner array is notable, as are the number of points which have been filtered out of the ZZ array for line 1 and the high RMSD values present in line 2.

		RMSD				No. points	
	Array	Test	Initial	Final	No. rounds	Pre filter	post filter
Line 1	Wenner	IP	12.32213	9.018175	19	651	651
		Res	12.32213	11.098702	18	651	651
	ZZ	IP	18.91643	6.590423	17	55821	19487
		Res	5.872458	2.32648	15	55428	19724
Line 2	ZZ	IP	28.28382	20.368452	12	29668	22402
		Res	68.81412	50.002338	15	29092	21607

Table 12: RMSD values of each array on both lines before and after the stated number of processing rounds, as well as the number of points taken by each survey and those filtered out.

The results of the surveys are represented as pseudo-sections using colour scales. Left to right on the sections represents electrodes 1 to 64 respectively. The bottom corners are subject to some misrepresentation due to extrapolation, given the conical shape of the data points collected in the survey, particularly that of the Wenner array sections.

Interpretation of the pseudo-sections is aided by a diagram produced by Palacky (1988), showing typical resistivity values of earth materials (figure 61).

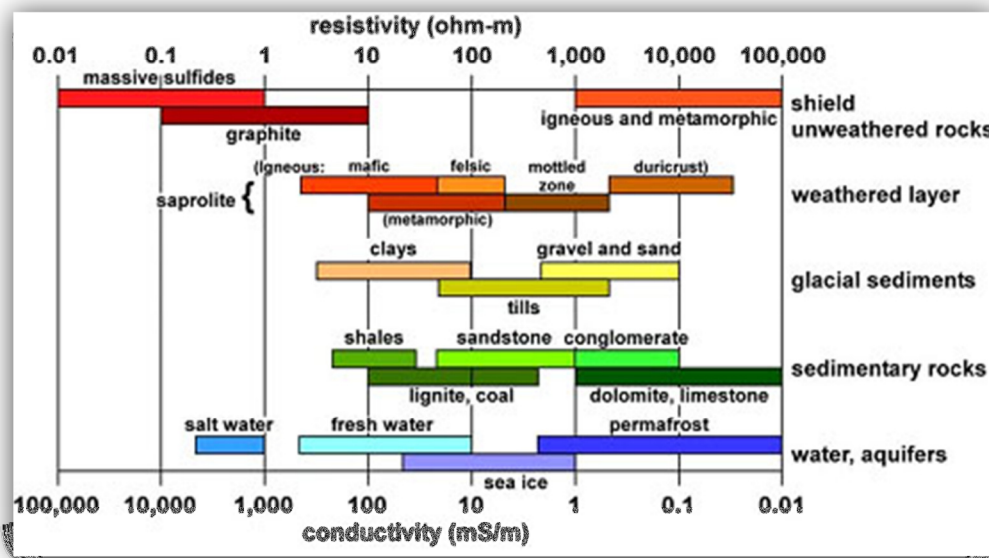


Figure 61: Typical ranges in resistivity values of Earth materials (Palacky, 1988).

16.3.1 Line 1 Resistivity

Wenner Array

Referring to figure 62, the high resistivity values of 400-700 Ω m at the surface (point 1) can be attributed most likely to the sand being drier. The level of both the high tide mark and the lake is lower than the elevation of the

line along which the resistivity was recorded. The only water source available to this upper area is therefore likely to be either from atmospheric sources, or by capillary action in an upwards direction through the sand, led by evaporation from the surface.

Under the resistive material at the surface, the layer beneath (point 2) shows a rapid decrease in resistivity from around 15 to 30m with values of 0-100 Ωm . This is possibly where the sediment in the bar becomes saturated with water and more specifically sea water, which shows a lower value than freshwater due to the ion content. Below this, the resistivity decreases, potentially as a result of compaction of the sediment, allowing for less water penetration.

The anomalously high value seen near the surface (point 3) coincides with the location of the cut carried out in 1984 (figure 59). According to Loke (1999), alluvium can show a resistivity value of up to 800 Ωm . This may be influencing the higher values seen here, with this alluvium material possibly having been deposited when this cut was made, particularly when taking into account the observation made that the cut reached a depth of approximately 10m.

The low number of points collected by the Wenner array can lead to inaccuracies in the representation of features and their interpretation. The image produced by the ZZ array has more than 30 times the number of points compared to the Wenner array, so will likely be more helpful when interpreting the results.

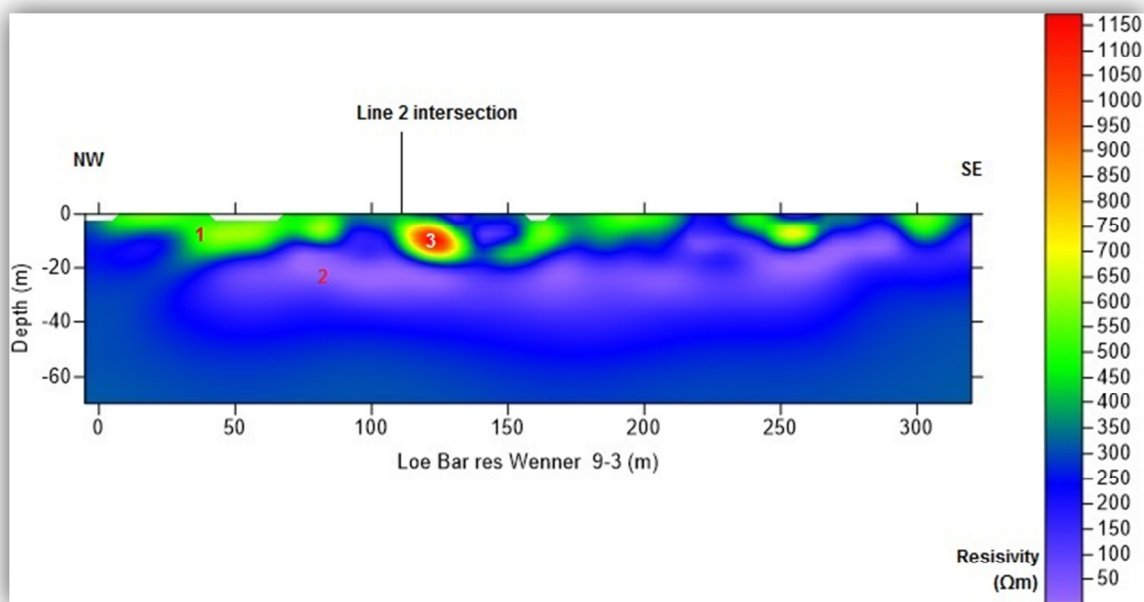


Figure 62: Resistivity pseudo-section of line 1 using a Wenner array (processed by Mr N.A. Wood). Smoothing coefficients: Horizontal = 9, Vertical = 3.

ZZ Array

The ZZ array (figure 63) shows more distinctive features than the Wenner array, such as the very linear appearance of the high resistivity values near the surface, upwards of 1200 Ωm (point 1). The sudden decrease in resistivity from values of around 1,200 Ωm to those close to zero, occurs at approximately 10m depth (point 2), and coincides with sea level and the likely injection of sea water into the sand.

Between 100 and 150m along the line an area of slightly higher resistivity occurs compared to the values of the surrounding material (point 3). This coincides with the area of the last cut carried out in 1984 and may represent fresh water in the sand rather than salt water. No mining has occurred in the Cober since the last cut, and low rates of deposition have taken place, meaning that minimal fine material is currently being deposited on to the bar's lake-ward edge and a channel may have remained present.

Point 4 shows a feature with a resistivity value of around 500 Ωm , consistent from the surface to around 20m depth. In studying the surface both in the field and using satellite imagery, this feature has no obvious cause and may require further investigation in order to determine the reason for its presence. Possible explanations for the presence of this feature may see a link to the bar's prolific history of shipwrecks and war defences or may even be remnants of an old 'scar' created by cutting the bar many years ago.

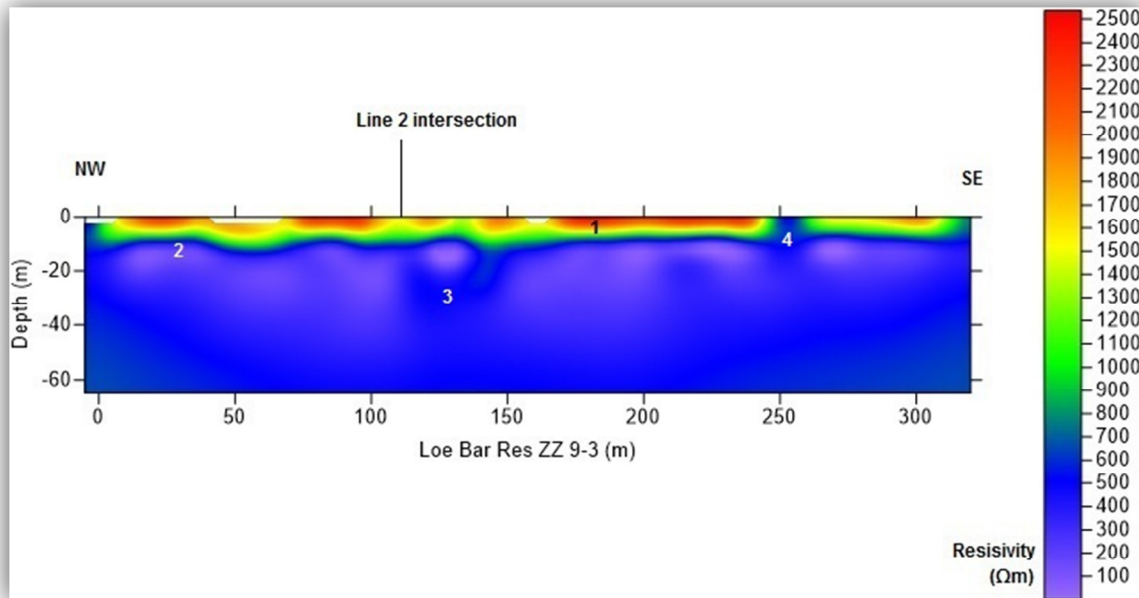


Figure 63: Resistivity pseudo-section of line 1 using a ZZ array (processed by Mr N.A. Wood). Smoothing coefficients: Horizontal = 9, Vertical = 3.

Applying contours to the image (figure 64) can clarify the large channel feature ranging in depth from approximately 10m at the edges to 60m towards the centre. Contours are created only from generic values and are not necessarily representative of the most definitive parts of features, however they do provide an effective aid in defining trends. The other clear features highlighted by the contours are the area under the scar as well as the mystery feature discussed near the surface at 250m along the line.

When the bar was last cut in 1984 a clear trend was seen in its regrowth and repair, with the closure of the cut occurring initially at the sea-ward side of the bar and gradually closing inwards, as is represented photographically in appendix A. The cut is documented as only reaching a depth of 10m, however freshwater would have been present in the channel for a number of years afterwards, with the photographs showing only partial fill up to June 1989, and total fill by the following December. In this time, fresh water may have seeped into the porous sand. The possibility may also exist for a freshwater channel to be present, taking water from the lake to the sea. Although it was stated in 1967 that no water passes through the bar, this information was gathered before the bar was last cut and may be outdated in terms of assessing the potential passages deeper within the bar. In order to further investigate this theory, some more resistivity lines would be required in order to distinguish the shape and extent of this feature, or boreholes drilled to obtain physical samples at known depths.

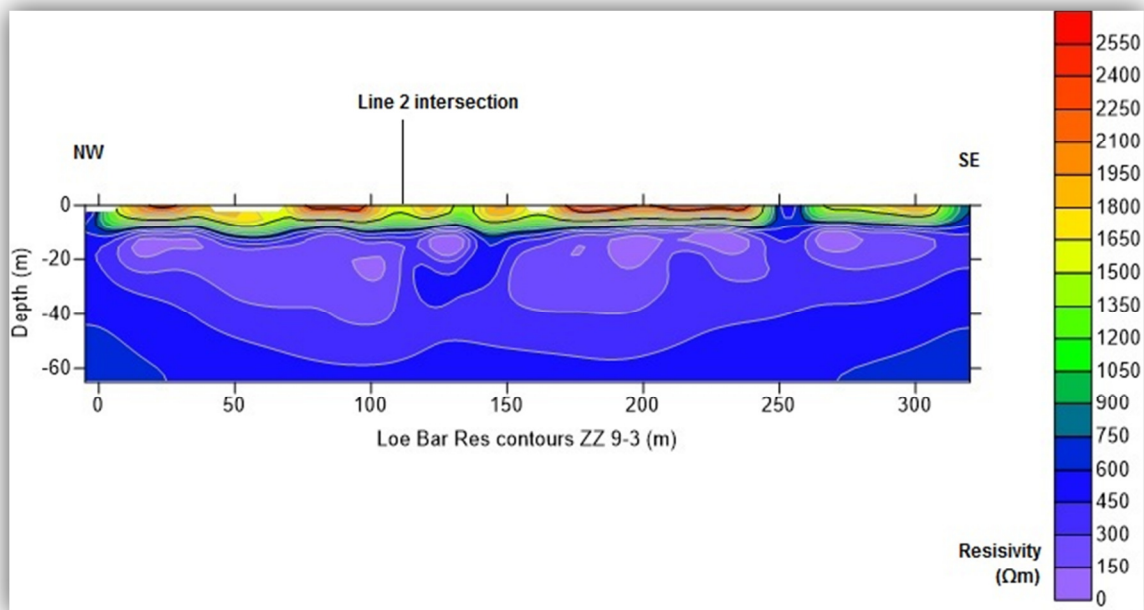


Figure 64: Resistivity pseudo-section of line 1 using a ZZ array. Contours are applied to clarify values in the image (processed by Mr N.A. Wood). Smoothing coefficients: Horizontal = 9, Vertical = 3.

Figure 65 shows the ZZ array data displayed with a maximum scale of 1,200 Ωm . This allows a more varied scale at increased depths, showing more clearly the larger lens-shaped channel running the length of the bar and the smaller channel between 100 and 150m along the line. While these two features show similar resistivity values, it does not necessarily indicate they are comprised of the same material.

Sand typically shows a high resistivity, as is seen in the upper layers of the bar, yet water, particularly saline, will significantly lower this, causing saturated rock to have lower levels of resistivity. The compaction of the sand within this channel would lead to the reduction in resistivity seen with depth. The suspected smaller channel 100-150m along the line could contain sand/shingle saturated with fresh water, while the rest of the bar is saturated with salt water. Water saturation counts for one of the biggest influencers of resistivity values of a medium. The formation in which the large channel is carved, shows a moderate value ranging from approximately 450 to 650 Ωm . According to the British Geological Interactive mapping, this is likely to be the Portscatho formation. As this lies beneath the water table and the sea, the rock is likely to be saturated, potentially with salt water, showing lower resistivity values.

Using the LiDAR data, a cross-section of the area parallel with the bar can be produced coinciding with the resistivity line (figure 66). When the resistivity values are superimposed onto this cross-section, the structure of the channel under the bar matches well to the morphology of the cliffs either side (figure 67). This provides further evidence for the large channel feature representing the base of the old ria, cut into the portscatho formation, with the potentially glacial sediments occupying the bar.

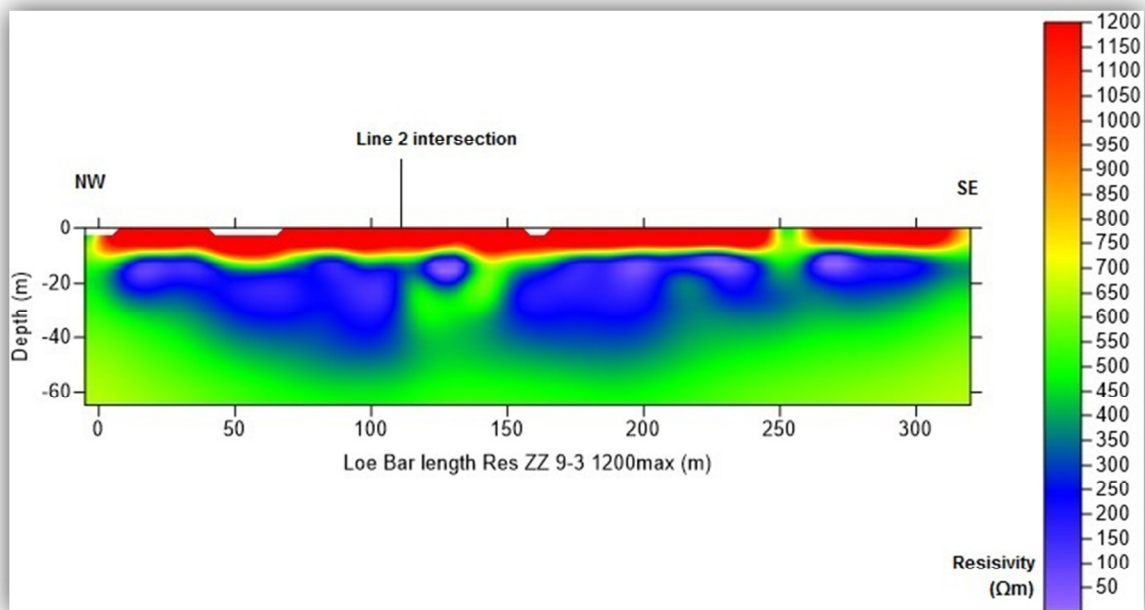


Figure 65: Resistivity pseudo-section of line 1 using a ZZ array. Scale is altered to show a maximum value of 1200 Ωm (processed by N.A. Wood). Smoothing coefficients: Horizontal = 9, Vertical = 3. Scale units Ωm .

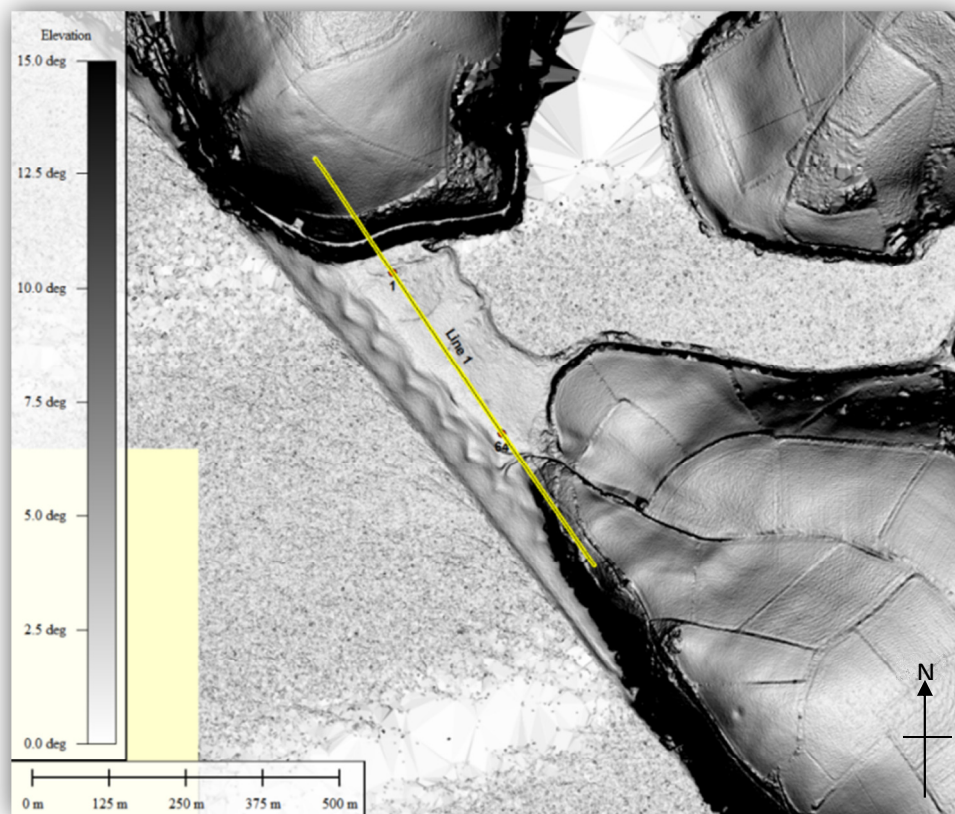


Figure 66: Position of cross section generated for comparing the morphology of the channel feature with that of the surrounding valley in figure 67.

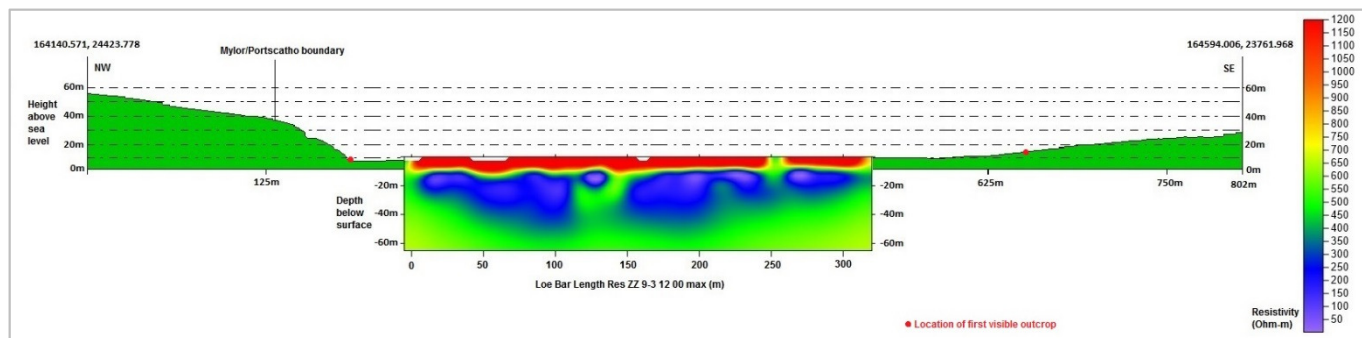


Figure 67: Cross section through LiDAR data (location marked in figure 66) with resistivity data superimposed (top scale of 1200 Ωm), showing a realistic match between the shape of the valley and the increase in resistivity potentially showing the bottom of the ria.

Outcrop localities of rocks at the northern end of the bar are visible at the contact between the sand and cliff, providing evidence of where the structure of the ria exists. The only section of the valley which therefore remains subject to interpretation, is the section between the outcrops and the resistivity line, yet with evidence such as that demonstrated in figure 67, a feasible connection can be drawn between these two features.

The boundary location separating the Mylor Slate and Portscatho formations according to the BGS is also visible in figure 67. A normal fault dipping in a South-easterly direction is said to separate the two units, yet the exact direction of dip is difficult to determine. The Carrick thrust which initially provides this boundary also dips to the south east and is said to vary in thickness by as much as several kilometres. In the data produced it is clear that no obvious fault exists as there is no clear evidence showing separation of two areas of differing resistivity. It must be remembered however that the outer lower corners of the pseudo-section are subject to error given the lack of data readings which are taken in these areas.

One feature missing from all of the profiles is the adit which takes water from the lake to the sea. This is because its location is too far north to have been captured by the line.

Coastal Salt Water Incursion

Todd (2005) states that the movement of seawater towards fresh groundwater occurs in the form of a curved slope due to the heavier saline water sinking beneath the freshwater. Figure 68 shows the typical interaction between salt water from the ocean meeting an unconfined coastal freshwater aquifer. With the resistivity values being as low as they are, it is likely that the interface between salt and fresh water under the bar could be further to the northeast of where line 1 was located. The strength of the sea pushing water inland is likely to be stronger than that of the freshwater pushing from the lake through the reportedly blocked bar and may have led to the interface moving inland by several metres on account of this very low resistivity.

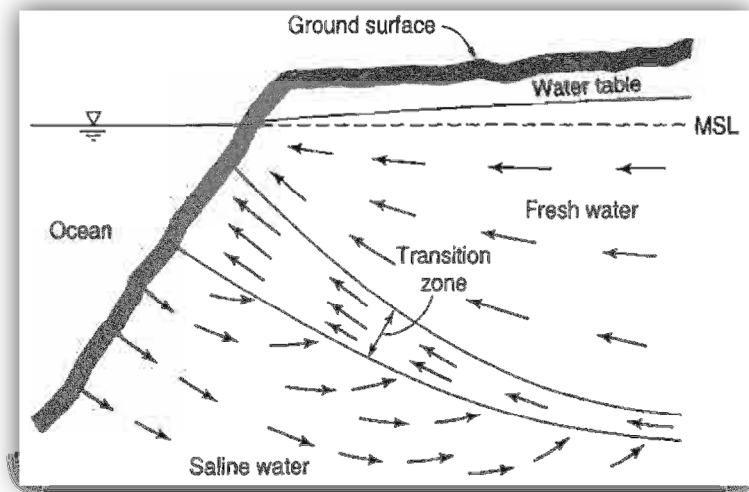


Figure 68: Vertical Cross-section showing typical interactions of fresh and saline water in an unconfined coastal aquifer (Todd, 2005).

16.3.2 Line 1 Induced Polarisation

Mapping salt water intrusions in coastal aquifers which include clay layers may be difficult if only resistivity is used. Sand which has been saturated with salt water shows similar characteristics to clay layers when seen in a resistivity survey. Induced polarisation however can differentiate between them due to clay having an increased chargeability (Jones, 2007; Gazoty et al, 2012). The high ionic conductivity of saline waters typically cause them to show a poor IP response (Sharma, 1997).

Wenner Array

The Wenner array IP image (figure 69) shows a linear distribution of higher values (1200 and above) up to 10m depth. At around 75m and 290m along the line, small areas exist containing IP values of more than 3000 at depths of around 4-8m.

At approximately 125m along the line, a small area of moderate IP values between 1000 and 1200 coincides with the location of the cut, its peak at 25-30m depth. Above this area, the surface shows lower IP values than along the rest of the line. This also coincides with the section of the bar where little or no vegetation exists.

At around 200m along the line and 30m depth, an area with IP values in the region of 1200-1800 can be seen. In general, higher levels of IP suggest the presence of material such as clays or ores, and are effective in showing up mine waste. This could be an explanation for the presence of these higher values, perhaps with this being the location of a previous cut. No definitive explanation for this feature exists without further exploration.

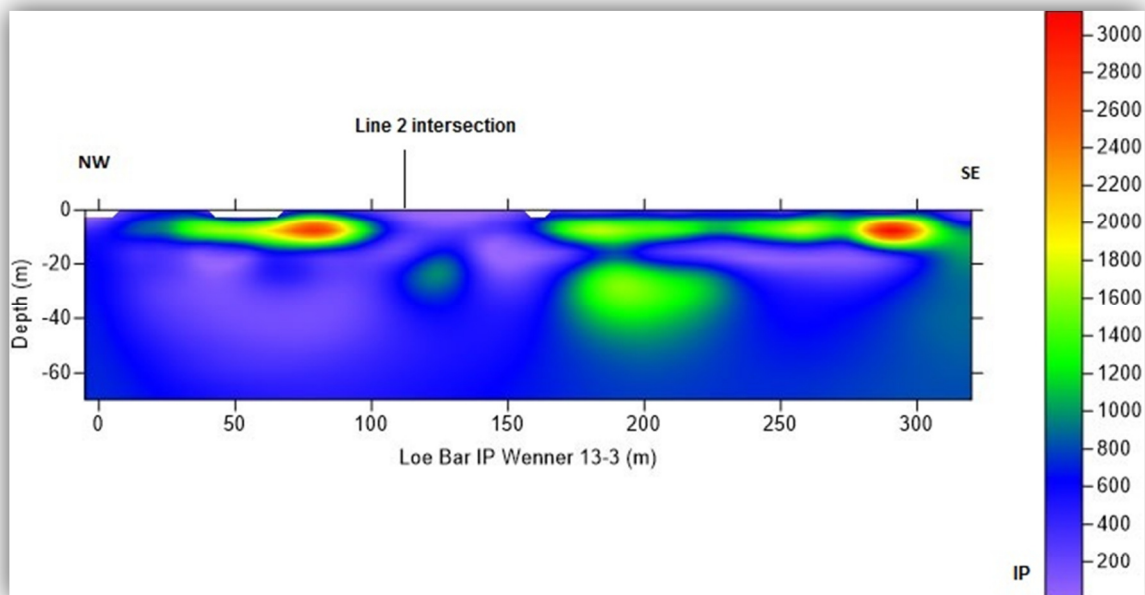


Figure 69: Induced polarisation pseudo-section of line 1 using a Wenner array (processed by N.A. Wood). Smoothing coefficients: Horizontal = 13, Vertical = 3.

ZZ Array

Quite differently to the Wenner array, and perhaps more accurately, the ZZ array shows more specific pockets and small lenses of higher IP values, mainly at a depth of 10m along the line (figure 70). This strong IP signature implies that the low resistivity band of around 10m depth believed to be sea water may have instead been caused by the presence of clay or possibly silt, given the description by Rendel that boreholes A and B have a layer of silt recorded at similar depths to this signature.

The increased data points collected by the ZZ array appear to have once again had an effect on the clarity and specific locations of features. A strong IP signature is present around 75m along the line, suggesting a deposit of clay-type material. While further investigation may need to be done to find more information on this feature, it is important to consider how the shape of the bar has changed over time. Figure 71 shows that line 1 crosses the paleo-shoreline of the lake which was in place in the late 1800s. This strong signature at 75m may be due to a larger deposit of clay-like materials which may also contain mine wastes given the likely provenance.

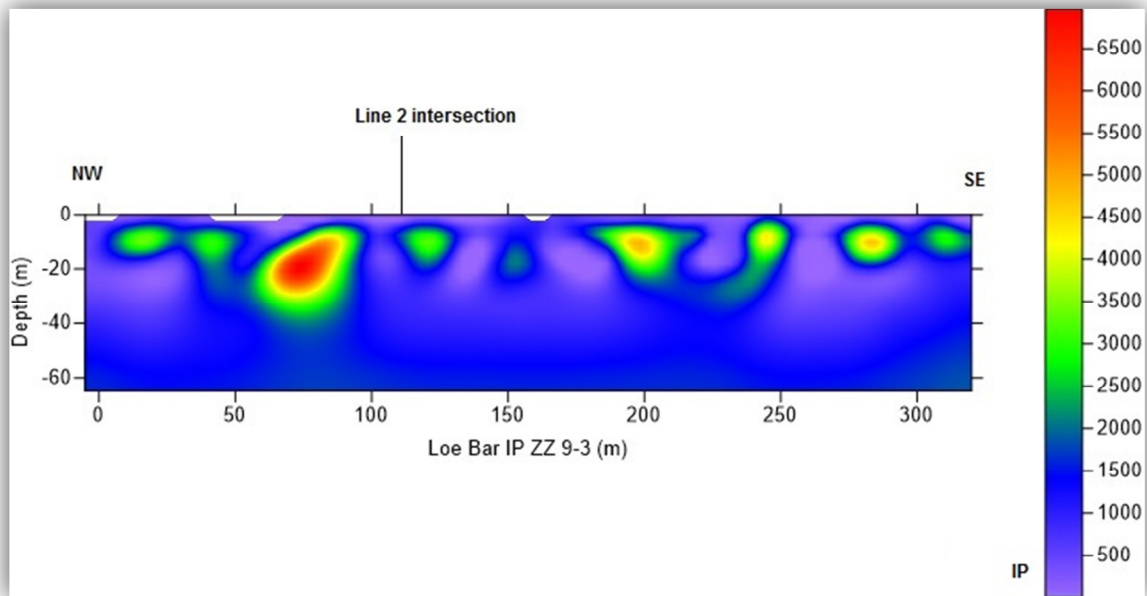


Figure 70: Induced polarisation pseudo-section of line 1 using a ZZ array (processed by N.A. Wood). Smoothing coefficients: Horizontal = 9, Vertical = 3. Scale units Ωm .

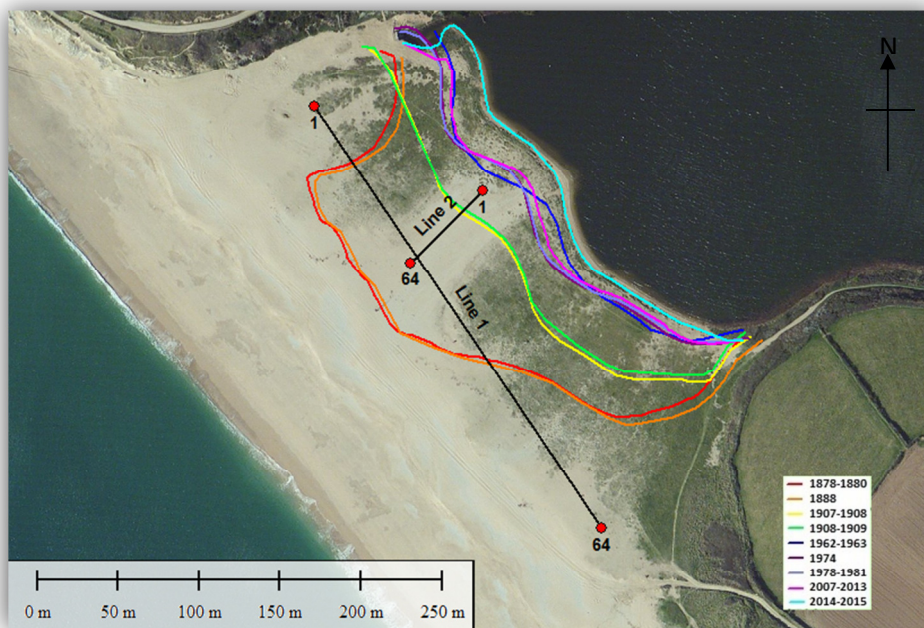


Figure 71: Spatial relationship between resistivity lines 1 and 2 and the changes in shoreline over time.

16.3.3 Line 2 Resistivity

For the transverse line, only the ZZ array was used, reaching a depth of around 13m. As a result, only the higher resistivity material at the surface is seen, although this does provide some clarity of features within this layer. The most highly resistive material exists from the surface to a depth of approximately 5m. This can again be explained by the sand being increasingly dry nearer the surface. Values seen along line 2 are higher than those experienced in line 1, showing up to $2000 \Omega\text{m}$ higher. At approximately 50m along the line, an area showing values above $4000 \Omega\text{m}$ is present, yet it is unclear what could be causing this result. A suggestion for the cause of this feature could be that a historical fragment exists there. Further investigation of the area using a magnetometer or intrusive techniques such as boreholes or test pits would supply more information and facilitate determining what this anomalous feature may consist of.

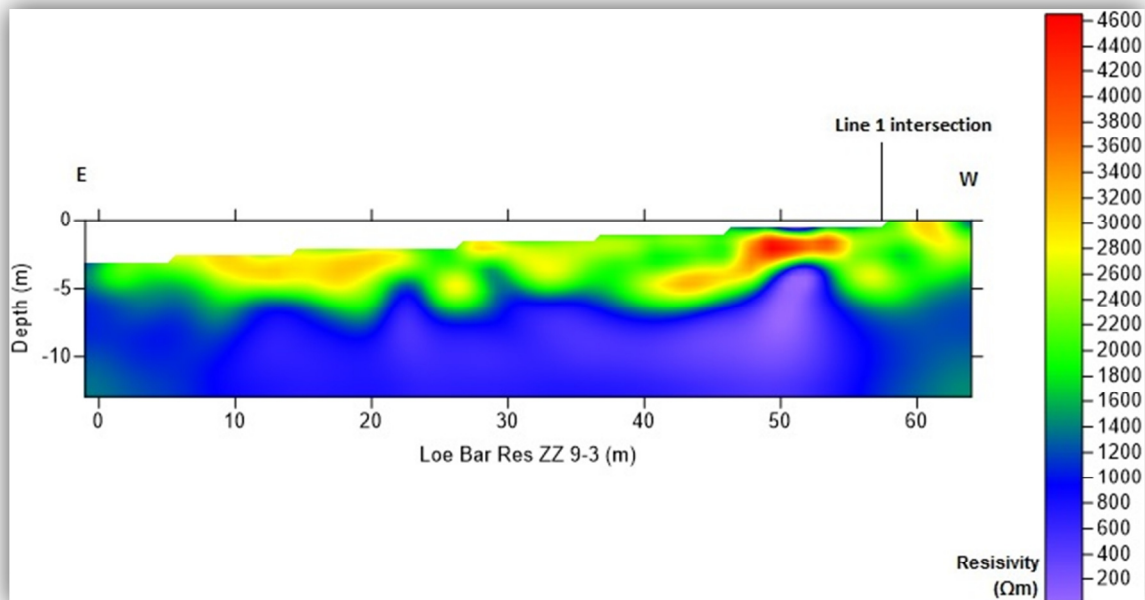


Figure 72: Resistivity pseudo-section of line 2 using a ZZ array (processed by N.A. Wood). Smoothing coefficients: Horizontal = 9, Vertical = 3. Scale units Ωm .

16.3.4 Line 2 Induced Polarisation

In the same way as line 1 showed sporadic lenses of material with a high IP value, line 2 also shows similar characteristics. The distribution of these features again contradicts the expectations. Rather than showing a high IP value near to the lake, a more varied distribution exists along the line. One possible explanation for this was that as the bar was repairing itself, from the seaward edge inwards, deposition of clay/silt possibly containing mine waste occurred in the closing channel. The bottom of the lake is well documented by O'Sullivan et al (1982) to consist of clay as much as several metres thick. The clay encountered in line 2 implies that in the time taken for the bar to heal after the last cut, quantities of the clay were deposited in the residual channel. The slow yet sudden growth patterns of the bar then allowed for the capture of this clay during storm events, when sand would be taken over the top of the bar and deposited, entrapping these clay pockets. Theories such as this could be looked into more by running more resistivity lines on the bar in multiple and differing locations.

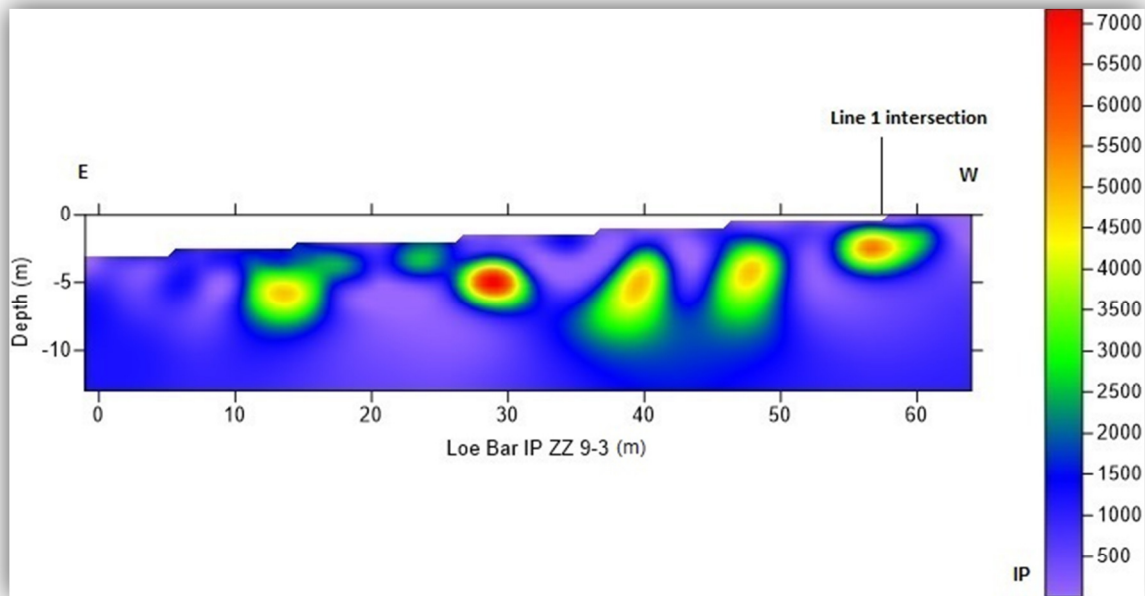


Figure 73: Induced Polarisation pseudo-section of line 2 using a ZZ array (processed by N.A. Wood). Smoothing coefficients: Horizontal = 9, Vertical = 3.

16.4 Correlation with Rendel's Bores

James Rendel's findings from the bores that were drilled in the 19th Century can be loosely applied to the results seen in line 1 of the resistivity data. In the absence of a map of the bores, some assumptions had to be made in order to determine the locations of the bores:

1. Carminow Point is at the Southern boundary of the bar (involving bores C, D and E).
2. Weeth Green is the northern end of the bar (involving bores F, G and H).
3. The elevation of the bar is the same level that is seen today.
4. Lateral continuity exists across the bar, allowing the points to be put on the cross section in the same point regardless of their position perpendicular to the line.

These assumptions have allowed the rough positioning of the bores onto the resistivity cross section, however a proportion of the ground over which line 1 is located (between 35 and 185m along the line), has been built up since 1878, meaning the observations made by Rendel in 1837 are not applicable to this part of the pseudo section and would most likely have been made closer to the sea. Figure 74 shows Rendel's findings marked on the pseudo section.

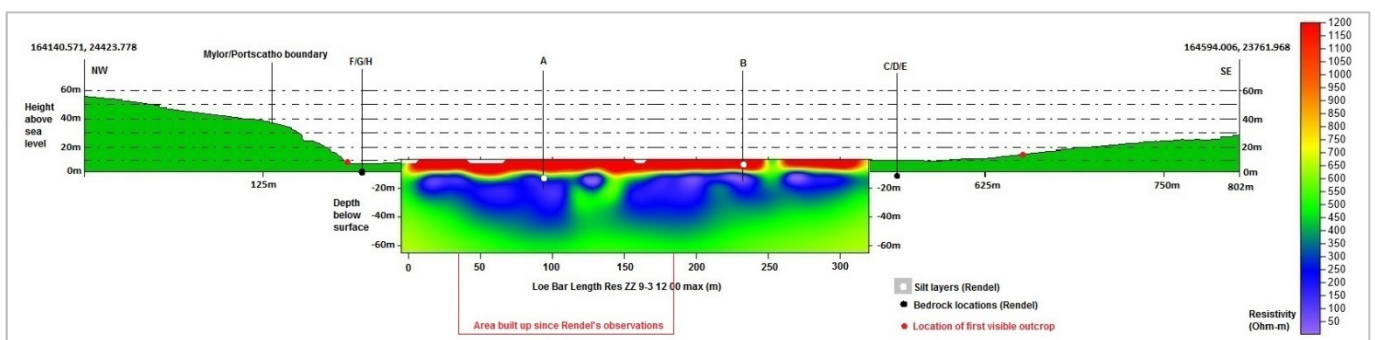


Figure 74: Cross section with pseudo-section superimposed (as in figure 67) with the addition of probable locations of Rendel's bores (subject to assumptions). Points on the bore locations represent features of interest found.

The points at which Rendel found underlying 'killas' or bedrock towards the edges of the bar coincide with the inferred boundary between the outcrops and the resistivity line.

The silt layer found in boreholes A and B (points marked on bore lines in figure 74) are at depths comparable to those at which a layer of clay or silt has shown in the IP results. Although borehole A would have been closer to the sea as previously mentioned, it seems that growth of the bar in this area has incorporated a layer of clay which has remained at a depth consistent to the observations of 1837. This implies that as the bar grows, this silt or clay layer is always incorporated as part of its growth.

The depth of rock and killas found in boreholes C, D and E, represented by the black point on the bore location, roughly coincide with the expected depths of the channel bed when a line is extrapolated from the nearest outcrop to where the channel is first seen in the resistivity results.

The presence of organic material and trees in bores F, G and H seem somewhat realistic considering the steep gradient of the slope. A number of trees and other species of vegetation appear unstable on this section and are likely to have fallen in the past and been covered by the rapid and abundant sedimentation rates.

16.5 Further Study

To develop more of an understanding of the lateral changes in resistivity and IP, several more resistivity lines would be required. Sophisticated equipment can be used to carry out 3D monitoring, such as was used by Allah et al, 2013 on a beach in Japan, yet is expensive given that sufficient data could be collected using a number of lines similar to those used in this survey. This method was effective when used by Beamish (2012). Establishing a grid pattern over which to record resistivity could greatly aid in understanding more about the characteristics and lateral changes in material of the bar.

The lack of prolific IP signatures towards the lake shore in comparison to the rest of the bar has shown an inconsistency to the eye witness accounts documented by Coard (1987) of there being a noticeable amount of clay in the area near the lake. More and longer transverse resistivity lines could be carried out in an attempt to discover if this clay area does exist in the lake-ward side of the bar in areas not recently cut.

Further understanding of the resistivity results would be aided by borehole drilling in order to confidently create links between resistivity values seen in the sections and physical data at specific locations. Attwa et al (2011) did exactly this in a study recording the extent of saltwater incursion on the Northern coast of Germany, drilling one borehole in a sunken, filled channel and two more at either side, to officiate proposed findings and aid in the completion of definitive cross sections of the subsurface geology and other characteristics.

16.5.1 Flooding in Helston – a solution?

With the town of Helston occasionally becoming victim to flooding, one possible solution to reduce the threat, in addition to those proposed by Northey et al (2013), may be to cut the bar in multiple locations at sequential times. The cut carried out in 1984 is most likely responsible for the presence of a freshwater channel which can be assumed is taking water from the lake to the sea. If this is proven to be the case through further tests, cutting the bar in other locations may disperse the clay which is currently blocking the passage of water and enable freshwater to once again flow to the sea. The quantities of water that will travel through the bar are unlikely to match those witnessed by Rendel in 1834 due to the bar's increased width, as well as the small amounts of clay which will inevitably be incorporated when the bar repairs itself, as have been noted by the resistivity results. This could still provide a relatively cost-effective solution to relieve pressures on the sluice in times of high rainfall, yet would require further study to quantify predicted volumes as well as highlight any environmental consequences. Some potential environmental issues can be deduced by studying the present scar, which shows the disturbance of vegetation on the bar, and the consequential destabilisation of the sand.

17 Recommendation for Further Study at Loe Bar

Conducting a magnetic survey of the area would provide another means for the investigation of the subsurface. Features such as debris left by shipwrecks and war defences would most likely show anomalies due to their predominantly metallic nature. Loe Bar is advised by a number of tourism websites as being both a good place for people who use a metal detector and an interesting place for divers keen to see shipwrecks just offshore. Other than finding historic objects, a trend may also exist in the metallic and more specifically iron content in the clay/silt layer seen within the bar reportedly at the lake edge. The presence of a haematite-rich layer in the clay at the bottom of Loe Pool hints that the clay present in the bar may show a trend in magnetic results.

A number of magnetic surveys around wreck sites have been carried out around the area but a magnetic survey of the bar is not documented as having been carried out. In 2005 Wessex Archaeology was commissioned by English Heritage to complete a site assessment of the wreck of the *President* which lies offshore from the bar. In 2007 they were also commissioned to carry out a similar assessment on *St Anthony*, wrecked off Gunwallow (Spalding, 2015). Other than specific site surveys of this nature, which mainly used underwater metal detectors, the bar itself has not been the subject of a full magnetic survey. A straight-forward magnetic survey could be carried out using the GSM-19 magnetometer which is kept by the Camborne School of Mines, to show the presence and extent of any potential magnetic anomalies.

18 Conclusion

Thanks to a well-documented history of Loe Bar, a substantial understanding of the area can be derived, allowing for methods of data collection to be fully prepared and pinpointed to specific areas of study.

The method of using a total station to complete a topographic survey worked successfully at Loe Bar and led to the production of an adequate plan showing the bar's main features on the lake-ward side. Surveys in the future can be compared to one another to accurately monitor the changing morphology of the bar. The speed of the survey will vary by how much data is required, for example if only the lake edge is required, the data can be collected in a matter of around half an hour.

The sentripod can provide sufficient resection results and show a clear advantage in the time taken to set up for the survey. The ease in removing and replacing them at various points, reduces the possibility of public interference. Another clear advantage of the sentripod was the reduction in heavy equipment required, particularly given the limited vehicular access to the site. However, accuracies in resection when using the sentripods were seen to decrease with distance, meaning future surveys will need to be completed from the northern end of the bar. Care must be taken to ensure that the sentripods are in good view when setting up the total station. If the sentripod at Base NW is obstructed by the cage then a bolt outside the cage can be used, for which coordinates have been derived. It is possible that one set-up will be sufficient to survey the bar. Any error expansion towards the southern end of the bar can be quantified by noting the coordinates of Base SE to compare with the recorded GPS points.

The resistivity survey provided an effective insight into subterranean features at Loe Bar. Underneath the dry sand on the surface, a layer of low resistivity showed either the injection of sea water or the inclusion of clay into the structure of the bar. The induced polarisation was proven to work well with the resistivity to deduce that this layer was in fact more likely to be clay. A proposed freshwater channel exists underneath the area of the scar created by the last occurrence upon which the bar was cut. This is shown by a layer of slightly higher resistivity than the surrounding sediments saturated with salt water. The sunken channel of the ria was seen to reach a maximum depth of approximately 60m and matches well to the subaerial topography either side of the bar. In further study, a magnetic survey would work well with the resistivity data, adding to interpretation of the very highly resistive objects seen in the sands at the surface, as well as determining the presence of any notable haematitic sediments in the bar.

References

- Allah, S.A., Mogi, T., Ito, H., Jomori, A., Yuuki, Y., Fomenko, E., Kiho, K., Kaieda, H., Suzuki, K. and Tsukuda, K., 2013, Three-dimensional resistivity characterization of a coastal area: Application of Grounded Electrical-Source Airborne Transient Electromagnetic (GREATEM) survey data from Kujukuri Beach, Japan, *Journal of Applied Geophysics*, Volume 99, December 2013, pages 1-11.
- Almeida, L.P., Masselink, G., Russell, P.E., Davidson, M.A., Poate, T.G., McCall, R.T., Blenkinsopp, C.E. and Turner, I.L., 2013, Observations of the swash zone on a gravel beach during a storm using a laser-scanner, *Proceedings 12th International Coastal Symposium (Plymouth, England)*, *Journal of Coastal Research*, Special Issue No. 65, pp. 636-641, ISSN 0749-0208.
- Almaeida, L.P., Masselink, G., Russel, P.E. and Davidson, M.A., 2014, Observations of gravel beach dynamics during high energy wave conditions using a laser scanner, *Geomorphology*, 228 15-27.
- Attwa, M., Günther, T., Grinat, M. and Binot, F., 2011, Evaluation of DC, FDEM and IP resistivity methods for imaging perched saltwater and a shallow channel within coastal tidal flat sediments, *Journal of Applied Geophysics*, Vol. 75, Issue 4, p 656-670.
- Austin, M.J. and Masselink, G., 2006, swash-groundwater interaction on a steep gravel beach, *Continental Shelf Research*, Volume 26, Issue 20, pp 2503-2519.
- Beamish, D., 2012, A study of saline incursion across an inter-tidal zone on Anglesey, Wales using airborne conductivity data, *Near Surface Geophysics*, 10, 171-184.
- Bird, E.C.F. and Schwartz (eds), M.I., 1985, *The World's Coastline*, Van Norstrand Rheinhold, New York, 1071 pp.
- Bray, M.J., 1990, Landslide and littoral zone sediment transport, in *Landslides of the Dorset Coast* (ed R.J. Allinson), British Geomorphological Research Group Field Guide, British Geomorphological Research Group, London, pp 107-117
- British Geological Survey, 2015, Interactive Mapping, Natural Environment Research Council, [ONLINE] Accessed on 10th July 2015, Available at <http://mapapps.bgs.ac.uk/geologyofbritain/home.html>.
- Buscombe, D. and Masselink, G., 2006, Concepts in Gravel Beach Dynamics, *Earth Science Reviews*, Volume 79, Issues 1-2, pp 33-52.
- Coard, M.A., 1987, Paleolimnological study of the history of Loe Pool, Helston and its catchment, Department of Environmental Sciences, Plymouth Polytechnic
- Coastal Processes Research Group, 2015, University of Plymouth, [ONLINE], Accessed on 23rd July 2015, Available at <http://www.research.plymouth.ac.uk/coastal-processes/projects/nupsigsite/science.html>
- Cornwall Guide, 2015, Legend of Jan Tregeagle, [ONLINE] Accessed 3rd July 2015, Available at: <http://www.cornwalls.co.uk/myths-legends/jan-tregeagle.htm>
- Cornwall River Authority (1946): Report on the canalisation of the River Cober below Helston. C.R.A., Truro.
- Cornwall River Authority (1967): South West Cornwall water supplies. Report of the Chief Engineer to the Water Committee, 29th September, 1967.
- Dahlin, T. and Loke, M.H., 1998. Resolution of 2D Wenner resistivity imaging as assessed by numerical modelling, *Journal of Applied Geophysics*, 38, 237-249.

Davidson-Arnott, R., 2010, *An introduction to Coastal Processes and Geomorphology*, Cambridge University Press, pp. 438, ISBN 978-0-521-87445-8.

Davies, D., 2012, *Loe Bar – A Chronological Photo History*, Presentation, [ONLINE] Accessed on 6th July 2015, Available at: <http://loepool.org/research-reports/>

Davies, D. and Matthews, G.G., 2002, *Loe Bar – A Geomorphological Analysis*, Helston History, [ONLINE], Accessed on 9th July 2015, Available at <http://freepages.history.rootsweb.ancestry.com/~helstonhistory/loebarpage.htm>

Day, G.A. and Edwards, J.W.F., 1983, Variscan thrusting in the basement of the English Channel and SW Approaches, *Proceedings of the Geologists Association*, 74, 265-287.

Designated Sites; Natural England, 1986, *SSSI Glossary* [ONLINE] Accessed on 9th July 2015; Available at: <https://designatedsites.naturalengland.org.uk/SiteDetail.aspx?SiteCode=S1003319&SiteName=loepool&countyCode=&responsiblePerson=>

Dornbusch, U., 2002, *Changes of Pagham Harbour*, Coastview, University of Sussex, [ONLINE], Accessed on 22/07/2015, Available at <http://www.sussex.ac.uk/geography/researchprojects/coastview/Estuaries/pagham-slides.htm>

English Heritage, 2015, *Defended Cornwall: Fear of Invasion*, Flying Through Cornwall's Past, [ONLINE] Accessed on 27th August 2015, Available at: <http://www.historic-cornwall.org.uk/flyingpast/fear.html#beach>

Ferraccioli, F., Gerard, F., Robinson, C., Jordan, T., Bieszczuk, M., Ireland, L., Beasley, M., Vidamour, A., Barker, A., Arnold, R., Dinn, M., Fox, A., Howard, A. (2014). *LiDAR based Digital Terrain Model (DTM) data for South West England*. NERC Environmental Information Data Centre. <http://doi.org/10.5285/e2a742df-3772-481a-97d6-0de5133f4812>

Gazoty, A., Fiandaca, G., Pedersen, J., Auken, E., Christiansen, A.V. and Pedersen, J.K., 2012, Application of time domain induced polarization to the mapping of lithotypes in a landfill site, *Hydrology and Earth System Sciences*, 16, 1973-1804.

Gerard, F., 2014, *LiDAR Quality Control Report: Processing of LiDAR data for the South West TELLUS Project*, Approved by Dr Alison Matthews, Geomatics, Environment Agency, National Operations.

Goudie, A., 2013, *The Human Impact on the Natural Environment: Past, Present and Future*, Seventh Edition, Published by John Wiley and Sons Ltd. 376 pp. ISBN 978-1405127042.

Johns, C.A., 1874, *A week at the Lizard*, S.P.C.K., London.

Jones, F., 2007, *Introduction to Induced Polarisation Surveying*, UBC Earth and Ocean Sciences, [ONLINE] Accessed on 27th August 2015, Available at http://www.eos.ubc.ca/ubcgif/iag/methods/meth_2/ip.pdf.

Kaplan, E. and Hegarty, C.J. (eds), 2006, *Understanding GPS Principles and Applications*, second edition, Artech House Inc., pp 703, ISBN 1-58053-894-0.

King, C.A.M., 1972, *Beaches and Coasts*, Edward Arnold, London, 2nd Edition, 570 pp.

Larn, R., and Carter, C., 1969, *Cornish Shipwrecks: the South Coast*, David and Charles, pp 254, ISBN 0330234749.

Le Gall, B., Le Hérisse, A. and Deunff, J., 1985, New palynological data from the Gramscatho Group at the Lizard Front (Cornwall); Palaeographical and geodynamical implications, *Proceedings of the Ussher Society*, 6, 237-253.

Loe Pool Forum, *Breaking the Bar*, 2015 [ONLINE] Accessed on 9th July 2015, Available at <http://loepool.org/loe-bar/>

Loke, M.H., 1999, Electrical imaging surveys for environmental and engineering studies, A practical guide to 2-D and 3-D surveys, From Geomatrix Earth Science Ltd, Available at: <http://www.geomatrix.co.uk/tools/application-notes/Lokenote.pdf>

Masselink, G., 2015, Impact of 2013-14 Storms on Coastal Geomorphology in SW England, Geographical Association, Presentation slides, [ONLINE] Accessed on 23rd July 2015, Available at: http://www.geography.org.uk/download/GA_conf15_impactof2013-4stormsoncoastalgeomorphologyinSWEngland.ppt

May, V.J. and Hansom, J.D., 2003, Coastal Geomorphology of Great Britain, Edited by Clayton K.M., and Bird, E.C.F., Published by the Joint Nature Conservation Committee, 737 pp.

McDonald, R.J., Russill, N.R., Miliorizos, M. and Thomas, J.W., 1998, A geophysical investigation of saline intrusion and geological structure beneath areas of tidal coastal wetland at Langstone Harbour, Hampshire, Uk. Geological Society, London, Special Publications 130, 77-94.

Natural England, 1986, Designated Sites, Loe Pool SSSI description, [ONLINE], Accessed on 21/07/2015, Available at http://www.english-nature.org.uk/citation/citation_photo/1003319.pdf

Northey, A., Hein, R., Widgery, D., Wallis, A., Lutyens, V., Boothroyd, M. and Payne, J., 2013, Helston (Cober) Appraisal, Long List of Options, Black & Veatch, Project No. 122234, for Environment Agency.

O'Sullivan, P.E., Coard, M.A. and Pickering, D.A., 1982, The use of laminated lake sediments in the estimation and calibration of erosion rates, Proceedings of the Exeter Symposium, IAHS publ no. 137.

Ordnance Survey, 2015, A Guide to Coordinate Systems in Great Britain, Crown Copyright, pp 43.

Orford, J.D., Murdy, J.M. and Wintle, A.G., 2003, Prograded Holocene beach ridges with superimposed dunes in north-east Ireland: mechanisms and timescales of fine and coarse beach sediment decoupling and deposition, Marine Geology, Volume 194, Issues 1-2, pp 47-64.

Palacky, G.J., 1988, Resistivity Characteristics of Geologic Targets, in Investigations in Geophysics chapter 3 of Electromagnetic methods in applied geophysics-theory, vol. 1, edited by M. N. Nabighian, Soc. Expl. Geophys., pages 53-129.

Poate, T., Masselink, G., Davidson, M., McCall, R., Russel, P. and Turner, I., 2013, High Frequency in-situ field measurements of morphological response on a fine gravel beach during energetic wave conditions, Marine Geology, Volume 342, pages 1-13.

Rendel, J.M., 1837, Report on the practicability of forming a harbour at the mouth of the Loe Pool in Mount's Bay, near Helston, Addressed to the Rev. Canon Rogers of Penrose, Helston, published by Graham G Matthews 2003, [ONLINE], Accessed 3rd July 2015, Available at: <http://freepages.history.rootsweb.ancestry.com/~helstonhistory/helstonharbourpage.htm>

RICS, Guidance Note, 2014, Boundaries: Procedures for boundary identification, demarcation and dispute resolution, 3rd edition, RICS Professional Guidance, England and Wales, Published by the Royal Institute of Chartered Surveyors (RICS), ISBN 978 1 78321 044 2.

Roberts, N., 1998, The Holocene: An Environmental History, Second edition, Blackwell Publishing, 328 pp., ISBN 978-0631186380

Rogers, J.J., 1859, Strata of the Cober Valley, Loe Pool, near Helston, Transactions of the Royal Geological Society of Cornwall, 7, 352-4.

Selwood, E.B., Durrance, E.M. and Bristow, C.M., (Eds) 1998, *The Geology of Cornwall*, University of Exeter Press, 298 pp, ISBN: 0859895297

Sharma, P.V., 1997, *Environmental and Engineering Geophysics*, Cambridge University Press, 475 pp, ISBN 0521576326.

Shoreline Management Plan Review (SMP2), 2011, Discussion and Detailed Policy Development, Final Report, Conducted for Cornwall Council by Royal Haskins.

South West Coastal Group (SWCG), 2015, Aims and Objectives, [ONLINE], Accessed on 12th July 2012, Available at http://www.southwestcoastalgroup.org/about_objectives.html

Spalding, A., 2015, *Loe Bar and the Sandhill Rustic Moth: The Biogeography, Ecology and History of a Coastal Shingle Bar*, BRILL, pp 372, ISBN 9004270302.

Steers, J.A., 1946, *The Coastline of England and Wales*, Cambridge University Press, Cambridge, 644 pp.

Todd, D.K., 2005, *Groundwater Hydrology*, 3rd Edition, Wiley, New York, 636 pp.

Toy, H.S., 1934, The Loe Bar near Helston, Cornwall, *Geographical Journal*, 83, 40-8.

Treglown, T., 2011, *Porthleven in years gone by: Local shipwrecks*, T.Treglown, ISBN 0953901971.

Uren, J. and Price, B., 2010, *Surveying for Engineers*, 5th edition, Palgrave Macmillan, pp. 805, ISBN 9780230221574.

ZZGeo Company Website, last updated 2014, [ONLINE], Accessed on 20th July 2015, Available at: <http://www.zzgeo.com/index.html>

Appendix A: Loe Bar Since 1984

The recovery of Loe Bar after the last cut in November 1984 in photographs collected and made available by David Davies (2012). Dates are as stated.

June 1985



April 1986



June 1987



May 1988



June 1989



December 1989



June 1990



January 1991



March 1993



March 1994



January 1997



September 1998



October 2001



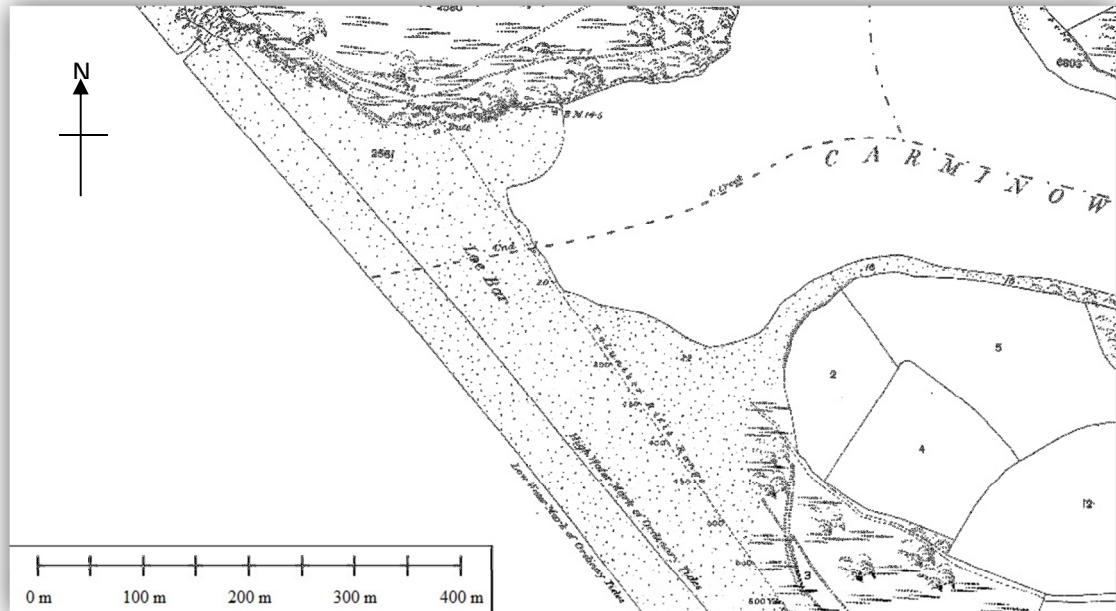
June 2003



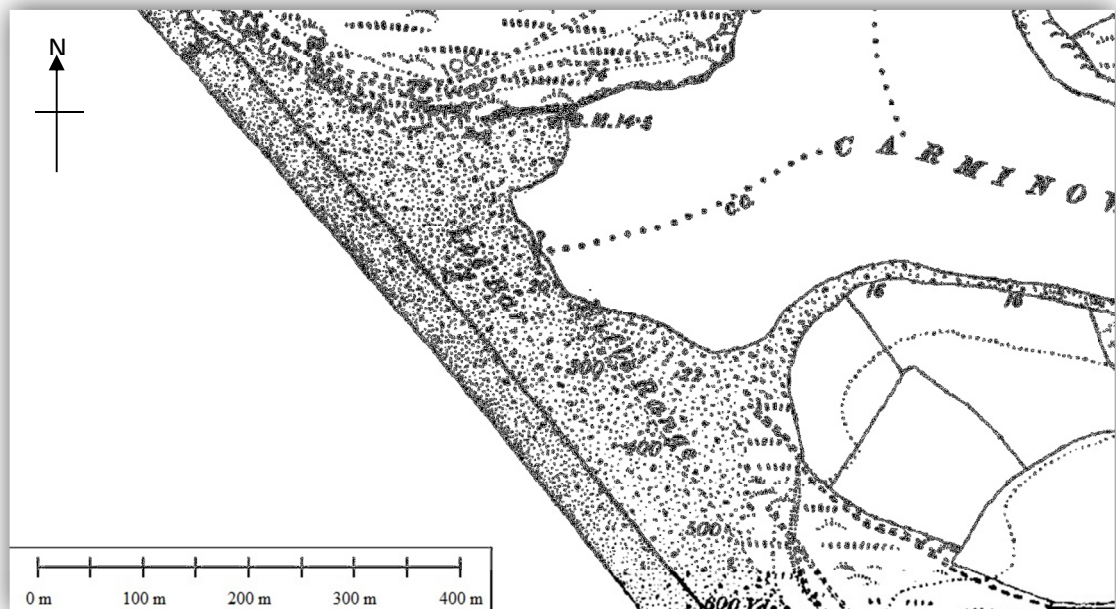
Appendix B: Loe Bar historical maps

The positions of Loe Bar have been mapped over time and are accessible from Edina Digimap Historic mapping. Below are maps of the bar which have been published in intervals of chronological order from 1887 to 1981 showing a distinct widening of the bar towards the lake.

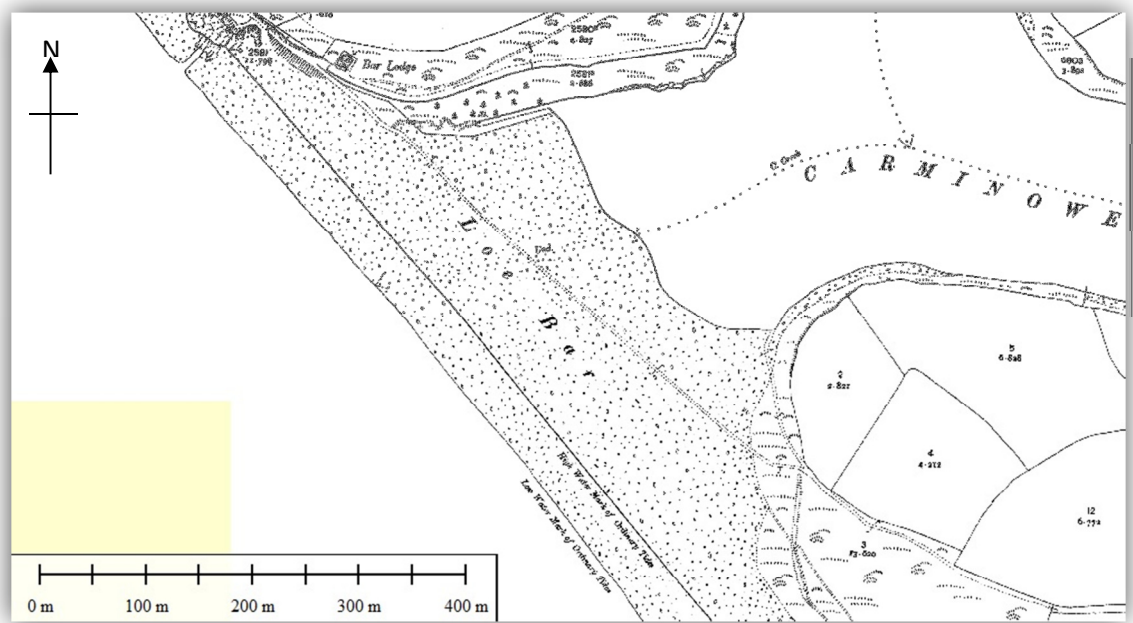
1878-1880



1888



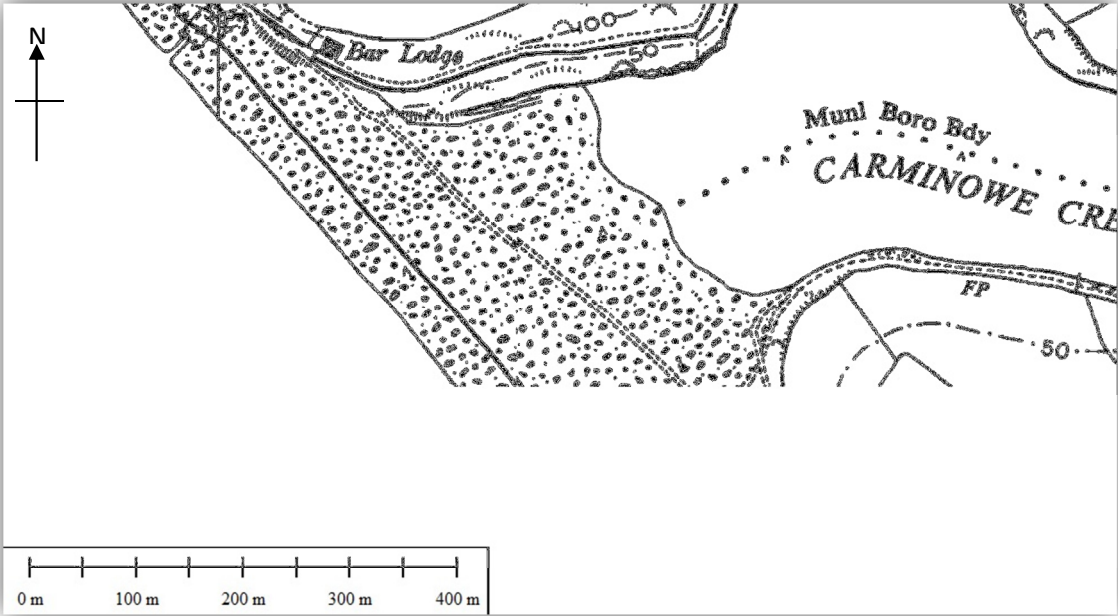
1907-1908



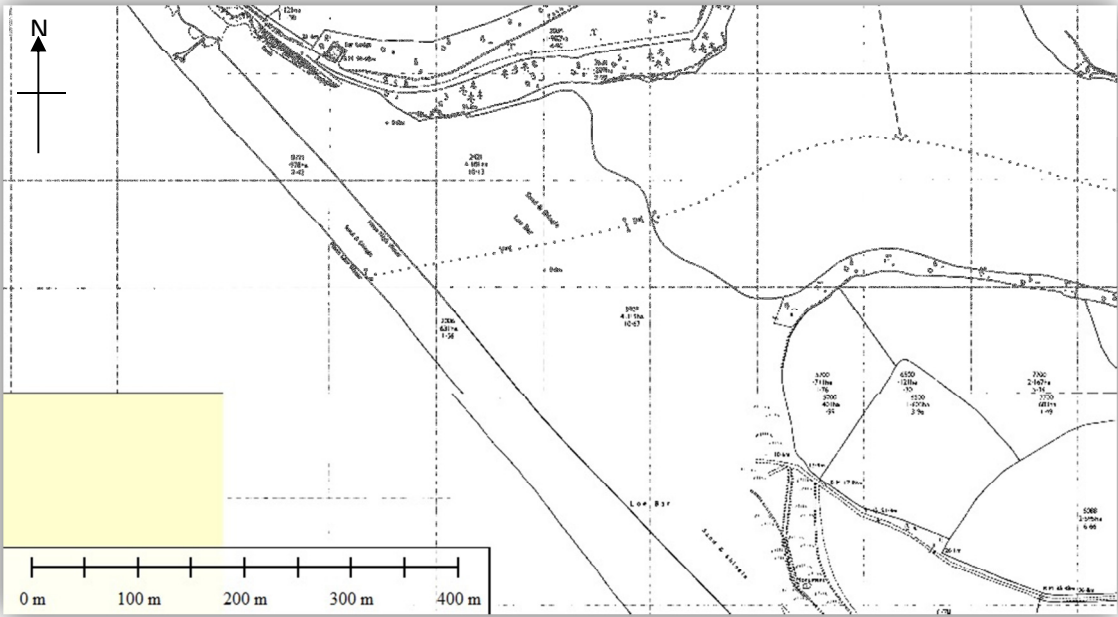
1908-1909



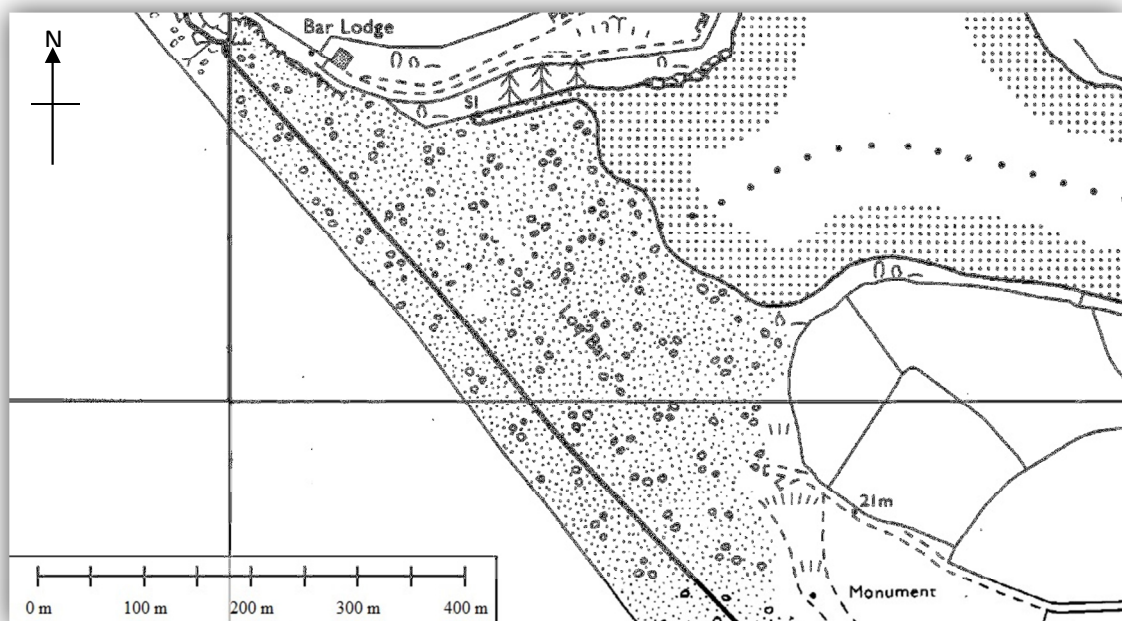
1962-1963



1974



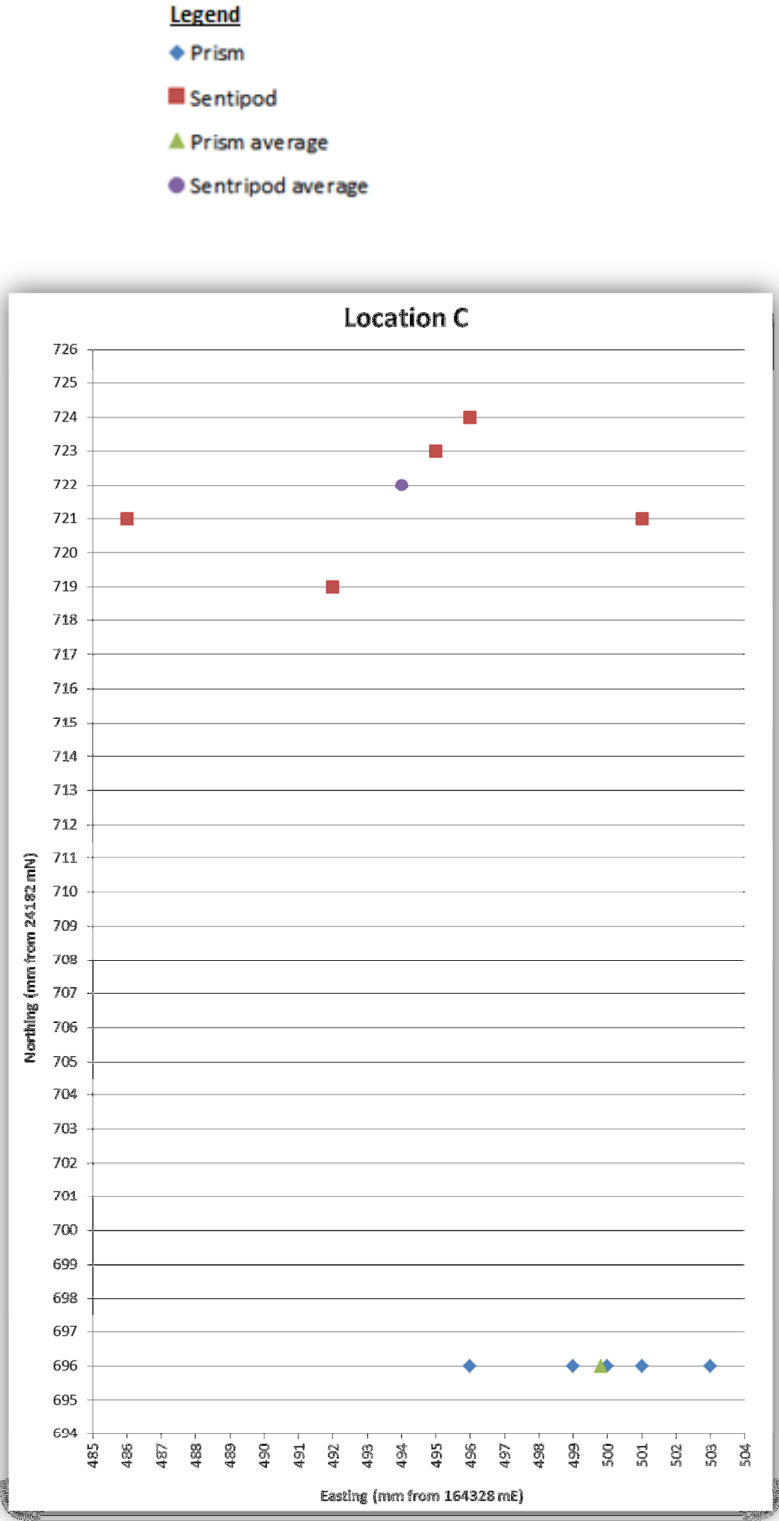
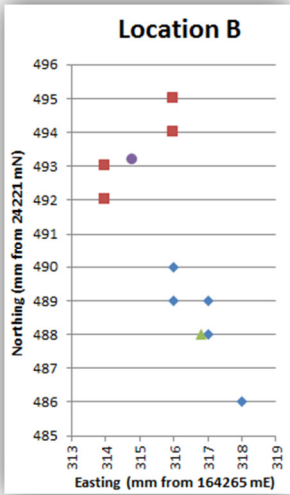
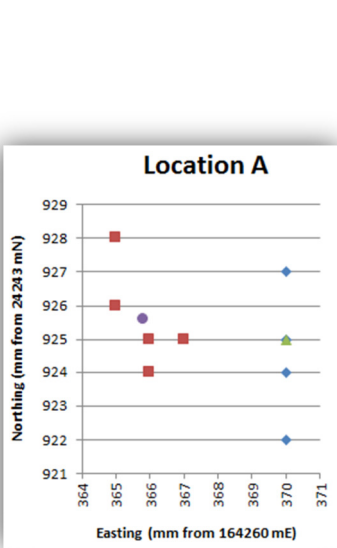
1978-1981

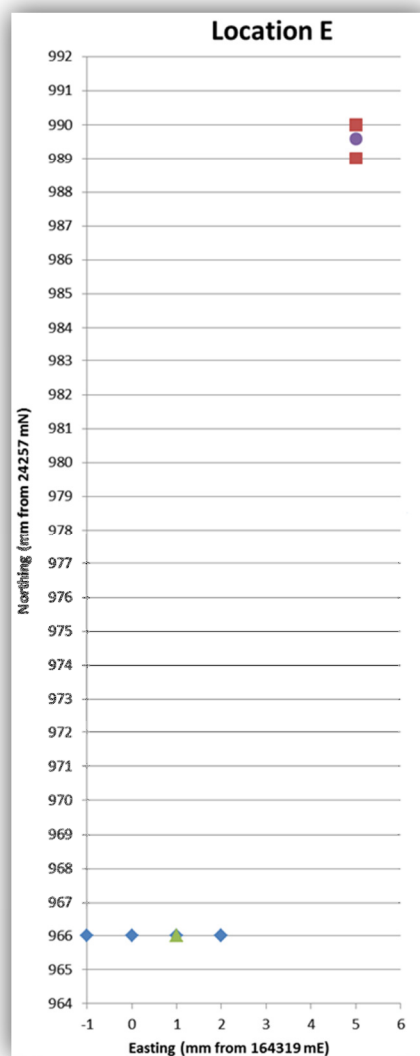
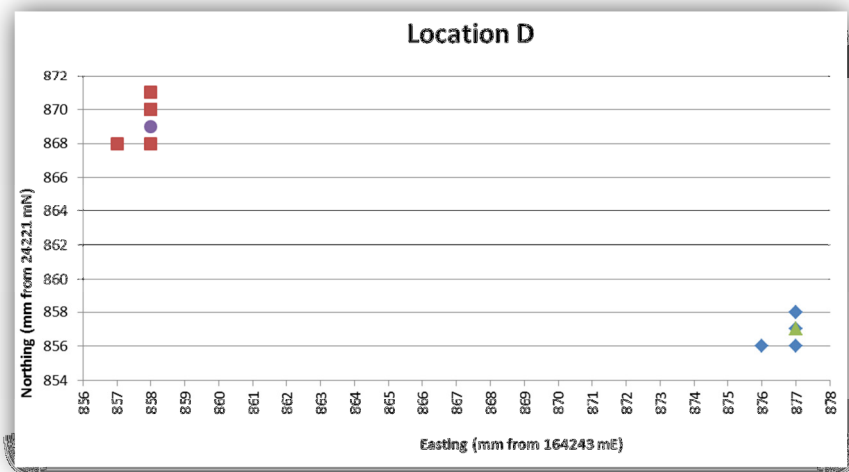


Appendix C: Sentripod Accuracies

C.1 Resection results

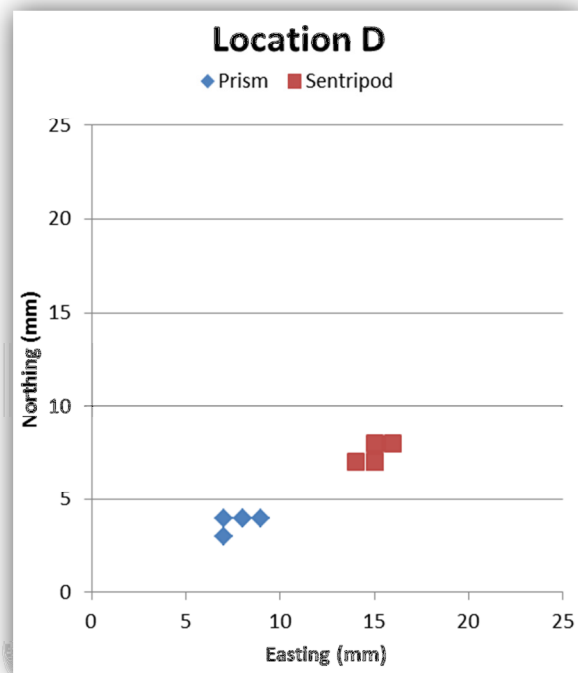
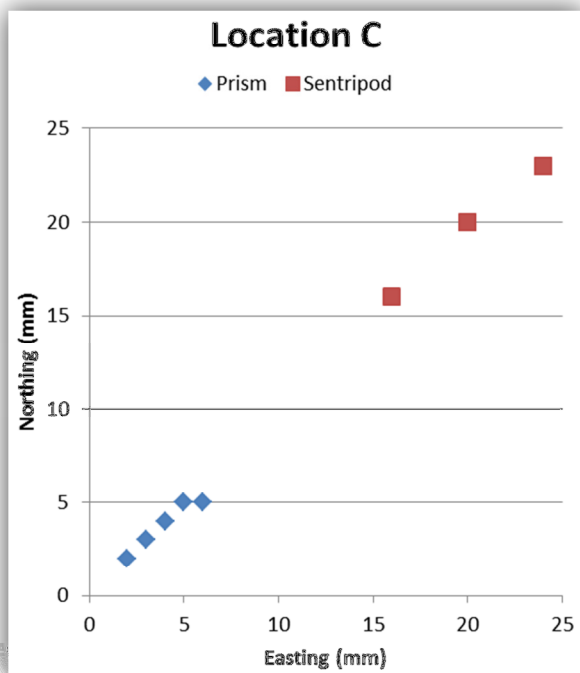
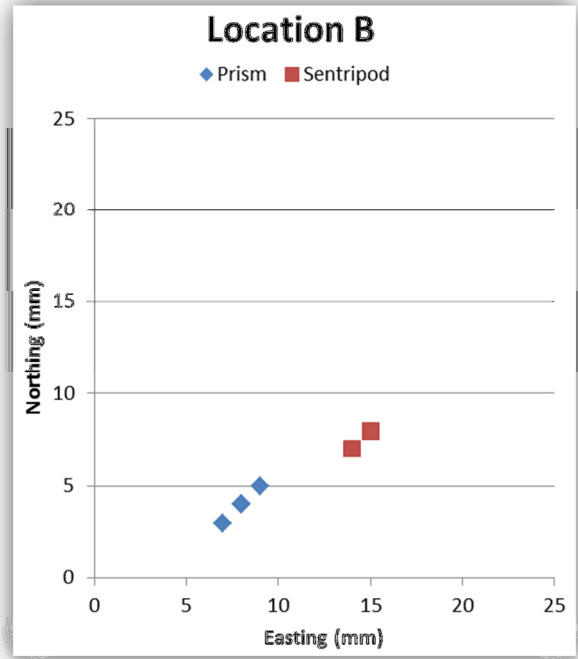
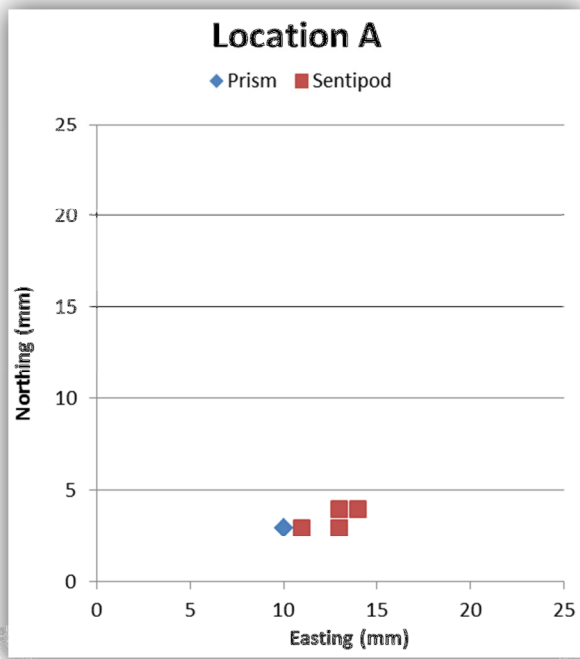
Below are the tables demonstrating the Easting and Northings of points derived from resections carried out using both a sentripod and a circular prism at a total of five locations. All scales are produced to match one another. Legend applies to all.

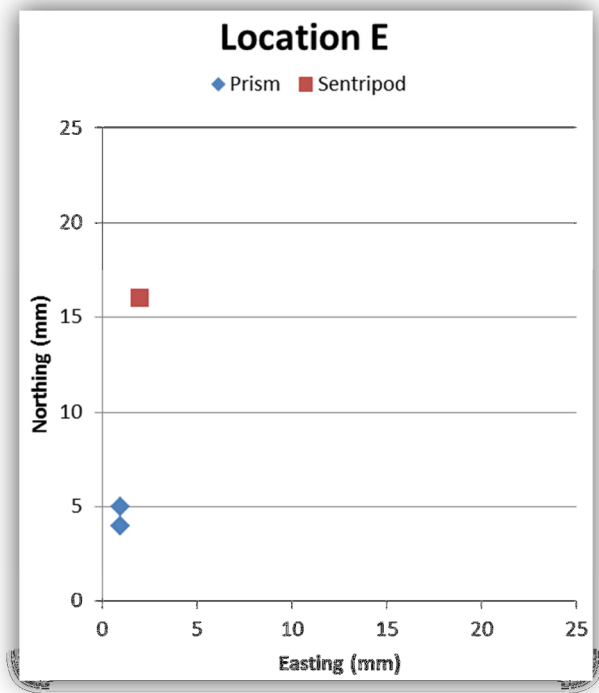




C.2 Resection Errors

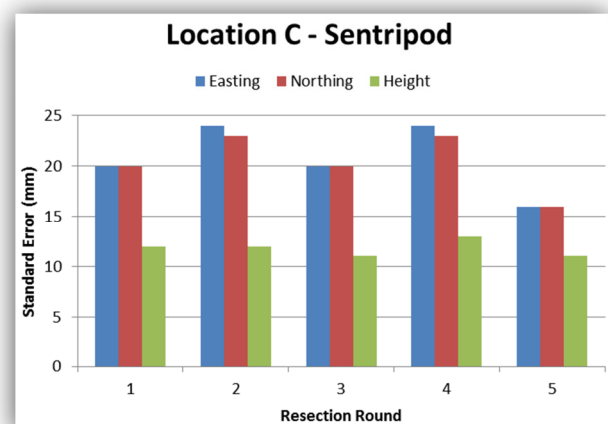
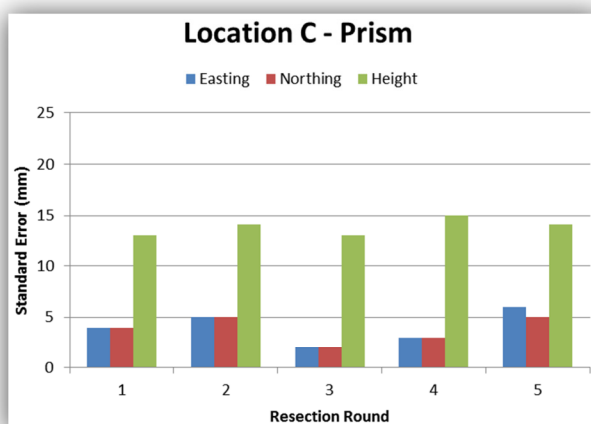
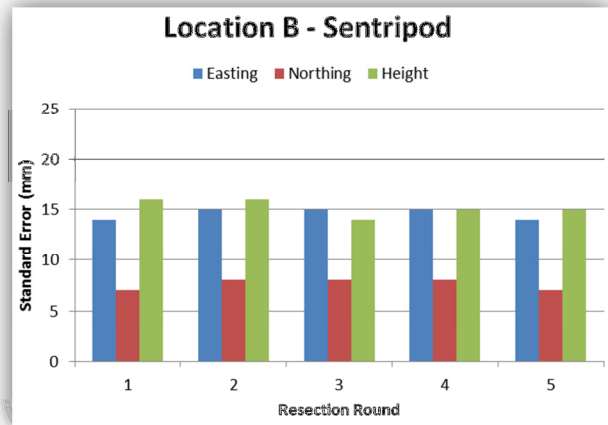
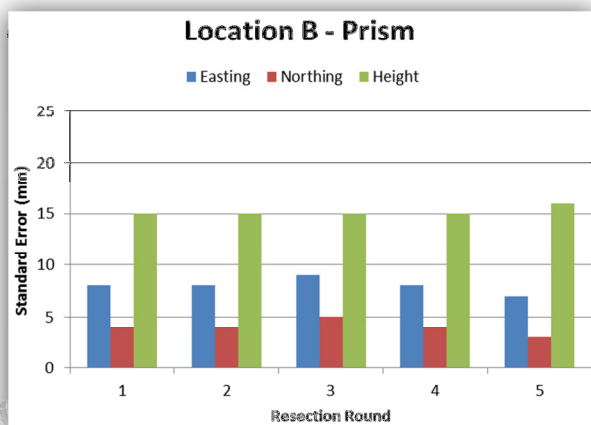
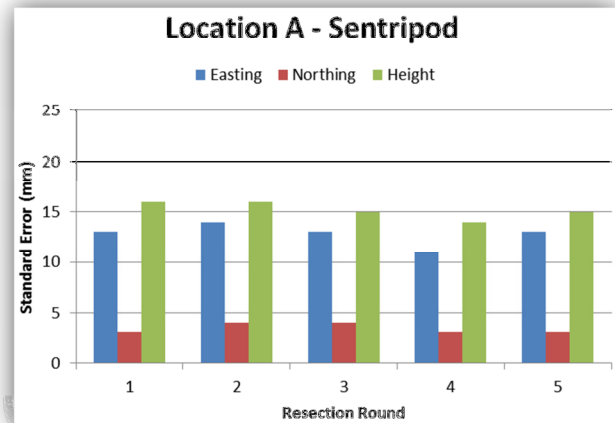
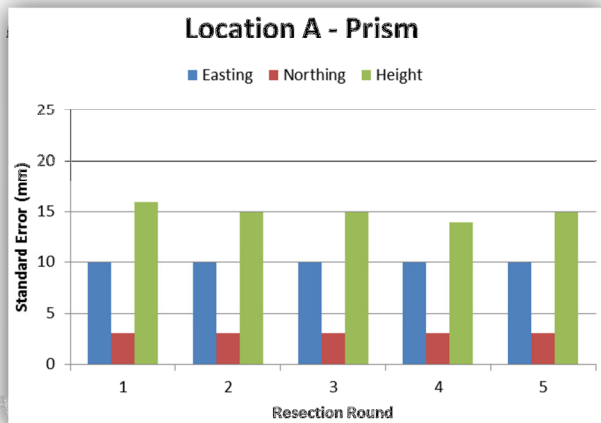
Standard errors of each resection for eastings and northings at each location are represented in the following graphs, showing errors for both the sentripods and circular prisms.

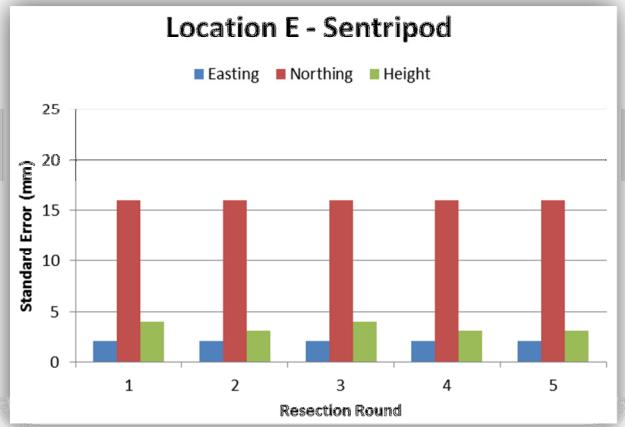
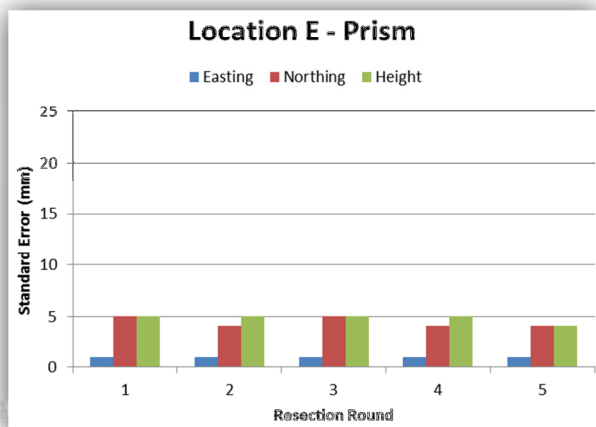
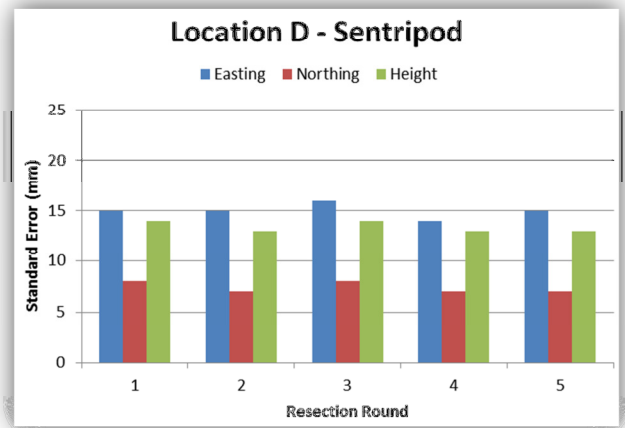
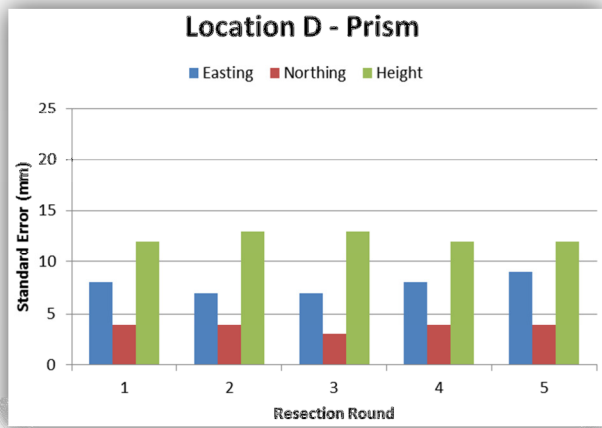




C.3 Errors encountered at Each Resection

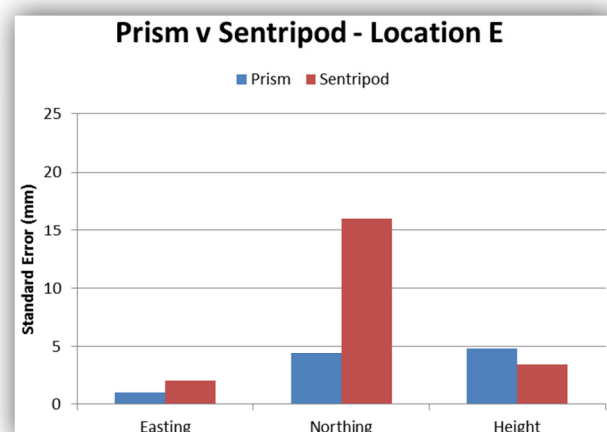
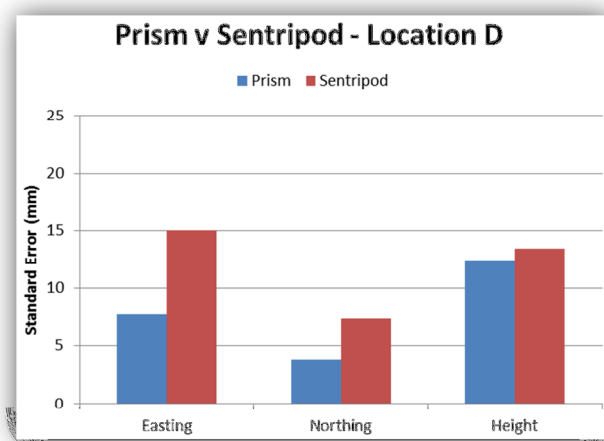
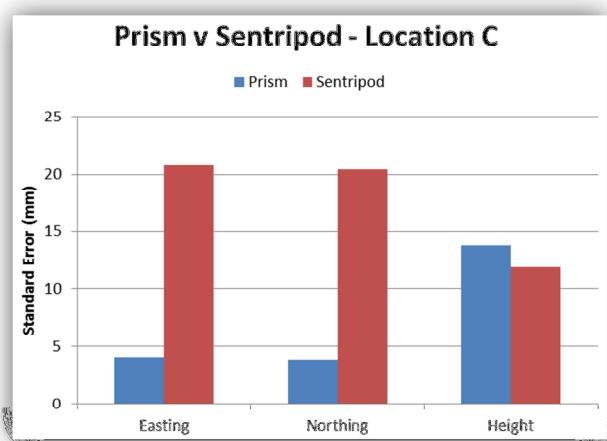
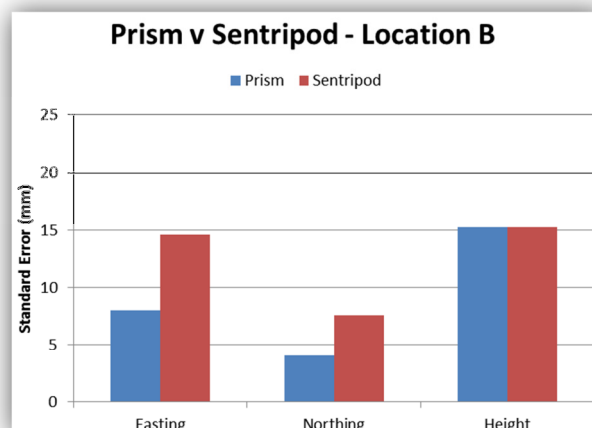
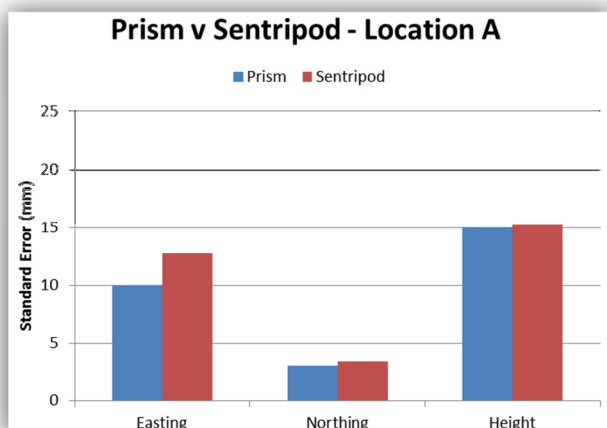
The errors of Easting, Northing and elevation encountered at each resection and each location for the circular prisms (left column) and sentripods (right column).





C.4 Average Errors of Each Prism

Averages of errors produced in Eastings, Northings and elevation using both the sentripods and the circular prisms at each site.



Appendix D: Bolt Coordinates

A total of 50 readings were taken to establish coordinates of the bolt (10 taken at each of 5 stations). A statistical analysis was carried out to determine the most accurate results possible, shown in the table below. Only one reading required eliminating, displayed in red. The elevation of the point was determined using levelling from Base NW.

Station	Resection coords	Resection errors	1	2	3	4	5	6	7	8	9	10	Average	SD (s)	2.5 x s	range [lower]	range [upper]
A	E	164286.875 E	0.007 E	164317.205	164317.201	164317.204	164317.201	164317.202	164317.203	164317.197	164317.203	164317.204	164317.2024	0.002319004	0.005797509	164317.1966	164317.2082
	N	24219.206 N	0.004 N	24275.780	24275.782	24275.781	24275.783	24275.782	24275.782	24275.785	24275.781	24275.781	24275.7819	0.00137032	0.003425801	24275.77847	24275.78533
B	E	164298.672 E	0.003 E	164317.196	164317.200	164317.201	164317.199	164317.201	164317.200	164317.200	164317.201	164317.199	164317.1999	0.00166333	0.004158325	164317.1957	164317.2041
	N	24218.606 N	0.003 N	24275.778	24275.778	24275.778	24275.777	24275.777	24275.777	24275.777	24275.777	24275.777	24275.7773	0.000483046	0.001207615	24275.77609	24275.77851
C	E	164307.557 E	0.005 E	164317.202	164317.207	164317.207	164317.201	164317.199	164317.198	164317.199	164317.197	164317.204	164317.2013	0.003622461	0.009056152	164317.1922	164317.2104
	N	24196.373 N	0.004 N	24275.770	24275.769	24275.770	24275.771	24275.771	24275.771	24275.770	24275.771	24275.771	24275.7705	0.000707107	0.001767767	24275.76873	24275.77227
D	E	164272.657 E	0.004 E	164317.200	164317.200	164317.201	164317.200	164317.198	164317.198	164317.201	164317.203	164317.203	164317.2005	0.001715938	0.004289846	164317.1962	164317.2048
	N	24203.433 N	0.001 N	24275.775	24275.775	24275.776	24275.776	24275.778	24275.776	24275.775	24275.774	24275.774	24275.7756	0.001264911	0.003162278	24275.77244	24275.77876
E	E	164309.536 E	0.003 E	164317.200	164317.202	164317.201	164317.199	164317.200	164317.199	164317.200	164317.199	164317.201	164317.2001	0.000994429	0.002486072	164317.1976	164317.2026
	N	24234.84 N	0.004 N	24275.777	24275.777	24275.777	24275.777	24275.777	24275.777	24275.777	24275.777	24275.776	24275.777	0	0	24275.777	24275.777

The coordinates derived are in the table below.

Final Coordinates	
Easting	164317.201
Northing	24275.776

Appendix E: Project Timeline

The table below shows significant dates of the project, including data collection, meetings and other notable correspondence.

Date	Task
June 30	Initial site visit and discussion of project scope with Neill Wood
July 1	Commencement of writing for the project
6	Meeting with Andy Wetherelt re: method to establish the baseline and use the GPS
11	Installation of two base points using Leica 1200 GPS
13	Completion of RINEX corrections of base stations by Andy Whetherelt
17	Field work: Collection of Resistivity data with Mr Neill Wood
20	Received Resistivity data after processing by Neill Wood
24	Email correspondence with Neil Wood re: topographic survey method
25	Field Work: Topographic Survey – water’s edge and main features
30	Field work: Topographic survey – main body of bar
August 1	Field work: Installing a third base station using Leica 1200 GPS
5	Completion of RINEX corrections of new base station by Andy Wetherelt
9	Field work: Topographic survey – sluice
11	Meeting with Andy Wetherelt re: method to test sentripods in the field
12	Email correspondence with Andy Wetherelt re: field method for testing the sentripods
13	Meeting with Neill Wood re: resistivity and survey parameters
15	Field work: Testing the sentripods in resection against circular prisms
17	Meeting with Dr Robin Shail re: resistivity data finds
19	Meeting with Andy Wetherelt re: results of resection trials with sentripods and circular prisms
19	Email correspondence with Dave Watkins re: resistivity data features
21	Email correspondence with Dave Watkins re: resistivity data features
23	Field work: transferring coordinates onto a bolt and levelling between bases
24	Email correspondence with Dave Watkins re flood risk in Helston
29	Field work: last test of sentripod resection to finalise future method
September 5	Project Completion